Optimised Radio over Fibre Links for Next Generation Radio Access Networks

A thesis submitted for the degree of Doctor of Philosophy

Department of Electronic and Computer Engineering

College of Engineering, Design and Physical Sciences

Brunel University London

By

Abdul Nasser Abdul Jabbar Abbood

Supervisor**: Prof. Hamed Al-Raweshidy**

June 2018

Dedicated to the loving memory of my father

To my wife Suhad

And

My two boys Ahmed & Haidar

And

My daughter Maryam

Abstract

Optical fibre has become the dominant theme of transmission in long haul, high data rate communication systems due to its tremendous bandwidth and low loss. Radio over Fibre (RoF) technology facilitates the seamless integration between wireless and optical communication systems and found to be the most promising solution to meet the exponential bandwidth demands expected for the upcoming years. However, the main bit-rate/distance limitation in RoF systems is the chromatic dispersion.

In this thesis, the two generations of RoF technologies, namely Analogue RoF (ARoF) and Digital RoF (DRoF) are investigated. The overall aim of this research is to optimise the optical bandwidth utilisation of these two approaches for a typical transmission of the fronthaul link proposed in the next generation Centralised Radio Access Network (C-RAN). Consequently, a number of physical layer design scenarios for the optimised transmission of the Radio Frequency (RF) signals over a Standards Single Mode Fibre (SSMF) are demonstrated.

Firstly, for an ARoF transmission, where the analogue RF signals are transported over SSMF using an optical carrier, a bidirectional link transmitting four Downlink/Uplink channels in a chromatic dispersion limited scenario is designed. Simulation results have shown a clear constellation diagram of a 2.5 Gb/s RF signal transmission over 120 km fibre length.

Secondly, a DRoF system with reduced optical bandwidth occupancy is proposed. This system employs an optical Duobinary transmission to the digitised RF signal at the transmitter side to reduce its spectrum and to address the chromatic dispersion effect, simultaneously. Simulation results demonstrate the capability of the proposed system to maintain high-quality transmission of the digitised signals over 70 km of fibre distance without dispersion compensation requirements.

Finally, an advanced DRoF transmission link based on integrating digital Optical Single Sideband (OSSB) transmission with Duobinary encoding scheme is designed. Simulation results have clearly verified system's robustness against transmission impairments and have better performances in terms of the obtained BER and EVM with respect to the 3GPP standardised values. Moreover, the results show that both transmission distance and power budget are furtherly improved in comparison with two other digital transmission scenarios.

Contents

Acknowledgements

First and foremost, I would like to express my sincere gratitude to my supervisor, Professor Hamed Al-Raweshidy for his continuous support, encouragement and guidance. I would like to thank you for your patience, valuable advises and beneficial discussions while giving me enough room to choose my study topics.

Secondly, my sincere gratefulness and appreciation would go to the Ministry of Higher Education and Scientific Research, Iraqi Cultural Attaché and Southern Technical University in Iraq for funding and support this study.

I owe my deepest gratitude to my mother, who has always been my main inspiration and always urged me to pursue a higher level of education.

Finally, I value the role of my colleagues in the Wireless Networks and Communications Centre (WNCC), who have been supportive throughout this period.

Declaration

I certify that the effort in this thesis has not previously been submitted for a degree nor has it been submitted as part of requirements for a degree. I also certify that the work in this thesis has been written by me. Any help that I have received in my research work and the preparation of the thesis itself has been duly acknowledged and referenced.

Signature of Student……. Date……

List of Figures

List of Tables

List of Abbreviations

ADC	Analogue-to-Digital Converter
A-FH	Analogue Fronthaul
AM	Amplitude Modulation
APD	Avalanche Photo Diode
ASE	Amplified Spontaneous Emission
ARoF	Analogue Radio over Fibre
BER	Bit Error Rate
BS	Base Station
BW	Bandwidth
CAGR	Compound Annual Growth Rate
CO	Central Office
CW	Continuous Wave
DAC	Digital-to-Analogue Converter
DAS	Distributed Antenna System
DCF	Dispersion Compensation Fibre
DFB	Distributed Feedback
D-FH	Digital Fronthaul
DGD	Differential Group Delay
DL	Downlink
DD-MZM	Dual Drive Mach Zehnder Modulator
DRoF	Digital Radio over Fibre
DSB	Double Sideband
DWDM	Dense Wavelength Division Multiplexing
EAM	Electro-absorption Modulator
EDFA	Erbium Doped Fibre Amplifier
EOM	Electro-Optical Modulator
EPON	Ethernet Passive Optical Network
EVM	Error Vector Magnitude

FBG	Fibre Bragg Grating
FP	Fabry-Perot
Fi-Wi	Fibre and Wireless
FP-DRoF	Fully-Photonic Digital Radio over Fibre
FWM	Four Waves Mixing
GPON	Gigabit Optical Passive Network
GVD	Group Velocity Dispersion
HDTV	High-Definition Television
IF	Intermediate Frequency
IMD	Intermodulation Distortion
IMDD	Intensity-Modulation Direct- Detection
ISI	Inter-Symbol Interferences
ITU	International Telecommunication Union
LD	Laser Diode
LiNbO3	Lithium Niobate
LSB	Least Significant Bit
LTE	Long Term Evolution
MIMO	Multi Input Multi Output
MMF	Multi-Mode Fibre
mm-Wave	Millimetre Wave
MSB	Most Significant Bit
MZI	Mach-Zehnder Interferometer
MZM	Mach-Zehnder Modulator
NRZ	Non-Return-to-Zero
OBPF	Optical Bandpass Filter
ODSB	Optical Double Sideband
O/E	Optic-to-Electric Converter
OPEX	Operation Expenditure
M-QAM	Multi-level Quadrature Amplitude Modulation
OSNR	Optical Signal-to-Noise Ratio
OSSB	Optical Single Sideband

PADC	Photonic ADC
PD	Photo Diode
PON	Passive Optical Network
QAM	Quadrature Amplitude Modulation
RAU	Remote Access Unit
RIN	Relative Intensity Noise
RF	Radio Frequency
RoF	Radio over Fibre
RZ	Return to Zero
SBS	Stimulated Brillouin Scattering
SCM	Subcarrier Multiplexing
SFDR	Spurious Free Dynamic Range
SMF	Single Mode Fibre
SNR	Signal-to-Noise Ratio
SPM	Self-Phase Modulation
SRS	Stimulated Raman Scattering
SSB	Single Sideband
UL	Uplink
VCSEL	Vertical-Cavity Surface-Emitting Laser
WDM	Wavelength Division Multiplexing
XPM	Cross-Phase Modulation

Chapter 1

Introduction

1.1 Background

The growth in data traffic demands has been attributed to the expanded use of mobile smartphones in addition to various bandwidth-hungry applications, such as video conferencing, High Definition TV (HDTV) and interactive video gaming. Figure 1.1 shows the Global Mobile Data Traffic Forecast from (2016 – 2021) [1]. It predicts that the overall data traffic is expected to grow from 7 Exabyte (EB), where an Exabyte is equal to one million terabytes, in 2016 to 49 EB by 2021, which means a seven-fold increase over 2016.

Figure1- 1: Cisco VNI, Global Mobile Data Traffic Forecast 2016 – 2021[1]

In addition, the Compound Annual Growth Rate (CAGR) of the mobile data traffic is expected to grow at 47% from (2016 – 2021). Wireless and broadband services represent the most prodigious growth stories in data traffic forecast. Consequently, transporting this massive amount of data would require a considerably huge transmission bandwidth which is much greater than that offered by the existing networks.

This traffic explosion is presently the major challenge to the existing Radio Access Networks (RANs). In response to that, fibre-optic technology, which is widely spread over the past few decades, provides a tremendous bandwidth and capacity in telecommunication networks. Fibre-optic communication systems are considered as the very promising technologies for next-generation networks. Beside its ability to carry extremely high data rates over long reach transmission distances with relatively low attenuation values, they have many other advantages over the conventional RANs. They are less influenced by noise, are totally unaffected by the radio frequency interferences, completely isolated medium, and finally unaffected by the weather conditions and high voltage exchanging [2]. Many techniques have been developed to offer the potential of Tera-bit per second transmission bandwidth in optical-fibre networks, such as Dense Wavelength Division Multiplexing (DWDM).

Therefore, Mobile Network Operators (MNOs) and service providers are in favour of integrating fibre and wireless (Fi-Wi) technologies to address the challenges of providing high data rate services to the end users [3], [4]. This presents the concept of Radio over Fibre (RoF) network as the futuristic solution for supporting super-broadband services in a cost-effective, solid and ecologically friendly way[5]. It opens the gate for a new era of an optical wireless converged network to be deployed.

1.2 Research Motivations

The significant growth in data traffic and the evolution in RoF technology have contributed to the innovation of a novel RAN infrastructure known as a Centralised Radio

Access Network (C-RAN) [6]. In C-RAN, a new concept of Base Station (BS) design is proposed based on co-locating the Baseband Processing Units (BBU) in a centralised BBU pool while keeping the relative Remote Radio Heads (RRHs) at the cell site. C-RAN provides many advantages over conventional RAN, such as BS design simplification, reduced power consumption even with the densely deployment of the RRHs, centralisation of the Radio Frequency (RF) signal processing, the ability to perform a dynamic resource allocation, cooperative radio techniques, and network functionalities virtualisation to perform dynamic load balancing [7]. This requires a more effective utilisation of the transmission system resources.

However, C-RAN advocates for a new paradigm of a transport network connecting the BBU pool to the RRHs known as the "front-haul" as shown in figure 1.2. Front-haul link is built using an optical distribution network to meet the increasing demands of the higher data rate.

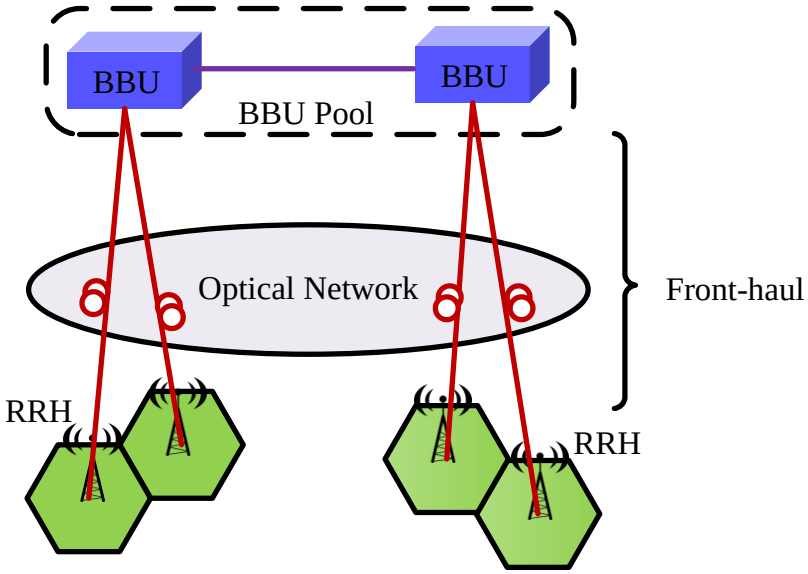

Figure1- 2: The Basic C-RAN Structure

Optical techniques applied for this transportation segment might make use of either analogue or digitise waveform of the RF signal to be transmitted over the front-haul.

Nevertheless, transmitting an extremely high data rates using any of these transmission scenarios impose stringent requirements on the design of the front-haul link.
Based on what has been mentioned above, the main motivation for this PhD research is the design of a cost-effective front-haul link for the next generation mobile networks that can cope with the challenging high data rate requirements and reduce the optical bandwidth.

1.3 Research Challenges

A physical layer design conceived for a fronthaul link relying on RoF technology is a challenging research area. Some of these challenges have been addressed through the work of this PhD research as follows:

- Generally, fronhaul link design based fibre-optic can be classified into Analogue fronthaul (A-FH) and Digital fronthaul (D-FH). Traffic in D-FH is based on Digital Radio over Fibre (DRoF) technology. The de facto standards for a fronthaul based DRoF is either the Common Public Radio Interface (CPRI) [8] or Open Base Station Architecture Initiative (OBSAI) [9]. However, CPRI is the most adopted standard for the fronthaul interface due to its efficient mapping methods. Considering CPRI protocol, the digitised signal is transmitted over the fronthaul by one of its standardised bit rate options which are multiples of (1, 2, 4, 5, 8, 10, and 16) by 614.4 Mbit/s. Therefore, D-FH must be capable of handling data rates that reach up to 10 Gb/s. This represents a highly challenging issue from the implementation point of view for the fronthaul as it requires a high optical bandwidth.

- The challenging bit rate requirements for the D-FH based DRoF can result in the implementation of A-FH based Analogue Radio over Fibre (ARoF) transmission technology. However, Signal transmission over the A-FH suffers from nonlinear effects, such as Intermodulation Distortion (IMD) and chromatic dispersion which

reduce the transmission distance to a few kilometres. Consequently, reducing these impairments in order to enhance the performance and to extend the transmission distance is a challenge needs to be addressed.

- Due to high data rates in DRoF, it seems unlikely to be integrated with the operational Passive Optical Network (PON) standards, such as Ethernet Passive Optical Network (EPON), Gigabit Passive Optical Network (GPON) and Next Generation-Passive Optical Network (NG-PON1) to achieve the cost-effectiveness. More recently, NG-PON2 has been standardised by International Telecommunication Union ITU-T G 989.2 [10] which brings more improvements to the bit rate capacity relative to the previous PON standards. This introduces a challenge represented by assuring the compatibility of DRoF link with the NG-PON2 from the perspectives of the wavelength plan and bandwidth requirements.

- With the current capacity expansion in optical fibre networks using technologies like WDM, the impact of the chromatic dispersion is one of the major challenges with regard to higher transmission rates and lengths. Particularly, at wavelengths around 1550 nm, which offers the most reduced attenuation, the impact of the chromatic dispersion must be considered for the assurance of ideal transmission approach. For this regard, bandwidth-efficient modulation schemes have been proposed to address this challenge.

1.4 Aims and Objectives

The main aim for this research study is to design an optimised radio over fibre physical link for the application in the fronthaul of next-generation radio access network and to investigate its performance to evaluate its physical functionalities. This design considers the two major types of RoF transmission systems, namely Analogue RoF (ARoF) and Digital RoF (DRoF). The aim of this thesis is addressed via the following objectives:

1- Review the methodologies which have been created, proposed or developed to compensate or limit the impact of the chromatic dispersion in optical fibre, particularly in the standard single mode fibre (SSMF).

2- Adopt a technique or a strategy which would address the impact of the chromatic dispersion in digital optical transmission systems. This includes applying an efficient encoding scheme to the digital data signal to optimise its spectrum and to counteract the chromatic dispersion effect as well.

3- The focus of this research is on reducing the optical bandwidth of the designed link so that to improve the transmission performance on one hand, and to increase the transmission distance on the other hand. This comprises the following sub-objectives:

    a) Employing a bandwidth efficient modulation scheme for both the baseband and optical signals for different transmission scenarios.
    b) Employing higher order modulation formats and making sure to keep the performance figure of merits, such as Error Vector Magnitude (EVM) below the standardised limits.
    c) Integrating multi-bandwidth optimisation schemes together to gain even more bandwidth reduction.

4- Propose a simplified wavelength reuse scheme to be implemented at the Base Station (BS) side to achieve a bidirectional cost-effective RoF link.

5- Analyse the performance of the optimised RoF link in terms of a simulation environment to verify its robustness. The simulation focuses on the optical link design only while the wireless transmission has not been considered.

1.5 Thesis Outline and Contributions

This thesis is composed into six chapters. Each chapter starts with a concise review featuring the contributions achieved in that chapter. Then, a brief presentation to the most recent related work is listed followed by a detailed introduction to the chapter explaining what has been done in it. Towards the end of the chapter, a summarised conclusion is presented.
The outline of this thesis contributions are as follows:

Chapter 2: Presents an overview of the optical communication system, and the operation principles of the components used in it including the transmission mediums and optical transmitters/receivers. Transmission main impairments that affecting the optical link performance, particularly dispersion effect with the major dispersion compensation schemes are described. The two types of RoF communication systems which are ARoF and DRoF are detailed. The basic operation principles, advantages/disadvantages and impairments presented in each RoF type are discussed. This discussion justifies the need for the techniques used in the design of the optimised links presented in the next chapters.

Chapter 3: Considers the design of a bidirectional ARoF system in details, proposing a scheme for transmitting four downlink signals each one with different Quadrature Amplitude Modulation (QAM) combination over long reach fibre using four Dense Wavelength Division Multiplexing (DWDM) channels. Addressing the impact of the chromatic dispersion has been achieved by using a Dispersion Compensation Fibre (DCF). As a further enhancement, employing higher order modulation formats have supported dispersion resiliency as they require less optical bandwidths. The duplex transmission has been facilitated using a new low complexity technique for reusing the downstream wavelength for upstream transmission without requiring a separate laser source at the BS side. The advantages of the proposed link conceived for fronthaul based ARoF technology

is presented and performance results are discussed on the basis of signal's EVM and BER showing the feasibility of the designed ARoF link.

Chapter 4: Aims for designing an optimised DRoF link. Following a concise introduction on DRoF, a discussion on the key components used in DRoF systems, namely Analogue to Digital Converter (ADC) and Digital to Analogue Converter (DAC) are presented showing their attribution in the highly produced data rate. A cost-efficient physical layer design for the optimised transmission of a digitised 16-QAM signal over fibre is presented. In this system, an optical Duobinary modulation scheme is realised with reduced complexity to optimise the optical bandwidth utilisation. More explicitly, the designed link is capable of transmitting a digitised 16-QAM signal over 70 km SSMF without dispersion compensation requirements. Furthermore, the performance of the system is investigated for different ADC quantisation levels as a separate transmission scenario.

Chapter 5: Introduces a concept of integrating the Duobinary encoding scheme with the digital Optical Single Sideband (OSSB) transmission to furtherly reduces the optical bandwidth to obtain even more performance improvements. Therefore, a brief introduction to the theory of the OSSB transmission technique is presented. For the sake of integration compatibility, many modifications have been done not only to gain more bandwidth reduction but also to achieve even more sideband suppression. Moreover, a physical design to a Finite Impulse Response (FIR) digital filter is proposed to provide the required Hilbert Transformation to baseband digital signal in the OSSB configuration. Again, the digitised transmission of a 16-QAM signal over an SSMF is demonstrated. The performance of the proposed system is analysed and compared with different digital transmission scenarios in order to highlight its proficiency.

Chapter 6: Concludes the research findings and highlights a range of ideas for the future work.

Chapter 2

Optical-Fibre Communication System

2.1 Introduction

The block diagram of the fibre-optic communication system is shown in figure 2-1 below. It consists of a transmitter, a communication channel, which is realised using optical fibre cable and a receiver. The optical fibre has mostly been developed for telecommunication networks as it offers an enormous transmission bandwidth. Optical fibre telecommunication systems can furtherly be divided into two categories: Long-Haul and Shot-Haul depending on the transmission distance [11]. Indeed, Fibre-optic systems are not only very attractive for high bit rate long-haul applications but also it is a cost-effective solution for short-haul multichannel networks with multiple services, such as broadband integrated services digital networks. In the next sections, we will provide an introductory review of the main components of the fibre-optic telecommunication system.

Figure 2- 1:Optical Communication System

2.2 Optical Transmitter

The main function of the optical transmitter is to convert the signal from Electrical to Optical (EO) domains and to dispatch the optical signal into the fibre. The main parts of the optical transmitter are an optical source, an optical modulator and a coupler as shown in figure 2-2. The optical source is configured using either semiconductor lasers or Light-

Emitting Diodes (LEDs). Most optical communication systems use semiconductor lasers rather than LEDs as they have many advantages which include low cost, reliability, small size and suitability for high frequency signals [12].

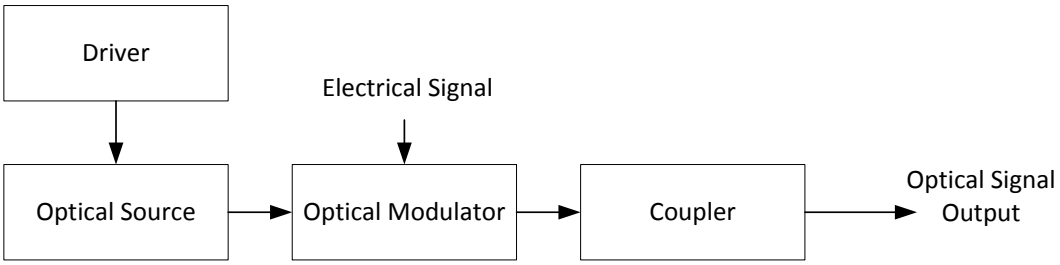

Figure 2- 2: Optical Transmitter Components

2.2.1 Continuous Wave (CW) Semiconductor Laser

A laser is a device used for emitting modulated data into the fibre. There are two kinds of lasers that are generally utilised in optical telecommunications: semiconductor lasers and fibre lasers. Semiconductor lasers are the most preferable in optical networking as they have narrow spectral line width, fast tunability and high output optical power. A semiconductor material can either be doped (adding impurities) with electrons to obtain (n-type) material or removing some of its electrons, which is so-called adding holes, to obtain (p-type) material. Therefore, a p-n junction is formed when the p-type and n-type materials are both intersecting each other with a common boundary between them [13].

The semiconductor laser is generally consisting of three parts: the optical gain, the optical feedback and the pumping mechanism as shown in figure 2-3.The optical gain is an atomic medium with two electromagnetic levels correspond to the ground (stable) state and the higher (excited) state. The electrons of the atoms are jumped to the excited level due to the external pumping mechanism effect. This is referred to as the population inversion. The operation principle of the semiconductor laser is governed by the stimulated emission, in which an external photon is bombarded onto excited electrons in the higher state.

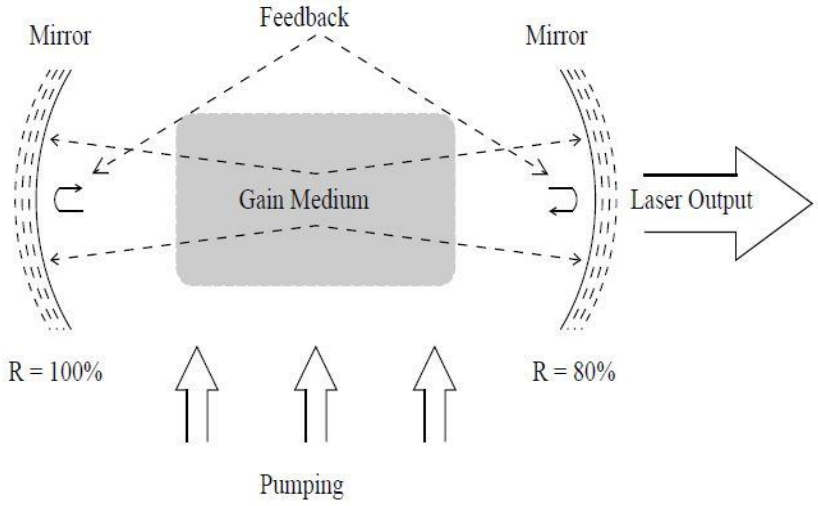

Figure 2- 3: Laser Operating Principles[12]

As a result, these electrons fall from the excited state to the lower energy state, emitting photons (light) that have the same phase and frequency of the incident stimulated photon [12]. However, frequency and phase of the laser light are affected by a phenomenon called spontaneous emission. It happens when excited electrons in the higher level fall into the lower energy level without stimulation, resulting in a photon emission with random frequency and phase distribution. Therefore, to sustain the emission of the laser light continuously, the number of electrons in the higher (excited) level must be greater than the number of electrons in the lower energy (stable) level. In another word, the rate of the spontaneous emission (R_{spon}) must always be less than the rate of the stimulated emission as given below [13]:

$$\frac{R_{stim}}{R_{spon}} = \left\{ e^{\left(\frac{hf}{k_B T}\right)} - 1 \right\}^{-1} \ll 1 \qquad (2.1)$$

where f is the frequency of the emitted light, h is Plank's constant, T is the temperature and k_B is Boltzmann constant.

There are two main sources of semiconductor laser noise, which is known as the Relative Intensity Noise (RIN). First, is the spontaneous emission effect, and second, is the absorption effect, which occurs as a result of filling of holes with some of the free electrons in the semiconductor material.

2.2.2 Optical Modulation

The optical signal generated by the laser source needs to be modulated by the information signal. This is referred to as the optical modulation, which can be divided into two schemes: Direct Modulation and External Modulation. Directly modulating an optical signal is limited for the modulation of the digital signal with a bit rate that scales up to 1 Gb/s [14]. The variation in the refractive index of the direct modulator is severely changed with high optical frequencies, causing variations in the output phase and frequency. The modulation current in such modulation schemes need to be minimal to suppress the frequency chirp, which is in turn, decreases the modulator's extinction ratio, and hence reducing the signal to noise ratio (SNR) [5], [13]. As a consequent, optical transmission of high data rate digital signal over long distances can typically be achieved by using external modulators. There are two main external modulators types used in the simulation processes carried out in this research, namely, Mach-Zehnder Modulator (MZM) and Dual-Drive Mach-Zehnder Modulator (DD-MZM). In the following sections, operation principles of these modulators are described in greater details.

2.2.2.1 Mach-Zehender Modulator (MZM)

It is one of the most widely used external modulators in optical communication networks, which also referred to as Mach-Zehnder Interferometer (MZI). The operation principle of MZM is based on the electro-optic effect that occurs in a particular material when the refractive index of that material changes due to the effect of an external electric field [15]. The most commercially used material for electro-optic effect employment in the Lithium Niobate ($LiNbO_3$) for its ability to work at high optical frequencies and low-frequency chirp characteristics [16]. The MZM structure is shown in figure 2-4.

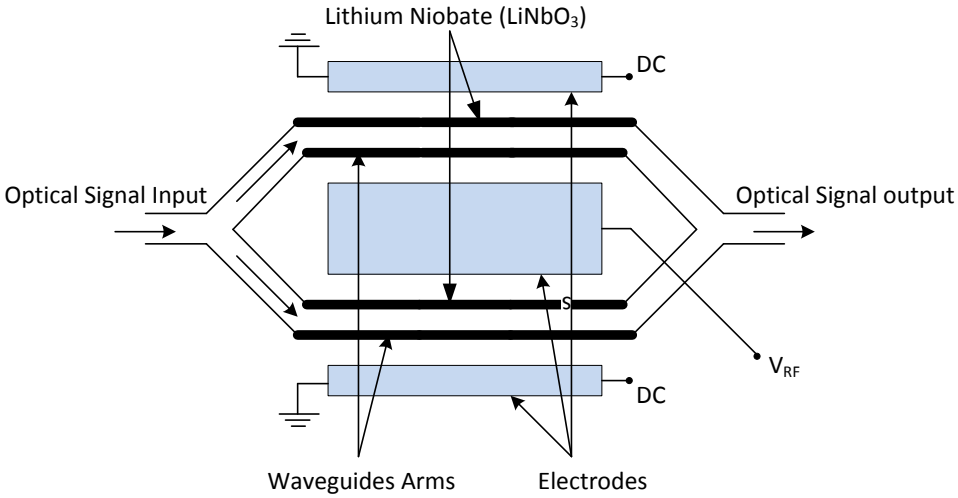

Figure 2- 4: Single-Drive MZM Basic Configuration[17]

As it can be seen from the figure (2.4), the continuous wave coming from the laser source is split equally between two optical waveguide arms. These waveguides are fitted in between two pairs of electrodes which are both connected to the modulating data signal and the DC bias signal. With the aid of the electro-optic effect, the optical phase of the optical signal in each waveguide path (arm) is going to be changed relatively quickly in accordance with the changes in the amplitude of the modulating signal voltage. Therefore, if only the DC bias signal is applied, there will be no change in the phase of the optical signals pass through the waveguide arms. As a result, MZM operation is controlled through the modulation of optical phase. Hence, the amplitude of the output optical modulated signal depends on the optical phase difference between the phase variation in waveguide path 1 (φ_1) and phase variation in waveguide path 2 (φ_2). Therefore, the output optical power of MZM depends on the phase difference between the modulator's arms, and so it can be written as [18]:

$$P_{out}(t) = P_{in}(t) \cdot \cos^2[\Delta\Phi(t)] \tag{2.2}$$

with

$$\Delta\Phi(t) = \frac{\Phi_1(t) - \Phi_2(t)}{2} \tag{2.3}$$

2.2.2.2 Dual Drive Mach-Zehnder Modulator (DD-MZM)

The DD-MZM has two inputs for the modulating drive signals (V_{RF1} and V_{RF2}) applied separately to the electrodes around the optical waveguide arms. Therefore, the optical phase shift in one waveguide arm is independent from the phase shift in the other arm. As a result, many applications would be allowed using this schematic of DD-MZM, such as the Optical Single Sideband (OSSB) modulation [18]. Figure 2-5 shows the basic structure of the DD-MZM.

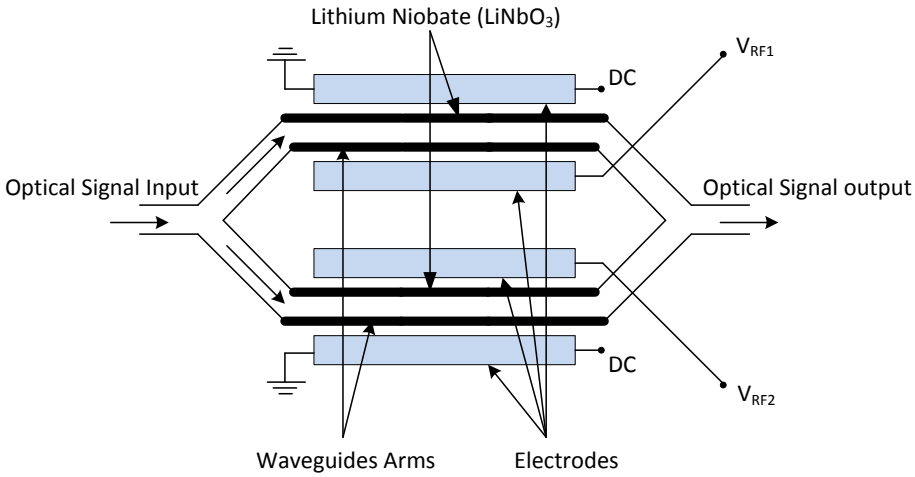

Figure 2- 5: Dual-Drive MZM (DD-MZM) Structure[17]

2.3 Optical Receivers

The main function of the optical receiver is to perform the Optical-to-Electrical (OE) conversion process to recover the transmitted data. This can be handled by using a Photo-Diode (PD) made out of semiconductor materials to be placed at the receiver side of the optical communication network. The operation principles of the PD are based on the absorption mechanism of the semiconductor material [2]. The PD is typically formed out of a combination of n-type and p-type semiconductor materials. Figure 2-6 shows a reverse biased PD with a p-n region known as the depletion region, formulated with free charge carriers.

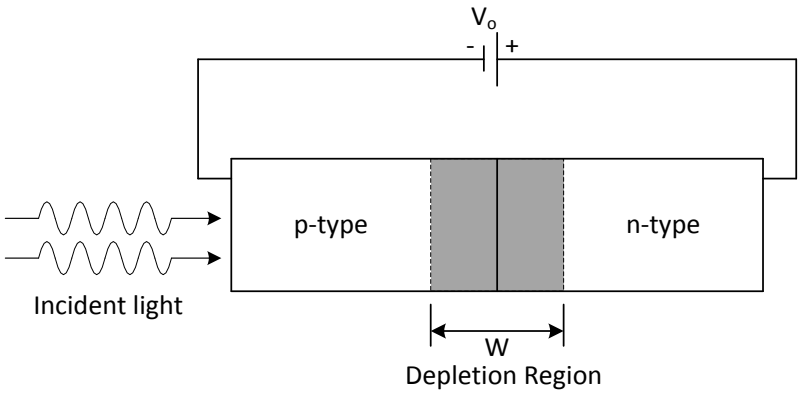

Figure 2- 6: p-n Photodiode[19]

The process of the photo-detection is as follows: when a p-n photodetector is bombarded with a beam of an incident light through a particular side, electrons in the depletion region absorb the incident light photons. These electrons gain some energy from the absorbed photons making them move towards the opposite side, creating an electron-hole pair inside the depletion region. Due to the reverse biased electric field across the PD terminals, as shown in figure 2-6, electrons and holes generated inside the depletion region are going to drift in the opposite directions of their corresponding region depending on the electric charge. Therefore, a flow of an electric current is resulted, which is known as a photocurrent (I_P). This current is proportional to the incident optical power (P_{in}), and hence, it can be given as [19]:

$$I_P = RP_{in} \tag{2.4}$$

where R is the responsivity of the PD measured in (A/W) units. The bandwidth of the PD is determined by how fast the electron-hole pairs travel through the depletion region due to the prompt changes in the incident light. This can be expressed in terms of the transit time, which is defined as the time required for the response of a system to increase from 10% to 90% of its final value for an abruptly changed input signal, such as step signal. Transit time can be given as:

$$\tau_{tr} = \frac{W}{\upsilon_d} \tag{2.5}$$

where, W is the depletion region width, and v_d is the electron-hole drift velocity.
The bandwidth of the PD can be increased by decreasingτ_{tr}. The reduction in τ_{tr} might be achieved by decreasing *W* in (2.5), which in turn will reduce the responsivity of the PD as the rate of the electron-hole generation will be decreased. The effective solution to increase the depletion region while reducing the τ_{tr} is achieved by inserting a layer of undoped semiconductor material (intrinsic material) in between the p-n junction forming what is it called PIN photodiode. A PIN PD that is used InGaAs material in the middle i-layer is commonly used in modern light-wave networks, with typical responsivity values between (0.6 – 0.9) A/W [20].
Another optical receiver type known as Avalanche Photo-Diode (APD) is widely used in optical networks as well. The main difference between APD and PIN PDs is that, in APD, an additional layer is sandwiched between the i-layer and n-type layer [20]. As a result, a secondary electron-hole pairs flow is generated due to the impact of ionization, and so, the optical receiver responsivity is greatly improved in this kind of PDs. However, noise and gain level in the APD PD is greatly influenced by the temperature. Therefore, PIN PD will mostly be adopted as the optical receiver in our designed simulation optical networks.

2.4 Optical Fibre

An optical fibre is a transmission medium used for the transmission of information as light pulses through a glass (Silica) or plastic fibre. It has been first established in the middle of 1980s and used most often in fibre-optic communications [2]. One benefit was to transport the data for longer distances as well as at much higher bandwidth with less loss, compared to the coaxial cables. The glass fibre core is surrounded by another glass layer called cladding as shown in figure 2-7.

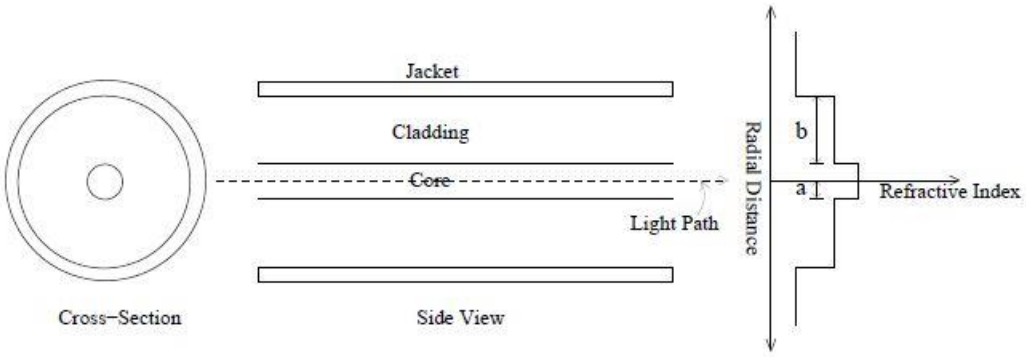

Figure 2- 7: Cross-Sectional Area of a Single Core Optical Fibre[2]

The cladding layer is made with lower refractive index than the core in order to confine the light entering the fibre within the core boundaries according to the principles of the Total Internal Reflection (TIR) phenomenon [21]. Optical communication systems are so attractive due to their capability to transport huge data along large distances with minimal transmission errors. Today, researchers are investigating the transmission of 100 Gb/s per wavelength by the employment of multilevel coding and bandwidth-efficient modulation schemes. Typically, there are two types of optical fibre cables, namely, Single Mode Fibre (SMF) and Multimode Fibre (MMF).

2.4.1 Optical Fibre Types

We will discuss the various types of optical fibres utilised in the optical communication. There are two types of fibre depending on the core diameter and paths of the light propagating through this fibre [20]. The difference between them is their relative size and optical performance. In step-index guides, single-mode operation occurs when the normalised frequency (V), which is defined in equation (2.21) is less than or equal to 2.405. Since the core radius of SMF is so small, it only allows the light to propagate in one mode: this is why it referred to as a single mode fibre as shown in figure 2-8(a). Similarly, an optical fibre cable with large core size (50 μm and more) permit the light waves to propagate in multiple modes, so as called a multimode fibre [2], [22]. In the following section, we will discuss the optical fibre types in more details.

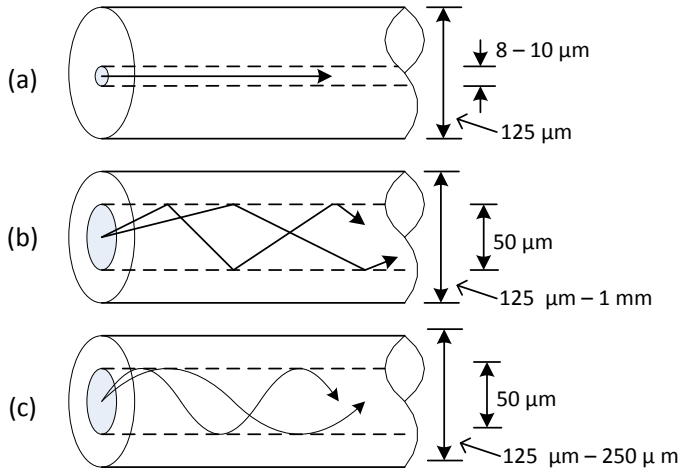

Figure 2- 8: Optical Fibre Types: (a) Single Mode Fibre, (b) Step-index Multi-Mode Fibre, (c) Graded-index Multi-Mode Fibre[2]

2.4.1.1 Multi-Mode Fibre (MMF):

In multimode fibre, the light waves travel through multi-paths inside the core, and so, they arrive at different time instances at the fibre output [2]. This is called the modal dispersion. Hence, the issue with MMF is that as some modes (paths) are longer than others, the light pulses will be spread out causing an effect called Inter-Symbol Interference (ISI), which in turn, restrict the distances that pulses can be transmitted over the MMF. However, as the MMF has a relatively large core size, it is ideally suited for high bandwidth transmission (10 Gb/s and more) over short haul distances (300 m -1 km), such as in buildings and on-campus applications [23].

There are two types of the MMF depending on the core's refractive index profile. MMF with constant refractive index across its core is called a step-index MMF, which is shown in figure 2-8(b). In which, the modal dispersion is severe as the light waves spread out at different angles and lengths. As a result, the transmission bandwidth would be fairly small in such fibres. In spite of the low bandwidth and high attenuation associated with step-

index MMF, its large core size (up to 1 mm) simplifies its connections and splice, which makes it typical in applications requiring distances less than 1 km [24].

Modal dispersion effect in the step-index MMF can be reduced by the graded design of the core's refractive index profile, which is referred to as the graded-index MMF depicted in figure 2-8(c). This can be achieved by gradually decreasing the refractive index profile from the centre of the core towards the outer edge. Due to the reduced refractive index at the core edges, the light waves on the peripheral paths will travel considerably faster than those on the axial, and cause the light waves to take almost the same travelling time through the fibre, thus minimising the dispersion effect. Therefore, the bandwidth of the graded-index MMF is larger than that of the step-index MMF. In contrast, the refractive index profile is more complex, and hence, it is more costly compared to the step-index MMF.

2.4.1.2 Single Mode Fibre

SMF also was known as monomode fibre allows for only one mode of light to propagate through it due to its small core radius, and hence, cannot suffer an intermodal dispersion. SMFs offer a huge bandwidth and are perfectly suited for the long haul, low cost and high capacity transmission. The outer cladding of the SMF is at least ten times the thickness of the core, and the refractive index between the core and the cladding is about 0.6 % [22].

By Design, the core diameter is very narrow compared to the wavelength of the light being used. Consequently, the confinement of the light inside the core is only controlled by the step-change in the refractive index between the cladding and the core of the fibre.

The major disadvantage of the SMF is the complexity experienced in attempting to the couple and/or splices it to another length of the fibre. SMF is widely used in the transmission of a Quadrature Amplitude Modulation (QAM) signals and Single Sideband (SSB) transmission.

Signals being transmitted through optical fibre impose to different types of impairments induced by the fibre media. In the following section, we are going to discuss these impairments n details.

2.5 Optical Fibre Attenuation

Signals transmitted through the fibre are subjected to attenuation. It causes a reduction in the signal power over the transmission distance and it is usually measured in decibel per kilometre (dB/km). In silica optical fibre, there are two main sources for the attenuation, in particular, material absorption and Rayleigh scattering.

2.5.1 Material Absorption

Each material absorbs light at a certain range of wavelengths in accordance to the electronic and vibrational resonances at a particular molecule of that material. This absorption results in a loss of the photons, and their energy therefore transformed into a heat. Material absorption in silica can be subdivided into two categories: intrinsic and extrinsic absorption mechanisms of the silica as the base material used in fibre manufacturing [13]. Intrinsic absorption occurs in two wavelength regions; one at the ultraviolet region caused by the electronic resonance, and the second in the infrared region due to the vibrational resonance. Figure 2-9 shows the reliance on the material absorption on the wavelengths. It can be observed from figure 2-9 that intrinsic absorption is less than 0.1 dB/km at a wavelength range (0.8 μm – 1.6 μm), which is commonly utilised in optical communication systems.

Extrinsic absorption, on the other hand, happens due to impurities in the silica itself. The main source of the extrinsic absorption is the presence of water vapours in silica. A vibrational resonance of the Oxygen and Hydrogen ions near the 2.73 μm wavelength causes these vapours. As shown in figure 2-9, there are three attenuation peaks caused by

the extrinsic absorption occurring near 1.39 μm, 1.24 μm and 0.95 μm wavelengths due to the existence of residual water vapours in silica [13].

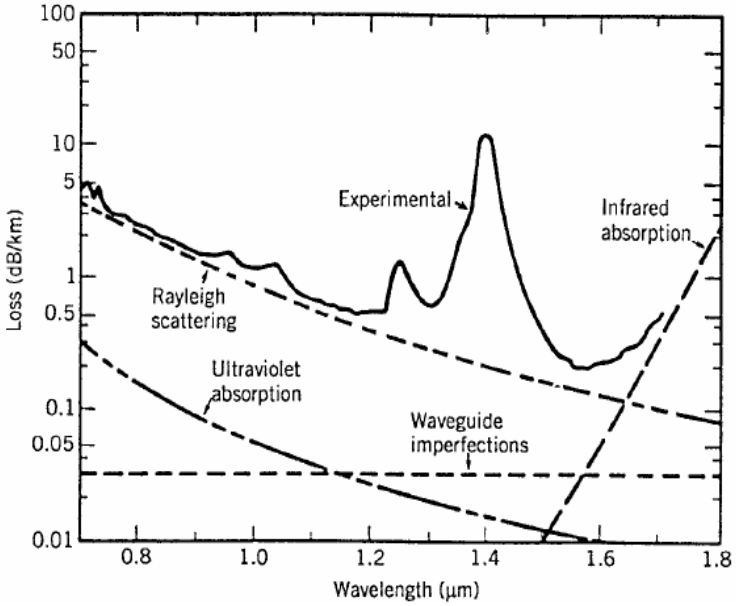

Figure 2- 9: Measured Attenuation versus Wavelengths in SMF[13]

2.5.2 Rayleigh scattering

Rayleigh scattering represents the second major source of attenuation in the optical fibre. The reason for this scattering is the minor variation in the refractive index of the fibre core [25]. Silica particles are haphazardly moving in the molten state and freeze in place during fibre manufacturing, which is, in turn, resulted in an inhomogeneous refractive index profile along the fibre core. Hence, Rayleigh scattering would result in a light diversity out of the waveguide and/or light reflection back to the source. As it can be seen in figure 2-9, Rayleigh scattering effect is inversely proportional to the fourth power of the wavelength. As a result, the intrinsic loss of silica fibre from Rayleigh scattering can be given as [13]:

$$\alpha_R = \frac{C}{\lambda^4} \qquad (2.6)$$

where C is in the range of (0.7–0.9 (dB/km)-μm^4), consequently, α_R will be in the range of (0.12–0.16 dB/km at λ =1.55μm, indicating that fibre loss is dominated by Rayleigh scattering at this wavelength. The attenuation due to Rayleigh scattering can be reduced by increasing the transmission wavelength.

The overall attenuation constant or the fibre loss (α) can be calculated in decibels as follows [13]:

$$\alpha_{dB/km} = \frac{10}{L}\log_{10}\left(\frac{P_{out}}{P_{in}}\right) \tag{2.7}$$

where, P_{in} is the input optical power, and P_{out} is the output power measured at length L of fibre in km. Figure 2-9 also shows that the lowest attenuation value of 0.2 (dB/km) can be obtained in the 1.3 μm and 1.5 μm wavelengths, which explains why they have been largely selected in optical communication systems.

2.6 Dispersion in Optical Fibre

The dispersion can be defined as the widening or broadening that happens to the light pulses as they propagate through the fibre. We have seen that the light-wave speed depends on the refractive index profile of silica utilised in fibre manufacturing. Hence the variation in the refractive index will result in a different propagation speed of the wavelengths travelling along the fibre. Therefore, the optical signal that composed of a finite range of wavelengths will be broadened at the fibre output owing to dispersion. As the dispersion widens the light pulse duration along the transmission distance, interference or overlapping between the consecutive light pulses might be experienced, resulting in inter-symbol interference, thus limiting the pulses (bits) intervals [18]. As a result, the transmission rate in optical communication systems will greatly be influenced by the dispersion effect, and so a reduction in the overall optical system performance, such as the signal to noise ratio and the received bit error rate. However, there are different types of

dispersion in the optical fibre. We are going to discuss these types in details in the following sections.

2.6.1 Modal Dispersion or Intermodal Distortion

The propagation velocity of the wavelengths inside the fibre is not the same for all modes as they travel through the fibre at the same time period. This means that the light pulse enters the fibre at a specific time instant will arrive at different times at the fibre end due to the multipath propagation along the fibre, resulting in a broadening or distortion to the light pulse received at the output of the fibre. This is referred to as the modal dispersion. As the modal dispersion associated with the multimode propagation in fibre, it occurs only in multimode fibre. Therefore, the intermodal dispersion is absent in single mode fibre as the light pulse is transmitted only in one mode [26].

2.6.2 Chromatic Dispersion or Group Velocity Dispersion.

It is another kind of dispersion that also causes a pulse broadening. The main reason for this phenomenon is the signal's angular frequency (ω) dependence of the refractive index on the light pulse speed as they travel in a dispersive medium, such as the silica (glass) [24]. As a result, different spectral components that belong to the same light pulse will travel at different group velocities. This is so-called the Group Velocity Dispersion (GVD). Pulse broadening due to chromatic dispersion increases linearly with the transmission distance. Therefore, after a particular length of fibre transmission will severely be spread out and so overlap with the neighbouring pulses, so that they cannot be distinguished at the receiver output [27], [28].

The propagation properties of the light pulse in a dispersive single-mode fibre of length (L) are primarily determined by the group velocity (v_g), which is given by:

$$v_g = \frac{d\omega}{d\beta} \tag{2.8}$$

where β is the propagation constant, ($\beta = \frac{n\omega}{c}$, c is the speed of light in vacuum)

The delay time (T) taken by the spectral components of the optical frequency to arrive at the end of the fibre can also be determined by means of the group velocity as follows:

$$T = \frac{L}{v_g} \tag{2.9}$$

Furthermore, the group velocity can be expressed as:

$$v_g = \frac{c}{n_g} \tag{2.10}$$

where n_g is the group refractive index.

The major consequence of the chromatic dispersion or the GVD is the pulse broadening ΔT, which can be measured as follows:

$$\Delta T = \frac{dT}{d\omega}\Delta\omega = \frac{d}{d\omega}\left(\frac{L}{v_g}\right)\Delta\omega = L\frac{d^2\beta}{d\omega^2}\Delta\omega = L\beta_2\Delta\omega \tag{2.11}$$

where $\Delta\omega$ is the spectral width of the pulse. From (2.11), the parameter β_2 represents the GVD parameter which determines how much the pulse would broaden as propagating through the fibre. As GVD changes with respect to the wavelength (λ), it is preferred to use $\Delta\lambda$ instead of $\Delta\omega$ by considering ($\omega = \frac{2\pi c}{\lambda}$ and $\Delta\omega = -\frac{2\pi c}{\lambda^2}\Delta\lambda$). Thus, equation (2.11) can be rewritten as:

$$\Delta T = \frac{d}{d\lambda}\left(\frac{L}{v_g}\right)\Delta\lambda = D.L\Delta\lambda \tag{2.12}$$

$$D = \frac{d}{d\lambda}\left(\frac{1}{v_g}\right) = -\frac{2\pi c}{\lambda^2}\beta_2 \tag{2.13}$$

where D is the dispersion parameter of the fibre and it is measured in (ps/(km-nm). The maximum transmission bit rate criteria B.ΔT<1 can be applied to examine the dispersion effect on the bit rate (B). By substituting ΔT from equation (2.12), this condition can be rewritten as:

$$B.L|D|\Delta\lambda < 1 \tag{2.14}$$

Generally, chromatic dispersion in fibre can be considered as the sum of two other quantities, namely material dispersion and waveguide dispersion. Material dispersion occurs due to the frequency dependence of the refractive index, while the waveguide dispersion caused by the frequency dependence of the propagation mode. The wavelength dependence of the dispersion is controlled by the frequency dependence of the refractive index. Therefore, the chromatic dispersion can be expressed in terms of the refractive index (n) as:

$$D = -\frac{2\pi c}{\lambda^2}\frac{d}{d\omega}\left(\frac{1}{v_g}\right) = -\frac{2\pi}{\lambda^2}\left(2\frac{dn}{d\omega} + \omega\frac{d^2n}{d\omega^2}\right) \tag{2.15}$$

$$D = D_M + D_W \tag{2.16}$$

where D_M is the material dispersion, and D_W is the waveguide dispersion. Figure 2-10 shows the variation of the dispersion with respect to the wavelength.

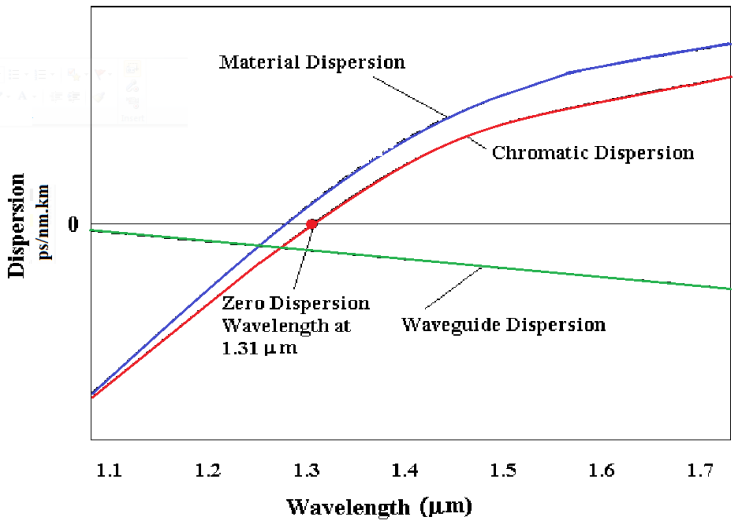

Figure 2- 10: Dispersion Variations against Wavelength Values[29]

2.6.2.1 Material Dispersion

Material dispersion happens because the refractive index of silica used in fibre manufacturing varies in accordance with the applied optical frequency (ω) [29], [30]. It is directly related to the resonance frequencies at which the material absorbs electromagnetic rays. The refractive index can be analysed as a function to the resonance frequencies in silica fibre using the Sellmeier equation as:

$$n^2(\omega) = 1 + \sum_{j=1}^{M} \frac{B_j {\omega_j}^2}{{\omega_j}^2 - \omega^2} \tag{2.17}$$

where B_j is the oscillator strength, and ω_j is the resonance frequency. Here, (n) might represent either the refractive index properties of the core or the cladding. There is a precise relation between the material dispersion and the slope of the group index (n_g):

$$D_M = \frac{1}{c}\left(\frac{dn_g}{d\lambda}\right) \tag{2.18}$$

The group index of silica fibre can be obtained as follows:

$$n_g = n + \frac{dn}{d\omega} \tag{2.19}$$

For a pure silica fibre, it has been found that the quantity $\frac{dn_g}{d\lambda} = 0$ at λ_{DZ} = 1.276 μm, which is referred to as zero dispersion wavelength. Therefore, the material dispersion equals to zero at λ_{DZ}, negative below λ_{DZ} and positive above λ_{DZ}.

2.6.2.2 Waveguide Dispersion

Wavelength propagation depends on fibre parameters such as core radius and core-cladding relative refractive index difference (Δ). The main reason for the waveguide dispersion is the inhomogeneities of these parameters along the fibre length [25]. Waveguide dispersion D_W can be given by [30]:

$$D_W = -\frac{2\pi\Delta}{\lambda^2}\left[\frac{{n_{2g}}^2}{n_2\omega}\frac{Vd^2(Vb)}{dV^2} + \frac{dn_{2g}}{d\omega}\frac{d(Vb)}{dV}\right] \tag{2.20}$$

where, *V* is called the normalised frequency, and it is equal to:

$$V = \frac{2\pi}{\lambda}a\sqrt{{n_1}^2 - {n_2}^2} \cong \frac{2\pi}{\lambda}an_1\sqrt{2\Delta} \tag{2.21}$$

and *b* is the normalised propagation constant:

$$b = \frac{{\beta}/{(2\pi/\lambda)} - n_2}{n_1 - n_2} \tag{2.22}$$

where n_1 and n_2 are the refractive indexes of the core and cladding respectively.

It is assumed that both derivatives in equation (2.20) are positive. Therefore, waveguide dispersion is negative for the whole wavelength range (0 – 1.6 μm). As a result, the major effect of the waveguide dispersion is shifting the zero dispersion wavelength (λ_{DZ}) by 20 – 30 nm, and so the chromatic dispersion is zero at 1.31 μm as shown in figure 2-10. It must be mentioned that the wavelength value of 1550 nm is of a great interest for optical-fibre communication systems as the attenuation loss is considerably low at this wavelength range. However, high dispersion values of (15 – 18) ps/(km-nm) limit the performance of 1550 nm light-wave systems. Remarkably, waveguide dispersion effect can be used to design a fibre such that λ_{DZ} is moved to 1550 nm. Such kind of fibre is referred to as dispersion shifted fibre (DSF) [20]. Another important facility offered by the D_W effect is the design of dispersion compensation fibre (DCF), in which the chromatic dispersion or GVD decreases along the transmission distance due to the variation in the core radius [19].

2.6.2.3 Polarization Mode Dispersion (PMD)

This kind of dispersion is attributed to the imperfect cylindrical symmetry of the fibre core, which results in what is called the birefringence. As a result, the orthogonally polarised components of the original fibre mode will have different mode indices, and so if they were both excited at the fibre input, they would disperse through the fibre as they have different group velocities as shown in figure 2-11 [31]. As any other type of dispersion, PMD causes a pulse broadening, which can be calculated by measuring the time delay (ΔT) between the orthogonal polarisation components as they travel along a fibre of length (L) as follows [32]:

$$\Delta T = \left|\frac{L}{v_{gx}} - \frac{L}{v_{gy}}\right| = L\left|\beta_{1x} - \beta_{1y}\right| = L(\Delta\beta_1) \qquad (2.23)$$

where, x and y are the orthogonal polarisation components of the pulse, while β_1 is the group velocity constant of the two states of polarisation. In a polarised maintaining fibre, the quantity ($\Delta T/T$) is the measure of PMD. It approximately equals 1 (ns/km) when both polarisation components are equally excited at the fibre input. However, PMD might be

reduced to zero when the two polarisation components initiated along one of the principle axes.

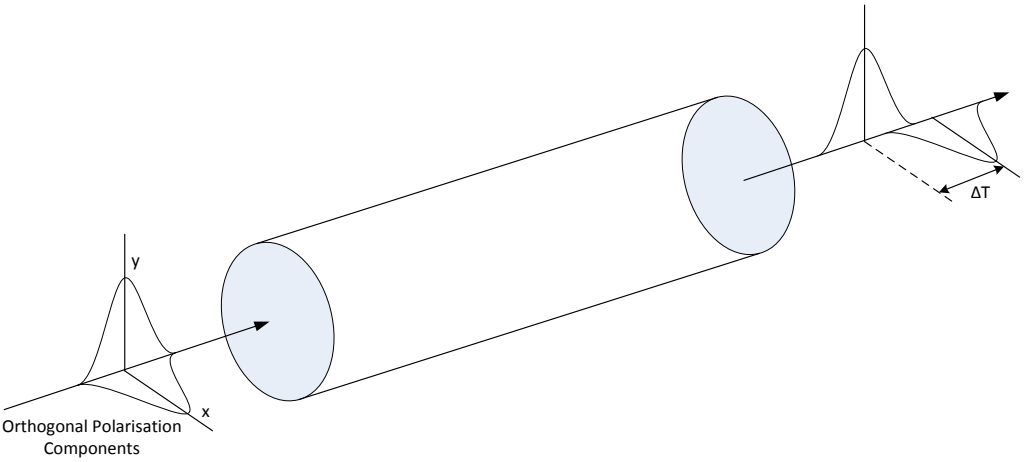

Figure 2- 11: Polarisation Mode Dispersion

2.7 Fibre Nonlinearities

Any dielectric medium shows a nonlinear response to a light with high intensity. Similarly, fibre optic behaves nonlinearly when an optical frequency with high electromagnetic field intensity passes through it. Although silica is not a highly nonlinear material, it is quite important to consider the nonlinear effects of fibre in the design of fibre-optic communication systems. In the following sections, we are going to examine the nonlinear effects that are most applicable in fibre-optic transmission systems.

2.7.1 Nonlinear Stimulated Brillian and Raman Scattering

Scattering losses in silica resulted from microscopic variations in silica density, composition fluctuation and from the imperfections happening during fibre manufacturing. There are two types of nonlinear scattering in optical fibre, namely Stimulated Brillian Scattering (SBS) and Stimulated Raman Scattering (SRS) [33].

These two nonlinear phenomena scatter the photon to a lower energy photon, and so the energy difference appears in the form of phonon. Raman scattering resulted in optical

phonons, while Brillian scattering contributed to acoustic phonons. The major effect of SBS is that the frequency of the scattered light is shifted downward by 10 GHz, whereas by 13 THz for SRS. At low power levels, loss due to nonlinear scattering is negligible as scattering cross section is adequately small. However, their effects become more significant when the power level exceeded the threshold value [34]. There are some differences between the impacts caused by SRS on a wavelength transmission over a single mode fibre relative to the ones caused by SBS. For instance, SRS occurs in both uplink/downlink directions, but SBS happens only in the uplink transmission. Moreover, the gain spectrum is less than 100 MHz at the SBS case, while it exceeds 20 – 30 THz in the case of SRS. Both SBS and SRS can beneficially be used in designing fibre optic communication systems. Recently, SBS effect has been used to generate an optical millimetre wave (mmWave) [35]. More importantly, SRS can be used to compensate for the fibre losses in modern light-wave systems due to its extremely high bandwidth [36].

2.7.2 Nonlinear Phase Modulation

Optical fibre shows a nonlinear response during the transmission of high-intensity light-waves. This nonlinearity is originally created in fibre as a result of enharmonic response electrons to the high-intensity optical field, which in turn results in a nonlinear susceptibility [37]. Therefore, it participates in producing harmonics to the optical spectrum, and hence resulting in bandwidth broadening. The nonlinearity of fibre can be characterised by means of its nonlinear parameter (γ), which is given as:

$$\gamma = \frac{2\pi\overline{n_2}}{\lambda_o c A_{eff}} \tag{2.24}$$

where c is the speed of light in vacuum, λ_o is the reference wavelength, $\overline{n_2}$ is the nonlinear index coefficient of the material and A_{eff} is the effective mode area of the fibre.

Not only the optical spectrum affected by nonlinearity in fibre but also the phase of each spectral component. As a result, new frequency components are produced due to this phase change, which gives an additional broadening to the optical spectrum. This phase-change

affects the long-haul optical transmission as it leads to the phenomenon of Self-Phase Modulation (SPM) and Cross-Phase Modulation (XPM) [18].

2.7.2.1 Self-Phase Modulation (SPM)

Phase modulation is a nonlinear phenomenon widens the spectral bandwidth of the optical signal along the fibre length. The term (γ) in equation (2.24) produces a nonlinear phase shift (φ_{NL}) which can be represented as [38]:

$$\emptyset_{NL}(t) = \gamma P_{in}(t) L_{eff} \qquad (2.25)$$

where L_{eff} is the effective fibre length and P_{in} is the optical input power. Practically, P_{in} is a time-variant parameter, and accordingly, $\emptyset_{NL}$ varies with time as well. Therefore, the optical phase of the optical signal changes in the same way as the optical spectrum, so it causes a frequency chirp that is spreading the optical bandwidth. As this phenomenon is self-induced, it is called self-phase modulation. Frequency chirp induced by the SPM results in additional pulse broadening through the fibre length, consequently, it limits the performance of the light-wave transmission system.

2.7.2.2 Cross-Phase Modulation (XPM)

The XPM is another nonlinear phase shift phenomenon occurs upon the transmission of a multichannel over fibre using Wavelength Division Multiplexing (WDM) techniques. In such systems, the nonlinear phase shift for a particular channel depends on the power of the channel itself as well as on the power of the adjacent channels [39]. Therefore, it can be written as:

$$\emptyset_{jNL} = \gamma L_{eff}\left(P_j + 2\sum_{m\neq j} P_m\right) \quad (2.26)$$

According to equation (2.26), the factor 2 indicates that the XPM is twice as harmful as SPM. The nonlinear phase shift also depends on the bit pattern of the adjacent channels, in which, two pulses at different group velocities and bit rate walk over each other, resulting in an induced phase shift. It is difficult to estimate the impact of XPM on the performance of the WDM systems [40]. However, it can be mitigated by carefully selecting bit rates of neighbouring WDM optical channels.

Since the nonlinear parameter γ depends inversely on the effective core area, the impact of fibre nonlinear phase modulation can be reduced considerably by enlarging the effective core area of the fibre core. In the design of light-wave systems, a power margin of approximately 0.5 dB is reserved to count for the power penalty caused by each of SPM and XPM.

2.7.2.3 Four-Wave Mixing (FWM)

If three optical frequencies ω_1, ω_2, and ω_3 propagate simultaneously along the fibre, they would interact with through the third order nonlinear susceptibility of the optical fibre, producing a fourth optical frequency (ω_4). This effect is called the four-wave mixing (FWM) [20]. In practice, ω_4 is related to the other frequencies as ($\omega_4 = \omega_1 + \omega_2 - \omega_3$) for modern multichannel communication systems. This is because wavelengths lie close to the zero dispersion wavelength become approximately phase matched.

FWM severely affects WDM systems by decreasing channel spacing of wavelengths with high signal power levels. Chromatic dispersion and inter-channel crosstalk are also increased due to FWM effects, in particular for equally spaced WDM channels. Therefore, one of the most effective mechanisms that used for FWM mitigation is the design of uneven channel spacing WDM systems. On the other hand, FWM can effectively be used in de-multiplexing channels transmitted using time division multiplexing (TDM)

techniques. It can be used as well in dispersion compensation and also can be used in wavelength conversion [41].

2.8 Dispersion Management Schemes

The major limiting factors in the design of optical communication networks are dispersion and nonlinear effects rather than fibre losses, especially after the advent of optical amplifiers. As described in section 2.6, chromatic dispersion is the main reason for bandwidth broadening of optical signals along the fibre length. Therefore, optical signal waveform deformation due to chromatic dispersion must be corrected. This can be achieved by compensating for the chromatic dispersion induced by fibre. This is referred to as dispersion compensation. Low bit rate network can operate without dispersion compensation. However, at high bit rate transmission over long-haul optical fibre, dispersion management is needed during the design of the transmission system. Various Dispersion Compensation Modules (DCMs) have been developed to address the dispersion problem [27], [42]. Fibre-based dispersion compensators are the most applicable, powerful and cost-effective technique utilised for the dispersion compensation. Conventionally, the main technique of DCM that is used widely in WDM and OTDM systems is accomplished using Dispersion Compensation Fibre (DCF) [43]. There is an alternative solution to control the chromatic dispersion and to expand the transmission distance. It is based on the use of Fibre Bragg Grating (FBG), which is the Chirped FBG (CFBG). In the following sections, we review will these techniques in details.

2.8.1 Dispersion Compensation Fibre (DCF)

DCF is a single mode fibre designed to produce a relatively negative waveguide dispersion value that may reach up to -80 ps/nm/km or even more. The chromatic dispersion induced in a Standard Single Mode Fibre (SSMF) is cancelled by inserting a DCF with a sufficient length to equalise the dispersion of that SSMF as shown in figure 2-12 below:

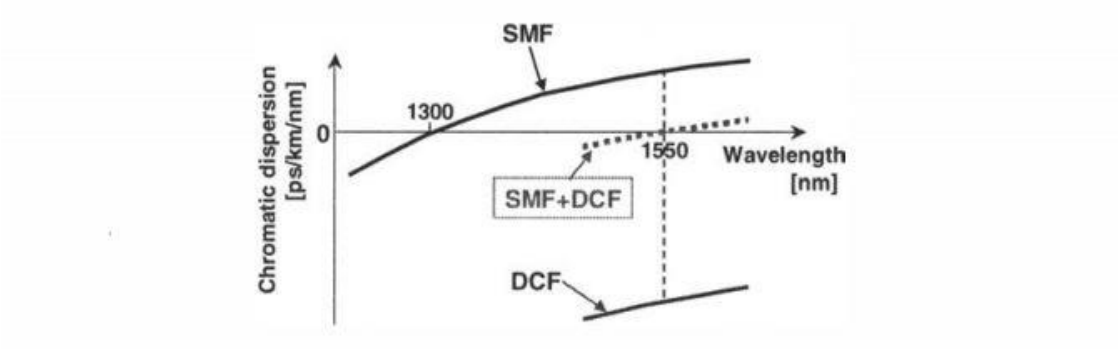

Figure 2- 12: Chromatic Dispersion Compensation using DCF[29]

The role of the DCF has become more and more important as both the bit rate and the transmission distance are dramatically increased. DCF is more advantageous and preferable than other DCMs as it can use to compensate for several WDM channels simultaneously because the residual dispersion after compensation becomes small enough within a certain wavelength band, not only at a single wavelength. Different types of DCF modules have been developed to cover most of the wavelength bands, such as C-band (1530-1565 nm), L-band (1565-1625nm) and S-band (1460-1530 nm), while it is less effective for wavelengths in the range of E-band (1360-1460nm) [44]. However, adding a DCF to the transmission network will increase the total attenuation. This can be addressed by using optical amplifiers and/or increasing the input optical signal power.

2.8.2 Chirped Fibre Bragg Grating (CFBG)

A Fibre Bragg Grating (FBG) is a Bragg reflector that can be used in optical communication networks as an optical filter to prevent a specific wavelength from passing through the fibre or as a reflector for a certain wavelength. Most importantly, it has been suggested to be utilised as a dispersion compensator [45]. Generally, Chirped FBG (CFBG) can be used as a DCM for a single channel transmission and for WDM systems as well. It has been widely employed in optical communication systems for its small size, low

cost and dispersion tenability. The chirp mechanism can take different forms over the length of the grating. The refractive index of the grating section is modified in a way that the reflected wavelengths will have the same speed as the output of the CFBG. As a result, the GVD effect experienced by the light components during the fibre transmission will be balanced, resulting in a reduction of the pulse broadening caused by dispersion [46]. The minimum grating length of the CFBG can be obtained as follows:

$$L_{min} = \frac{1}{2}\left(\frac{c}{n_{eff}}\right)\Delta\lambda.D.L \tag{2.27}$$

where $\Delta\lambda$ is the compensating bandwidth, D is the total dispersion, L is the whole fibre length and n_{eff} is the effective index of the guided mode.

2.9 Radio over Fibre Technology

Information to be transmitted through any communication system is represented as an electrical signal that may take either analogue or digital format. Radio frequencies can be used as a carrier signal to transmit this information to the mobile users through wireless networks as it offers mobility. However, wireless networks cannot provide sufficient bandwidth required to cope with the increasing demands of high data rate applications. On the other hand, optical network possesses a huge bandwidth, but it does not support roaming connections. The seamless integration of wireless and optical networks has enabled the transmission of high bandwidth services to both mobile users and fixed terminals (broadband services) [47]. This was firstly accomplished in the middle of 1990s by modulating the RF signal over an optical carrier and transmitting the modulated signal over fibre using a technology known as Radio-over-Fibre (RoF) technology [48]. RoF communication system can be designed to analogue and digital signals depending on the format of the RF signal transported over the fibre [49]. Two different scenarios of RoF communication systems, namely Analogue RoF (ARoF) and Digital RoF (DRoF) are

described in this thesis. In the following sections, the main two methods of transmitting and multiplexing the RF signals are discussed in details.

2.9.1 Intensity Modulation and Direct Detection in RoF

It can be considered as the simplest method of transporting RF signals over optical fibre. It entails the variation of the optical carrier intensity in a proportional way to the intensity variation of the modulating RF signal and then directly detect the transmitted RoF signal using a PD at the receiver side [49], [50] There are two ways of implementing the intensity modulation (IM): direct modulation and external modulation as shown in figure 2-13. Indirect modulation, The RF signal is used to directly modulate the LD's current, whereas the external modulation involves using a CW light source and an external modulator, such as MZM, to modulate the intensity of the CW in accordance to the RF signal intensity variation. In both cases, the RF signal must be superimposed with a DC biasing voltage and also must previously be modulated with the data need to be transmitted using a sufficient modulation scheme (analogue or digital).

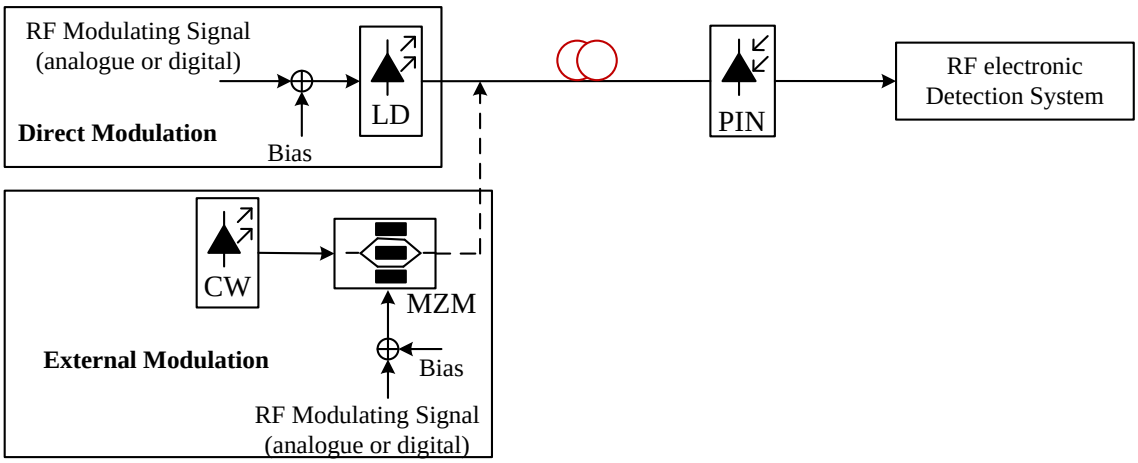

Figure 2- 13: Intensity Modulation and Direct Detection Schematic Diagram Showing Both Direct Modulation (Upper Branch) and Eternal Modulation (Lower Branch)

It can be seen from figure 2-13 that direct method is simple and cost-effective as well. However, it is inefficient for the transmission of high RF signals (greater than 10 GHz). On the other hand, external intensity modulation may provide further advantages relative to the direct method. For instance, external modulators can be used to modulate high-frequency signals, such as millimetre wave (mm-wave) signals, but at the expense of utilising costly drive amplifiers. In addition, some external modulators, such as DD-MZM, can be structured to perform a Single Sideband (SSB) modulation, which in turn reduces the dispersion effect on RoF transmitted signals (as it will be explained later in chapter 5).
Most RoF communication systems use IM-DD technique for the transmission of both single and multi-level modulating RF signals, such as mQAM signal, which can then be detected using an electrical detection system after the PD.

2.9.2 RoF Multiplexing Techniques

2.9.2.1 Subcarrier Multiplexing (SCM)

In this technique, multiple RF signals are multiplexed in the electrical domain by superimposing them electronically. Then, the resultant signal is used to modulate the intensity of the optical carrier at the transmitter side [51], [52]. It is, therefore, the most cost-effective RF multiplexing approach used to exploit the optical network's available bandwidth as it only utilises one optical source. In SCM, the modulation of the optical carrier signal can be achieved either by an external modulator or by directly modulating the laser source [51]. Each RF signal may use a different modulation scheme. Figure 2-14 shows the schematic diagram of the SCM technique, where each subcarrier (f_{sc}) can be modulated with different information signal (analogue or digital). However, the main disadvantage of the SCM approach is that it is susceptible to the fibre nonlinear effects. Here, the RIN is the main source of noise [51].

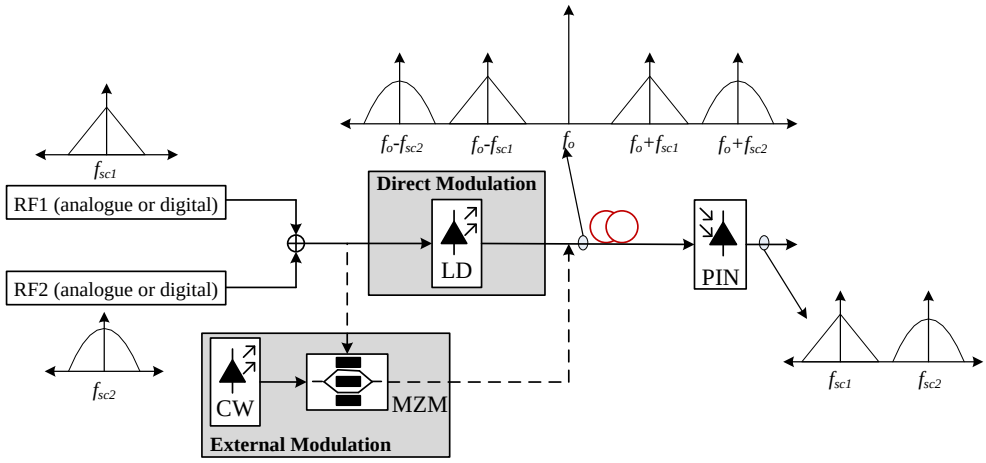

Figure 2- 14: Sub-Carrier Multiplexing Technique of Two RF Signals

2.9.2.2 Wavelength Division Multiplexing (WDM)

Multiplexing RF signals using WDM technique has recently gained a considerable attention since it provides better exploitation of the optical fibre bandwidth as well as, it addresses the laser RIN noise [53], [54]. In WDM, each RF signal is modulated separately over a single optical carrier, and the resultant signals are multiplexed in the optical domain as shown in figure 2-15.

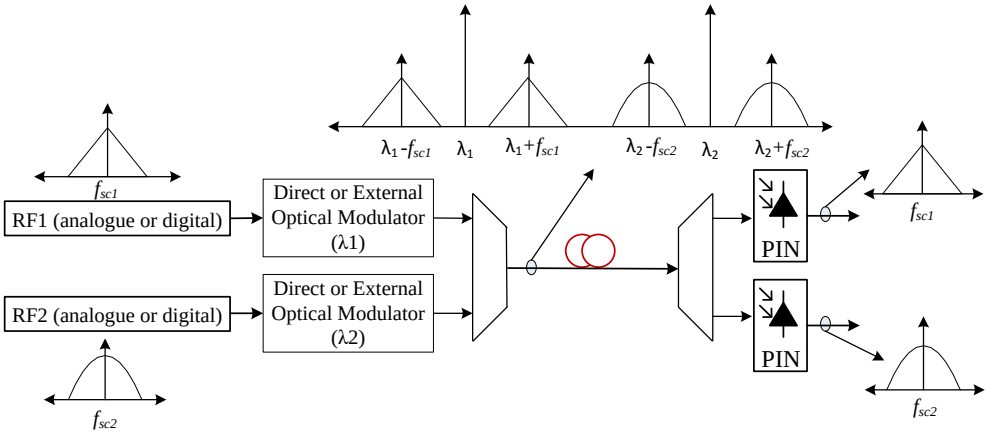

Figure 2- 15: Wavelength Division Multiplexing

Another significant advantage of employing WDM in RoF transmission networks is that it can allocate a specified wavelength to each Base Station (BS), enabling a simple network management [55]. As a result, transporting mm-Wave using WDM topology has increasingly been studied [56]–[58]. Apart from the cost constraints of using separate laser source to each RF signal, WDM networks might be involved in the XPM effect, which was explained in section (2.7.2.2). Recently, optical communication networks that combine both multiplexing techniques explained earlier are presented in [59], [60] to exploit the advantages of these two techniques. However, mm-Wave transmission spectral width might exceed the WDM channel spacing. Dense WDM (DWDM) technique is proposed to increase the number of the available wavelengths for further BS deployment in RoF networks [58]. Moreover, it is required in bidirectional optical transmission networks to have a singular wavelength for each BS, which can be recovered and used for upstream transmission [61], [62]. In chapter 3, an optical carrier reuse scheme is proposed in a designed bidirectional DWDM-RoF system.

2.10 Analogue Radio over Fibre (ARoF)

In an ARoF transmission system, the information signal transmitted over fibre in the analogue format. The RF carrier signal is first modulated by the baseband downstream data signal using a particular modulation, such as mQAM. The produced RF signal is then used to modulate an optical carrier signal at the Central Station (CS) side. A bi-directional ARoF transmission system structure is exhibited in figure 2-16. In which, the EO conversion is performed at the transmitter side by using either a direct or external optical modulation scheme depending on the value of the modulating RF signal. The optical modulator produces a DSB-ARoF signal, which is then transmitted to the BS, where the antenna installed, over an SMF to achieve a long reach transmission system. At the receiver side, the OE conversion is accomplished using a PD, such as a PIN to recover the transmitted RF signal. The demodulated RF signal is then passed through a Band Pass

Filter (BPF) to filter out the unwanted frequency components resulted from the photo-detection process. The filtered RF signal is then power amplified so that to be transmitted to the Mobile Subscribers (MSs) through the antenna.

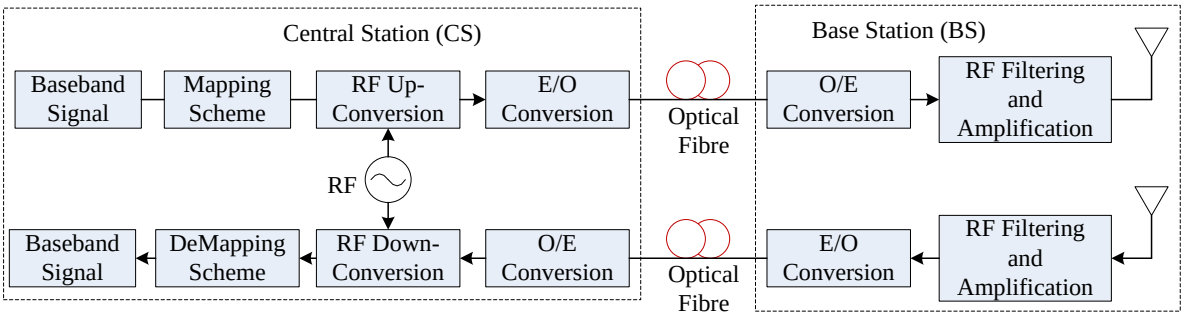

Figure 2- 16: General Architecture of Bidirectional ARoF System

In the upstream direction, the antenna at the BS can be used to receive the incoming signals from the MSs and send them to the amplifier before being optically up-converted using a specified EO conversion scheme. The resultant upstream optical signal is transmitted back to the CS over the same SMF or different one. At the CS, the received optical signal is demodulated using PD to obtain the RF signal that was transmitted by the BS.

2.10.1 Analogue RoF Impairments

Optical signal exposes some impairment while travelling through the optical communication system due to the nonlinearity of optical components and the transmission medium as well. These impairments cause degradation in the performance of the ARoF transmission system. In another word, it distorts the received RF signal. The major source of these impairments is the nonlinear characteristics of the optical modulators. In the case of transmitting high RF signal with high spectral bandwidth, an external modulator is required as mentioned in section (2.9.1). Due to the external modulator's nonlinearities, extra out-of-band spectral components are generated causing an Inter-Modulation

Distortion (IMD) components received at the receiver [63]. A large number of spurious IMD components appear on both sides of the original ARoF signal spectrum. However, some of these components can easily be filtered out using a BPF, but some others are closely located to the desired frequency components and hence, they cannot be filtered out. These non-removable IMD components have a significant impact on ARoF system performance as their power might be greater than the noise power [63].

Further to the IMD components effect, ARoF signal transmission is susceptible to some minor impairment during the EO conversion process as follows:

- The residual chirp. It causes distortion to ARoF signal as it travels through a dispersive optical fibre since it converts the phase modulation to amplitude variation with the aid of the dispersion effect.
- Residual phase modulation. It resulted from the difference in the modulation efficiency of the two branches of the external modulator, such as MZM, [64]. Due to the effect of the dispersion, residual phase modulation causes an intensity modulation [65], [66].

These impairments have clearly shown the impact of the chromatic dispersion on ARoF communication systems. Additionally, ARoF transmission system as any other analogue system is subjected to nonlinearities induced by the transmission medium. In analogue optical systems, nonlinearities induced by fibre limits the signal's dynamic range [67].

2.11 Digitised Radio-over-Fibre (DRoF) Technology

In this technology, The RF signal is transformed into a digital format at the CS side to be transmitted over the optical fibre [68]. DRoF technology has been proposed as an alternative to ARoF as it is more flexible, reliable and resistant to nonlinear effects imposed by the optical components and transmission channel [69]. Unlike ARoF technology, DRoF assumes the digitisation of the RF signal before being transmitted optically to the BS. Digitisation process is performed at the CS using an Analogue-to-

Digital Converter (ADC). The digitised RF signal is modulated using either a direct or external optical modulator and the produced optical signal is then transmitted over the fibre. At the BS side, the optical signal is demodulated using a PD, and the detected digital signal is retrieved to the analogue format again using a Digital-to-Analogue Converter (DAC). The obtained analogue RF signal is then filtered, power amplified and transmitted to the end users through the antenna. Figure 2-17 shows the basic structure of a DRoF transmission system. The same process is repeated for the upstream transmission of a digitised RF signal as presented in figure 2-17.

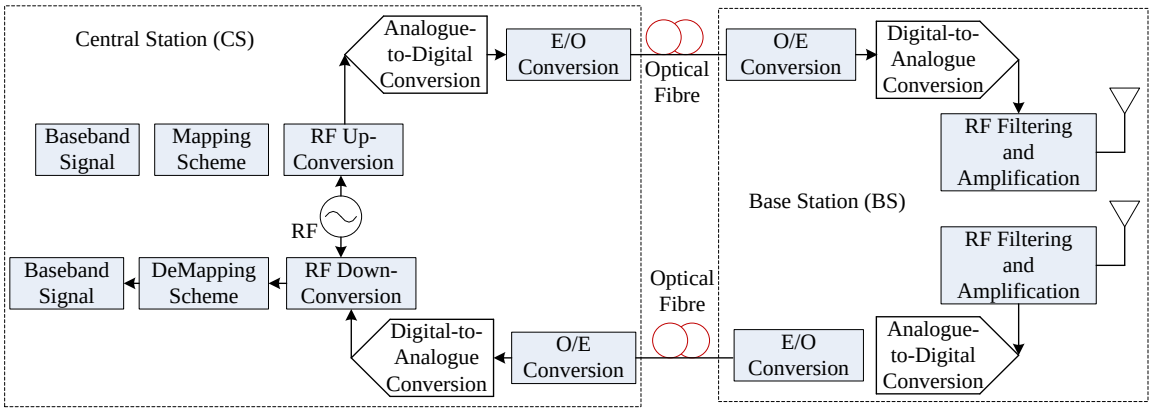

Figure 2- 17: General Architecture of Bidirectional DRoF System

Many factors have motivated the preference of this technology against ARoF. As mentioned in section (2.10.1), the received ARoF signal at the RAU might be distorted due to the nonlinearities of the optical fibre and some of the optical components. Not to mention the IMD noises occurrence especially when SCM is applied. On the other hand, DRoF technology has addressed these transmission impairments according to the state of the technology [70], [71]. Furthermore, DRoF system can preserve the dynamic range of the transmitted signals along the transmission distance regardless to the accumulated attenuation values with the increased fibre length until the received optical power goes below the sensitivity limits of the optical receiver [72]. For this regard, two industrial approaches, namely Open Base Station Architecture Initiative (OBSAI) [9] and Common Public Radio Interface (CPRI) [8], have been proposed to achieve the DRoF interconnection rules between the CS and multiple RAUs.

However, RF signal's digitisation produces a high bit rate baseband signal, which requires high optical channel bandwidth, and hence, impairments induced by the fibre, such as the chromatic dispersion, become more severe [73]. Moreover, for a highly performance DRoF system, ADC/DAC devices with a high sampling frequency (high speed) and resolution are required [71]. Such an operation should be too costly and/or not quite feasible because of the constraint forced by Nyquist theorem, which states that the sampling frequency required for an analogue signal must be at least two times greater than the highest frequency component contained in that analogue signal [74]. For example, to digitise a WiMAX 802.16a RF signal of 2.475 GHz, an ADC with at least 5 GHz sampling frequency is required. Such a digital circuitry is not available, and if so, it would not be at reasonable prices. Therefore, ADC/DAC quantisation and jitter noises are very critical issues in DRoF link implementation since they represent the major source of impairment in such technology.

2.12 Transmission of a Digital Optical Signal

The first step in the optical transmission of digital signals over fibre is to convert the digital data into a digital electrical waveform called a baseband signal using a process known as coding [74]. In another word, digital data is encoded at the transmitter side to obtain the baseband digital signal and then recreated at the receiver side by decoding the received digital signal. Therefore, the digital optical transmission is simply a frequency up-shifted version of that baseband signal. Two coding schemes are used for the digital-to-digital conversion process referred to as line coding and differential coding schemes. In the following sections, we are going to go through the details of these coding schemes.

2.12.1 Line Coding

It is a digital-to-digital conversion process, in which, the digital sequence is represented by a pulse waveform or a baseband signal [75]. There is two major line coding categories that

developed for the digital transmission, namely Non-Return-to-Zero (NRZ) and Return-to-Zero (RZ), where the waveform returns to zero level for a portion of the bit's time interval. NRZ and RZ can be furtherly subdivided into the following modes based on the rules by which the voltage levels are assigned to represent each binary digit:

1- Unipolar Signalling: Digit 1 is represented by a high voltage level (+V), whereas digit 0 by a zero level. It is also known as On-Off Keying (OOK).
2- Polar Signalling: Digit 0 is represented here by a negative voltage level (-V).
3- Bipolar Signalling: It is also called "Pseudoternary" or Alternative Mark Inversion (AMI) signalling. In which, digit 1 is represented alternately positive or negative voltage level, while digit 0 is always represented by level zero.

Figure 2-18 shows the waveforms of the basic line coding schemes. These coding schemes are different in their performances, which will lead to different features to the applications that they used with. The following are some of the features that may offer by line codes:

- Time synchronization: This requires that the line coding scheme must provide a sufficient transition time to recover the received data sequence correctly. A long bit stream should not cause any unsynchronized time recovery.
- Bandwidth: This should be selected so that to provide as narrow bandwidth as possible for the resultant baseband digital signal. Transmission bandwidth can be reduced either by filtering or by employing a multilevel signalling. The penalty for transmitting higher bandwidth is an increase in ISI and degradation in SNR.
- The available channel spectrum: Sometimes, the assigned channel bandwidth is so small. Therefore, line coding scheme must be selected to provide a sufficiently small signal bandwidth to prevent ISI, as it will be discussed later in chapter 4.
- Low bit error probability: Line code with low bit error probability that is caused by noise and/or ISI is preferable, while another characteristic, such as bandwidth and synchronization should be put into the consideration.
- Error detection: The selected scheme should be capable of detecting errors at the received data sequence. This can be used to evaluate the performance of the transmission system by measuring the received Bit Error Rate (BER).

- Transparency: Line coding scheme must be able to encode and/or decode and kind of data sequence regardless of the transmitter and/or receiver used, respectively.

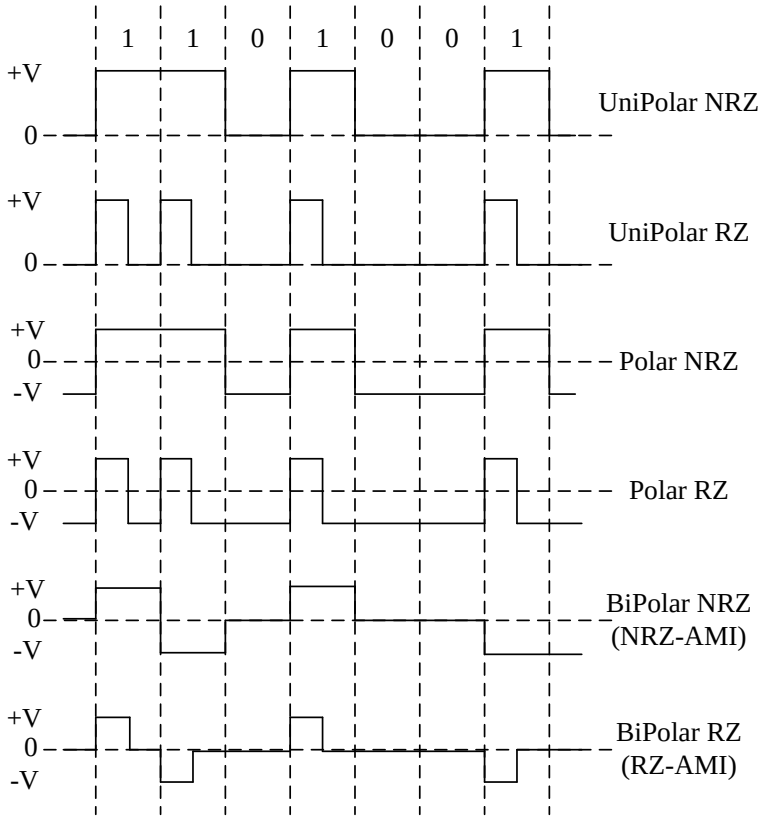

Figure 2- 18: Waveforms Representation of Various Line Coding Schemes

2.12.2 Differential Coding

It is another kind of coding that is used to obtain a baseband signal before being modulated onto a carrier. The differentially encoded data are given according to the rule [76]:

$$e_n = d_n \oplus e_{n-1} \tag{2.28}$$

where d_n is the original digital data sequence, e_n is the differential encoder output and $\oplus$ denotes the modulo-2 or exclusive OR (EOR) operation. This means that the encoder output compares the present and previous encoded outputs. The encoder gives digit 1 output only when the present and past encoded bits are of different states, whilst a binary

output of 0 is encoded if they have the same state. This is why this encoding scheme is called differential encoding. An example of a differentially encoded data sequence is shown in the figure 2-19, where a reference digit denoted by e_o is needed.
At the receiver, the encoded signal is decoded using the following rule:

$$\tilde{d}_n = \tilde{e}_n \oplus \tilde{e}_{n-1} \tag{2.29}$$

where the tilde sign is an indication for the received data. Figure 2-19 shows the block diagram of both differential encoder and decoder defined by (2.28) and (2.29), respectively.

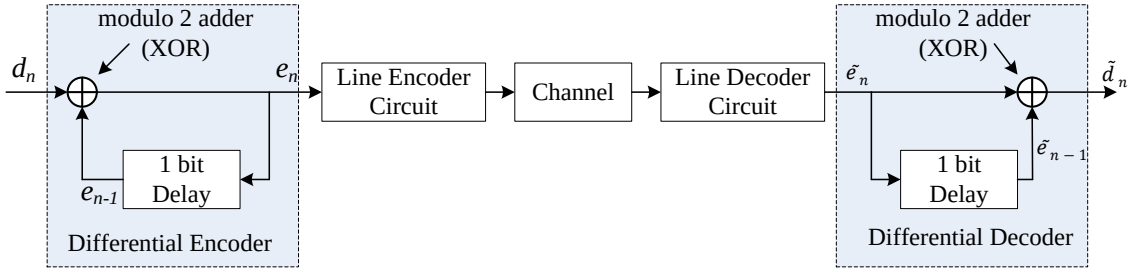

Figure 2- 19: Differential Coding System

The polarity of the received data might be reversed at the receiver due to the noise of the transmission channel. In this case, the whole sequence will be reversed as shown in figure 2-20. It can be seen from figure 2-20 that one of the most important benefits of employing the differential encoding is that it eliminates the polarity reversal effect on the received data because of the decoder output remains the same as the difference between any adjacent bit stays the same. The other benefits of using the differential encoding will become clearer when we will discuss its utilisation in Duobinary signal generation later in chapter 4.

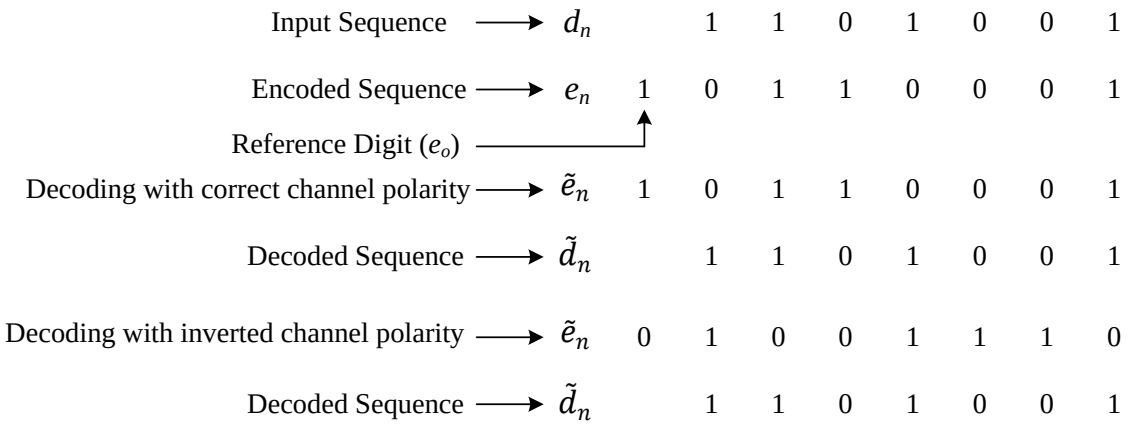

Figure 2- 20: Example of Differentially Encoded Data Sequence

2.13 Bandwidth-Efficient Modulation Formats for Digital Optical-Fibre Communication Systems

The growing demands of higher capacities and longer reach optical networks have dramatically increased the need for wavelength multiplexing networks, such as DWDM. However, increasing the number of wavelengths results in a decrease of the channel spacing and increases the impact of the dispersion and fibre nonlinearities. A promising technology that can improve the system's performance in terms of reducing the dispersion effect and/or nonlinear impairments while providing higher spectral efficiency is the use of bandwidth-efficient transmission format [77]. If the transmission format is adapted, so that, it produces a narrower spectrum than the commonly used formats, a reduction in the dispersion and nonlinear effects will result, and consequently, the necessity for dispersion compensation is omitted at all or even less compensation is required.

The theme of this section is to explore and review the digital transmission formats that would permit increasing the spectral efficiency, dispersion immunity and fibre nonlinearities. We will emphasise transmission formats that have spectral occupancy less than the traditionally used ones, such as NRZ. It will be shown that some formats are more

immune to dispersion effects than others, however, considerations to some other impairments need a closer attention. Various transmission formats have been proposed for this subject [78], [79]. This thesis has concentrated only on those that have potential applications to digital optical communication systems, in particular, Duobinary signalling, which is a type of partial response coding schemes, and also on the Optical Single Sideband (OSSB) modulation.

2.14 Duobinary Encoding

Duobinary is a bandwidth efficient coding scheme, in which the binary digital signal is encoded into a three-level baseband signal using a particular precoding technique [77]. The performance of high data rate optical communication systems is primarily dispersion limited. Duobinary signalling can be considered as an effective way to reduce the influence of chromatic dispersion in the optical fibre. It reduces the bandwidth requirement for transmitting a data rate of *R* bit/s to less than *R/2* Hz of the transmission bandwidth. It has been proven in[80]–[82] that ISI can be mitigated by using one of the partial response signalling techniques, such as the duobinary signalling, by introducing a deterministic amount of ISI into the transmitted signal so that it can be counteracted upon detection at the receiver. This, in fact, constitutes another advantage of using this encoding scheme in addition to the reduced bandwidth. In order to understand why this makes sense, one must understand how duobinary data is generated. The coding rule for the duobinary signal is given by [83]:

$$c_k = b_k + b_{k-1} \tag{2.30}$$

where b_k is the k^{th} element of the binary sequence. Meaning that the duobinary encoder output c_k correlates present binary input bits and the previous input bits (i.e. there are three output levels {-1 0 1} depending on b_k and b_{k-1}). An important property of the three-level sequence is that the combinations {1 0 1} as well as {-1 0 -1} can never occur at the output

of the encoder; only {-1 0 1} and {1 0 -1} can occur as shown in figure 2-21. This sequence is another reason why duobinary encoding is resilient to dispersion.

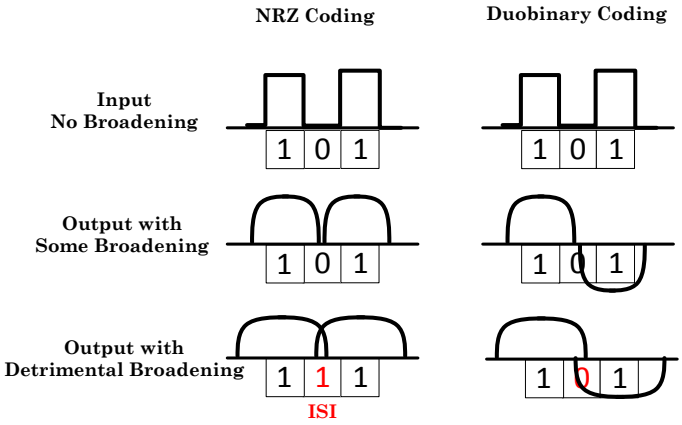

Figure 2- 21: Dispersion Effect on NRZ and the Duobinary Coding Schemes

The receiver can recover the transmitted data sequence b_k by the following rule:

$$b_k = c_k - b_{k-1} \tag{2.31}$$

This means that a single ISI error will propagate at the receiver due to the correlation between symbols. To overcome this, a precoding scheme is used before the duobinary encoder at the transmitter. The data bits are pre-coded or differentially encoded as follows:

$$c_k = b_k \oplus c_{k-1} \tag{2.32}$$

where $\oplus$ denotes the modulo-2 addition. Hence, the receiver samples the value:

$$c_k \oplus c_{k-1} = c_{k-1} \oplus b_k \oplus c_{k-1} = b_k \tag{2.33}$$

To implement the differential encoder, an exclusive OR (XOR) gate can be used, as shown in figure 2-22.

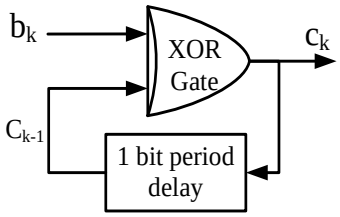

Figure 2- 22: Conventional Duobinary Pre-Coder

However, the implementation of the 1-bit delay feedback precoder does not support the transmission of high data rate beyond 10 Gb/s based on the simulation results. Figure 2-23 illustrates the functionality of the designed precoder measured at a bit sequence of 10 Gb/s.

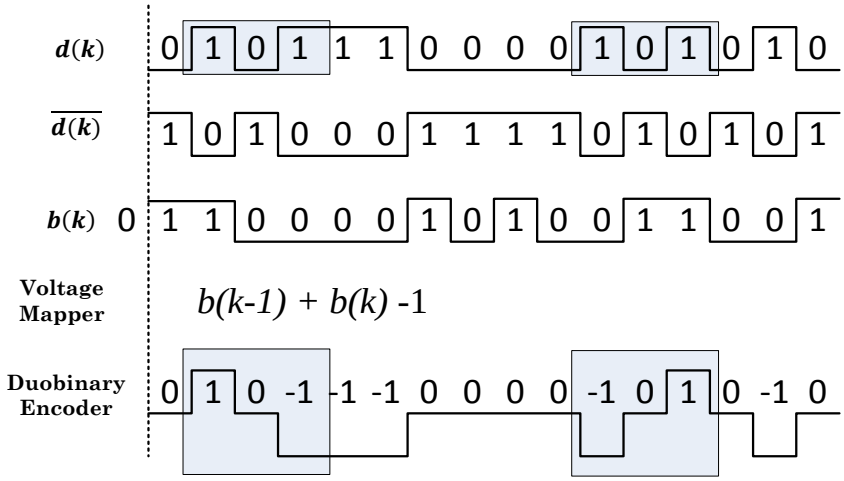

Figure 2- 23: Bit Sequences illustrate the operation of Duobinary Coding System

2.15 Chapter Conclusion

In this chapter, the basic components utilised in the design of the optical fibre telecommunication system have been discussed. These components are used in both analogue and digital optical transmission networks. The conclusion of this chapter can be summarised as follows:

1- Optical transmitters mostly composed of a CW laser diode which can be modulated either directly or externally using an optical modulator with the information data signal in order to be transmitted over optical fibre.
2- The optical fibre, which is mainly manufactured from Silica, induces some impairment, such as dispersion, attenuation and nonlinearity over the transmitted signals.
3- Optical-to-Electrical (OE) conversion process takes place at the receiver side. The detection is generally established using a photodiode, such as PIN or APD.
4- Optical amplifiers are used to compensate for the attenuation caused by fibre, while the dispersion is compensated using different techniques, such as DCF and CFBG.
5- Optical transmission capacity can be increased by multiplexing wavelengths using WDM or DWDM technologies. To ensure the cost-effectiveness, wavelength re-use schemes are proposed.
6- The RF signal can generally be transmitted over fibre via RoF technology using either an external or direct intensity modulation or direct detection techniques.
7- The RF signal can be multiplexed either in the electrical domain using SCM or optically using WDM.
8- There are two types of RoF communication systems divided on the basis of the transmitted RF signal format, they are ARoF and DRoF.
9- The ARoF system exhibits impairment upon the transmitted RF signal caused by IMD, optical components nonlinearities, reduced dynamic range and impairment induced by fibre.
10- The key components in DRoF systems are ADC and DAC, and hence, DRoF system performance is limited by their sampling frequency and resolution.
11- The high optical bandwidth produced in DRoF is reduced using bandwidth-efficient modulation formats, such as OSSB and multilevel modulation schemes like Duobinary.

Chapter 3

A Bidirectional DWDM Analogue-RoF Transmission

3.1 Overview

Optical wireless access technology has been considered as the most effective solution to meet the increased bandwidth demands and to extend the transmission reach at a relatively low power budget. The integration of the wavelength division multiplexing (WDM) technique in RoF technology can provide a much higher data rate transmission over longer distances [84].

In this chapter, a bidirectional Dense Wavelength Division Multiplexing Radio-over Fibre (DWDM-RoF) transmission link has been designed. In this system, four carrier signals each of 5 GHz have been modulated using different combinations of Quadrature Amplitude Modulation (M-QAM) schemes with a 2.5 Gb/s data rate per channel and transmitted over a Standard Single Mode Fibre (SSMF) to the Base Station (BS). For the upstream transmission, a very simple and cost-effective technique based on employing an Optical Band Pass Filter (OBPF) at the BS side to filter out the transmitted wavelength and reuse it for the upstream transmission of a 2.5 Gb/s On-Off Keying baseband signal, after being externally modulated, over fibre to the Central Station (CS). The dispersion effect has been investigated and counteracted by employing a Dispersion Compensation Fiber (DCF). Simulation results showed an approximately negligible power penalty between Back to Back (B2B) and after 120 km transmission distance. System Performance has been evaluated by measuring Error Vector Magnitude (EVM) and constellation diagram with respect to the fibre distance. Finally, the upstream signal performance has been

evaluated by measuring its Bit Error Rate (BER) and eye diagram at the CS side. As a result, error-free transmissions of 10 Gb/s for both upstream and downstream signals over 30 km and up to 120 km (SMF-DCF) are demonstrated to verify the suitability of the proposed link in A-RoF technology.

3.2 Introduction

The architecture of the next generation Radio Access Network (RAN) has to manipulate the growing demands of high bit-rate and bandwidth requested by the end users. Radio over Fibre (RoF) technology can be considered as a promising solution for the increased capacity and mobility in RAN since it introduces a good data transmission rate and large bandwidth [5]. In RoF system, Radio Frequency (RF) signals are modulated by light either directly or at intermediate frequency and then transmitted over an optical fibre to raise transmission as well as wireless access. It transmits RF Downlink/Uplink (DL/UL) signals between a Central Station (CS) and Base Stations (BSs), where the RF signal is transmitted wirelessly to different users. Therefore, RoF system should have many BSs connected to the CS.

It has been mentioned in section (2.9.2.2) that the WDM technique has been proposed to enlarge the optical bandwidth utilization of the RoF link connecting the CS to the corresponding BSs. Such WDM-RoF architecture could be capable of reducing antenna site complexity, dynamically assigning RF signals to different antenna sites, reducing power consumption and it will be easy in its installation and maintenance [85], [86]. In the same context and to achieve better bandwidth exploitation, DWDM technique has been proposed to increase the number of the available wavelengths in order to expand BSs deployment within RoF network [84]. Bidirectional WDM-RoF systems require expensive optical source assigned to each of the DL/UL signals transmission so that it has not been largely deployed. For this reason, an access network architecture utilizing a central light source at the CS with data re-modulation using the DL wavelength received at the BS is an

effective solution for low-cost implementation of an upstream transmitter as it requires no wavelength management and needs no external light source [87].

In order to achieve high data rate as well as to optimize bandwidth utilization, RoF signals have been integrated with Dense WDM. DWDM is a multiplexing system with channel spacing less than or equal to 200 GHz [88]. Thus DWDM-RoF architecture can provide the most extensive and cost-effective way to expand the bandwidth of fibre-optic channels to support a huge number of distributed antenna stations. Quadrature Amplitude Modulation (QAM) has been chosen to be the modulation format for the proposed downstream RF signal. Recently, m-QAM RF signals have become the potential candidate for transmission in the next generation access network because of its high spectral-efficiency and its resilience to chromatic dispersion [89].

In this chapter, we propose and demonstrate the transmission of 4 RF channels over a DWDM-RoF bidirectional system. In this system, the downstream signals are resulted from modulating a data rate of 2.5 Gb/s per channel on a 5GHz RF carrier signal using 4-QAM, 16-QAM, 64-QAM and 256-QAM modulation schemes. The upstream signals are produced from OOK baseband signals each of 2.5 Gb/s externally modulated using an OAM modulator. In the proposed scheme, we have utilized, for the first time, an Optical Band Pass Filter (OBPF) with a Gaussian transfer function to filter out the downstream optical carrier and reuse it for the upstream transmission. Furthermore, we have successfully proposed an effective solution for the long-haul transmission of DL/UL signals over more than 100 Km long SMF by adding a Dispersion Compensation Fibre (DCF) to adaptively compensate the dispersion caused by SMF and to increase the transmission distance. Finally, the effect of dispersion power penalty on the performance of the transmitted wavelengths has been studied. The obtained results showed an error-free performance for different transmission distances, which makes our proposed structure as one of the potential candidates to the next generation access network.

3.3 Related Work

Many systems have been proposed for the sake of reusing the received downstream optical carrier for the upstream transmission:

1- A DPSK RF signals transmitted over fibre using a WDM based Passive Optical Network (PON) is demonstrated in [90]. The upstream transmission of a 2.5 Gb/s data rate is realized by directly modulating a Fabry-Perot (FP) laser placed at the Optical Network Unit (ONU) side.

2- A 16-QAM RF signal transmission over fibre to the Remote Antenna Unit (RAU) by phase modulating an optical frequency is presented in [91]. The upstream transmission is achieved by intensity modulating the upstream data with the received optical carrier.

3- A method of implementing an upstream transmission based on spectral slicing with wavelength seeded Semiconductor Optical Amplifier (SOA) modulators are described in [92]. An upstream data of 1.25 Gb/s transmitted over 25 km SSMF with relatively low dispersion penalty was achieved using WDM-PON system.

4- According to [93], a Vertical-Cavity Surface Emitting Laser (VCSEL) has been used at the ONU side and injected by an Amplified Spontaneous Emission (ASE) light to provide the light source needed for the upstream transmission.

5- Recently, cost-effective approaches to achieve upstream data transmission have been mentioned in [94] and [95] based on using a Reflective Semiconductor Optical Amplifier (RSOA) at the OUN side. The WDM-PON system based on RSOA doesn't require an optical amplifier, the transmission length between CS and BS can be extended and there will be no need for an external modulator because RSOA can perform the two functions of amplification and modulation. The research finding has shown that the modulation bandwidth of RSOA is limited to 2 GHz by carrier lifetime in the active layer, which consequently limits the value of upstream data-rate to less than 2.5 Gbps in these schemes.

3.4 System's Theory

Transmitting RF signals over fibre has created a revolution in telecommunication systems not only because of the huge bandwidth available but also because of its resiliency against electromagnetic interference. The basic optical transmitter contains a light source which is modulated by the electrical signal and transmitted through the fibre to the receiver. As mentioned in chapter 2, different wavelengths travel at different speed through fibre due to the chromatic dispersion. Consequently, optical pulses are broadened after travelling through a particular length of the fibre. As a result, these pulses will interfere with each other causing BER degradation at the received signal. It has been also explained in chapter 2 that the chromatic dispersion value is zero at a wavelength of 1310 nm, but the attenuation is relatively high at this wavelength due to the Rayleigh scattering phenomenon. Therefore the wavelength of 1550 nm is highly preferable in modern telecommunication optical systems, and so, it has been considered as the reference transmission wavelength in our designed system.

3.4.1 Chromatic Dispersion Management

The dispersion effect can be reduced by using a dispersion compensation fibre (DCF), which can be designed for different transmission lengths. DCF has negative dispersion characteristics with respect to the material dispersion in the SMF. Therefore, the chromatic dispersion can be equalized and set to zero by adding a DCF to the SMF link. The standard dispersion value at a wavelength of 1550 nm is 16 ps/nm.km.

Accordingly, a combination of DCF and SMF has been considered in our simulation design to minimize the dispersion caused by the SMF as low as possible. By inserting a DCF into the transmission link, the accumulated dispersion caused by the SMF is compensated. The Total dispersion and attenuation of the SMF-DCF combination are given by:

$$D_T = D_{SMF}.L_{SMF} + D_{DCF}.L_{DCF} \quad (3.1)$$

$$A_T = A_{SMF}.L_{SMF} + A_{DCF}.L_{DCF} \quad (3.2)$$

The main drawback of employing the DCF is the high attenuation values in this special kind of fibres, which is practically, around 0.4 dB/km at 1550 nm. Therefore, DCF length should be minimised. In our design, DCF parameters have been adaptively adjusted so that to maintain the total dispersion produced as low as possible, while an EDFA optical amplifier has been used to compensate for the added attenuation by the DCF.

3.4.2 M-QAM signals Transmission Based DWDM

As described in section (2.9.2.2), applying WDM in RoF systems enlarges its capacity and increases the number of the BSs supported by a significant CS. In the proposed system, DWDM technique has been adopted as it can achieve even more bandwidth utilisation and expand the transmission capacity.

M-QAM signals are preferable for multi-band WDM based RoF transmission of analogue signals because of their spectral efficiency and noise immunity [96]. The proposed modal provides a schematic test-bed to investigate the transmission of ARoF downstream signals with different QAM combinations (4, 16, 64 and 256) QAM. Each one of these QAM signals is frequency up-converted using a carrier frequency of a 5 GHz and then transmitted over fibre using a separate wavelength.

3.4.3 Wavelength Reuse and Uplink Transmission

Wavelength reuse refers to the ability to use the same wavelength of the downstream channel for the transmission of the uplink channel. It can also be used for the communication between multiple BSs deployed using ring topology within a singular CS, which increases the number of channels in the network [97].

Instead of having a separate light source at the BS side, wavelength reuse scheme would significantly reduce the cost and simplify BS structure. In the proposed system, a simplified structure based on employing a passive splitter followed by an optical BPF is considered to achieve the requirement of the fully duplexed transmission system.

3.5 The Proposed Bidirectional ARoF System's Architecture

The schematic diagram of the proposed bidirectional DWDM-ARoF system is shown in figure (3.1). This work has been designed, simulated and analysed using VPITransmission Maker^{TM} software packages V. 9.5 [17]. This software creates real-time simulation closer to most practical optical transmission systems.

In the downlink direction, a four RF signals, namely (4-QAM, 16-QAM, 64-QAM and 256-QAM), respectively were generated by separately modulating a carrier frequency of 5 GHz with a data rate of 2.5 Gb/s by using a different kind of QAM mapping as nominated earlier. These for QAM signal are used to modulate a series of four CW lasers of (192.5, 193.05, 193.15 and 193.25) THz, each with an average power of 5 mW and laser linewidth of 10 MHz, by using a conventional MZM to generate a DSB optical signal. The generated optical DSB signals are multiplexed using 4:1 DWDM multiplexer with channel spacing Δf =100 GHz, which translates into a $\Delta\lambda$ of 0.8 nm wavelength spacing, to achieve a total downlink rate of 10 Gb/s transmitted to the BSs side over a combination of an SMF-DCF transmission link. An Erbium Doped Fiber Amplifier (EDFA) with its standard gain value of 20 dB was used to compensate the added attenuation by the DCF at the end of the transmission link, so that to strengthen the transmitted QAM signals before being de-multiplexed to four channels by (1:4) DWDM de-multiplexer where various optical signals are sent to different BSs.

At the BS side, each optical signal is divided into two portions by using a passive splitter (PS). One portion is sent for detection to a PIN (with 0.9 A/W responsivity and 10 nA dark current) to perform the (O/E) conversion process. The produced electrical signal is then fed to the corresponding QAM receiver block, which is provided by the simulator to

observe the constellation diagram of the received QAM signal and to measure the SER and EVM with the received power for different transmission distances. The other portion of the PS is passed through an optical BPF of a 5 GHz bandwidth and Gaussian transfer function with filter order of 5 to completely remove the sidebands and filter out the optical carrier to be reused for the upstream transmission.

In the uplink direction, a 2.5 Gb/s OOK baseband signal is externally modulated with the filtered optical carrier using an optical amplitude modulator (OAM) to produce the optical upstream signal. The upstream signals from each BS are multiplexed and then transmitted over the same SMF-DCF transmission link to the CS. The received upstream signal at the CS side is detected using a PIN detector and fed into error detection circuit to estimate the BER and to observe the eye diagram.

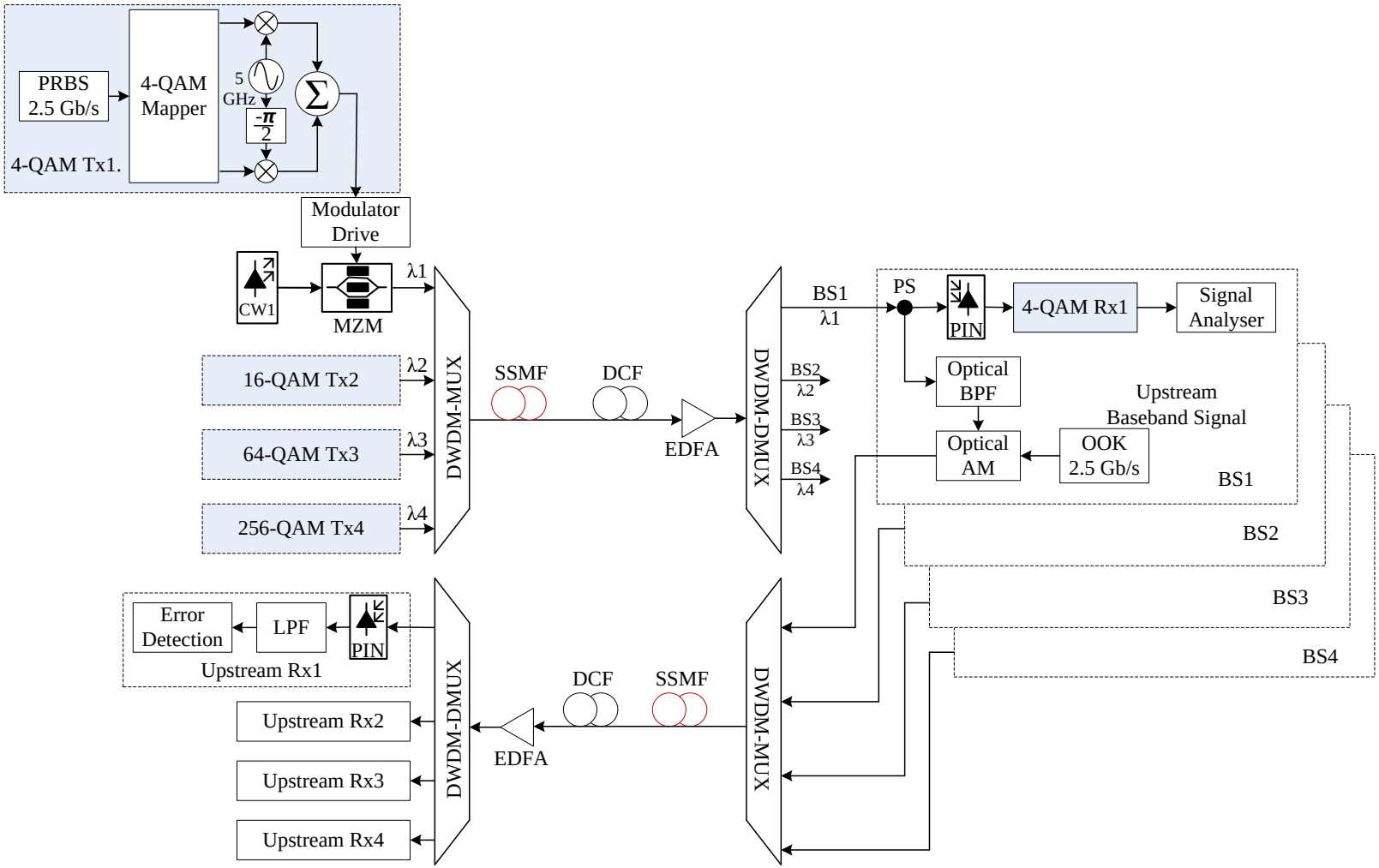

Figure 3- 1: Architecture of the Proposed Bidirectional DWDM-ARoF Transmission System

3.6 Simulation Results and Discussion

The simulation of the system in this research represents the setup of a physical layer transmission link which increased the scalability of the analogue RF signals transmitted over fibre with different modulation schemes of 4-QAM (or QPSK), 16-QAM, 64-QAM and 256-QAM. Firstly, each QAM combination is modulated with an optical carrier using MZM. The wavelength difference between each two adjacent optical carriers is 0.8 nm. The output optical signal of each MZM is launched into the DWDM multiplexer to be merged together into one signal and injected to the fibre. Figure 3.2 shows the optical spectrum of the four multiplexed optical channels before being transmitted over the fibre link.

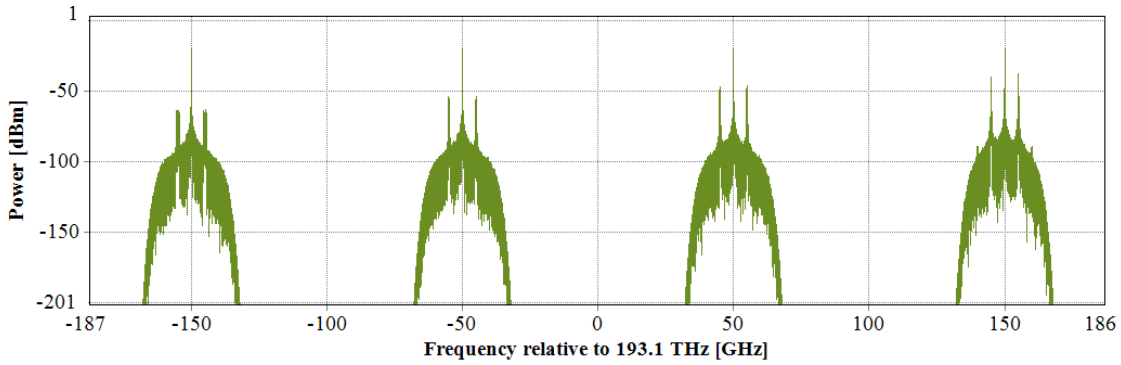

Figure 3- 2: The Optical Spectrum of the four ARoF Signals

The proposed system achieves compensation for the dispersion in SMF by using a DCF, and hence ARoF transmission can be extended. Subsequently, These ARoF signals are transmitted over two stages of fibre, namely SMF (100 km) and DCF (20 km).

Table 3.1 illustrates the parameters used in the simulation program for both SMF and DCF; keeping in mind that the reference wavelength used in both fibre segments is 1550 nm.

Table 3- 1FIBRE PARAMETERS

Parameter	SMF	DCF
Dispersion	16 ps/(nm.km)	-80 ps/(nm.km)
Fiber Attenuation	0.2 dB/km	0.4 dB/km
Dispersion Slope	0.08 ps/(nm^2.km)	-0.21 ps/(nm^2.km)
Non-linear index	2.6e-20 m^2/W	4e-20 m^2/W
Reference Frequency	193.1 THz	193.1 THz

According to the given parameters, the accumulated dispersion in SMF of 100 km long is (16 x 100 = 1600 ps/nm.km). The DCF is configured to a negative dispersion of a -80 ps/nm.km. Therefore, according to equation (3.1), a 20 km DCF is required to maintain zero dispersion over the total distance of SMF-DCF transmission link. The problem of high attenuation and dispersion penalty in DCF is handled by utilizing an EDFA of gain 20 dB. The transmitted ARoF signals are de-multiplexed by a DWDM-DMUX and each signal is delivered to a 3 dB Passive Splitter (PS) to divide the signal into two parts at each BS. The first part is injected to a PIN photodetector with 10 nA dark current to detect the electrical RF QAM signal. For instance, the electrical spectrum of the transmitted and received 4-QAM RF signal is exhibited in figure 3.3.

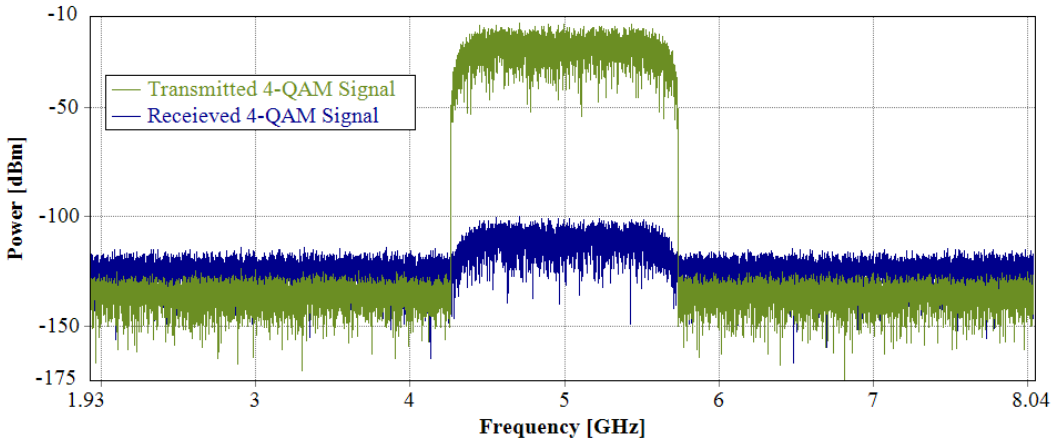

Figure 3- 3: Electrical spectrum of both transmitted and received 4-QAM signal After 120 km (SMF-DCF) measured at 2.5 Gbps, RF= 5 GHz and optical carrier= 193.25 THz

The second output of the PS is fed to an OBPF with a Gaussian transfer function. The filter order is chosen to be 5 so that to completely remove the DSB components of the received signal. A power controlled amplifier of 1 mW is utilised after the OBPF to amplify the output optical carrier to be reused for the upstream transmission as shown in figure 3.4.

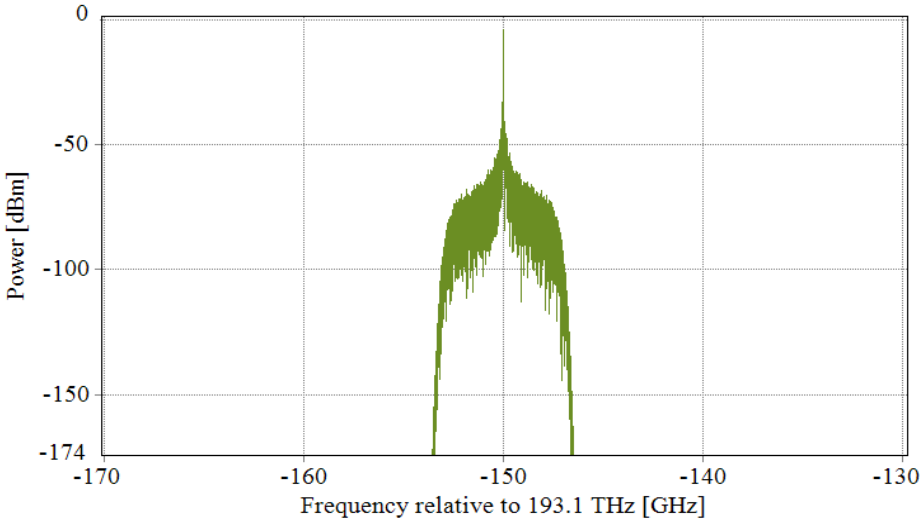

Figure 3- 4: Spectrum of the Optical BPF Output Signal

At the receiver side, QAM demodulator splits the received bit sequence into two parallel sub-sequent; in-phase (I) and Quadrature-Phase (Q) components. This is achieved by using QAM decoder. The QAM demodulation is performed by multiplying Q and I components by two quadrature carrier signals obtained from a local oscillator of 5 GHz. The I and Q electrical signals are transmitted to a DSP module provided by the simulator known as "Rx_El-mQAM_BER" which is used to estimate the SER and EVM of an electrical M-QAM signal.

Figure 3.5 shows the EVM performance for the four downstream channels over the SMF length. Most notably, the EVM for all QAM signals remains below 17.5%, which is the threshold that the 3GPP standards requires for QPSK (or 4-QAM) transmission in LTE [98] for distances up to 99.5 km. After this transmission point, a severe degradation in the EVM performance of the 4-QAM signal is occurred due to the chromatic dispersion effect with respect to the actual bandwidth resulted for this channel.

In order to reduce the penalty of the chromatic dispersion and other optical impairments, a bandwidth optimization process is performed based on using higher-order modulation formats. The accumulated bandwidth for each QAM combination (BW_{ch}) is given by [79]:

$$BW_{ch} = \frac{R}{\log_2 M} \tag{3.1}$$

Where R is the channel capacity, M is the number of bits per each symbol QAM. Accordingly, the resulted bandwidth per each QAM signal for the same channel capacity of 2.5 Gb/s per channel is reduced as follows:

Table 3- 2 BANDWIDTH FOR EACH QAM COMBINATION

M-QAM Signal	**Produced BW**
4-QAM	1.25 GHz
16-QAM	0.625 GHz
64-QAM	0.417 GHz
256-QAM	0.3125 GHz

As expected, the EVM performance for the remaining three channels is still below their corresponding EVM limits for longer transmission distances as follows: For the 16-QAM channel, the average EVM stays below 12.5%, which is the 3GPP standard threshold value for up to 110 km length. The 64-QAM signal achieved an EVM below 8% for SMF distances up to 117 km. Finally, the fourth channel (256-QAM signal) was capable to maintain the desired EVM limit of 3.5% up to 120 km distance. The simulation results of figure 3-5 clearly show that the chromatic dispersion which is the main source for the transmission length and data rate limitation in RoF systems can effectively be controlled by the use of an accumulated dispersion compensation (SMF + DCF) adapted with employing high order modulation schemes.

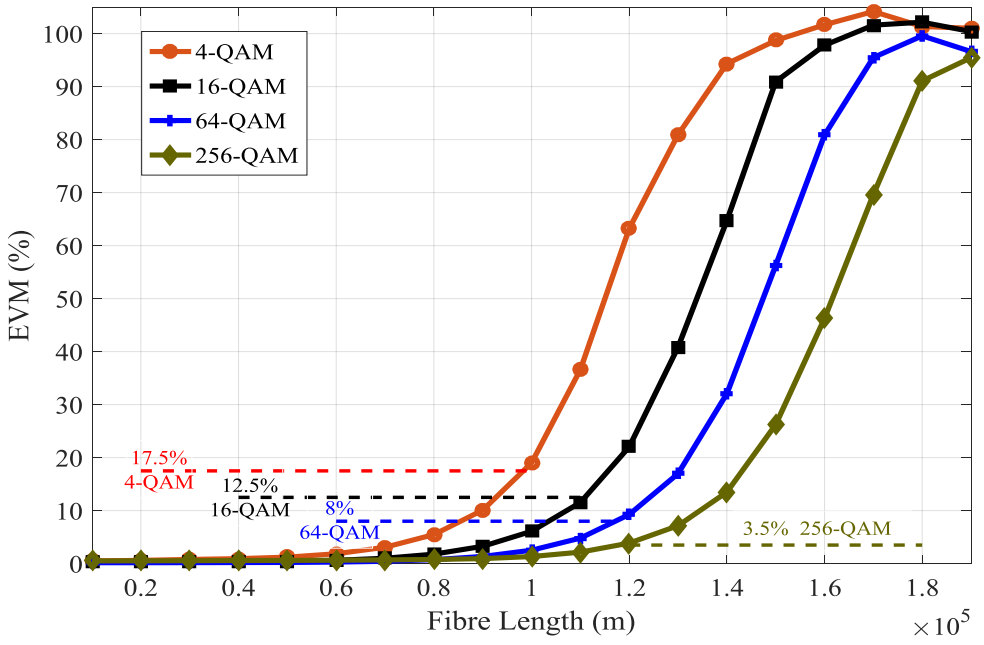

Figure 3- 5: EVM of the (4, 16, 64 and 256) QAM Analogue Signals over Fibre Length

Figure 3.6 shows the SER performance for all QAM channels with respect to the Optical Signal-to-Noise Ratio (OSNR). The OSNR was set using the "SET OSNR" module provided by the simulator tool which is placed before the PIN. This module adds ASE noise (emulated as a Gaussian-distributed optical white noise) to the input signal in order to reach the specified OSNR. The input signal is assumed to be noise-free and all channels are assumed to have identical power. The OSNR is changed by creating a sweep control parameter that varies the OSNR values between (10 – 30) dB using this module and running the simulation repeatedly in accordance to the variation happening in the OSNR while measuring the received SER at each iteration. The SER measurements were evaluated for all channels simultaneously at a transmission distance of 100 km SMF plus 20 km DCF. It can be seen that higher order QAM schemes can offer better SER performances in terms of the obtained OSNR for a particular SER value. This is attributed to the degradation in the chromatic dispersion effect associated with the bandwidth reduction from adopting a higher order QAM formats. It is evident that an SER value of 10^{-4} is an acceptable value for wireless transmission systems without the requirement of

error correction [99]. Consequently, this SER value is considered as a threshold value for comparison. Table 3.3 contains the obtained OSNR results for different QAM combinations.

Table 3- 3 OSNR FOR EACH QAM COMBINATION

M-QAM Signal	Obtained OSNR @ 10^{-4} SER
4-QAM	25.2 dB
16-QAM	23.1 dB
64-QAM	22 dB
256-QAM	21.3 dB

This confirms that the chromatic dispersion is tolerable for higher order QAM signals.

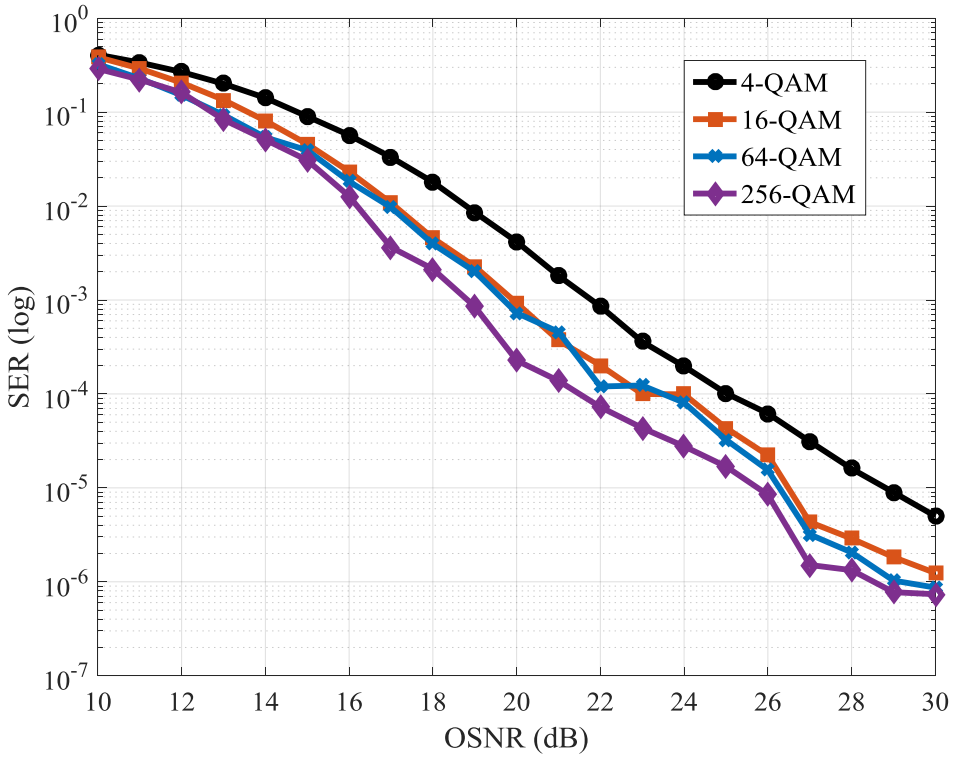

Figure 3- 6: SER of the (4, 16, 64 and 256) QAM Signals versus OSNR Measured at 100 km SMF + 20 km DCF

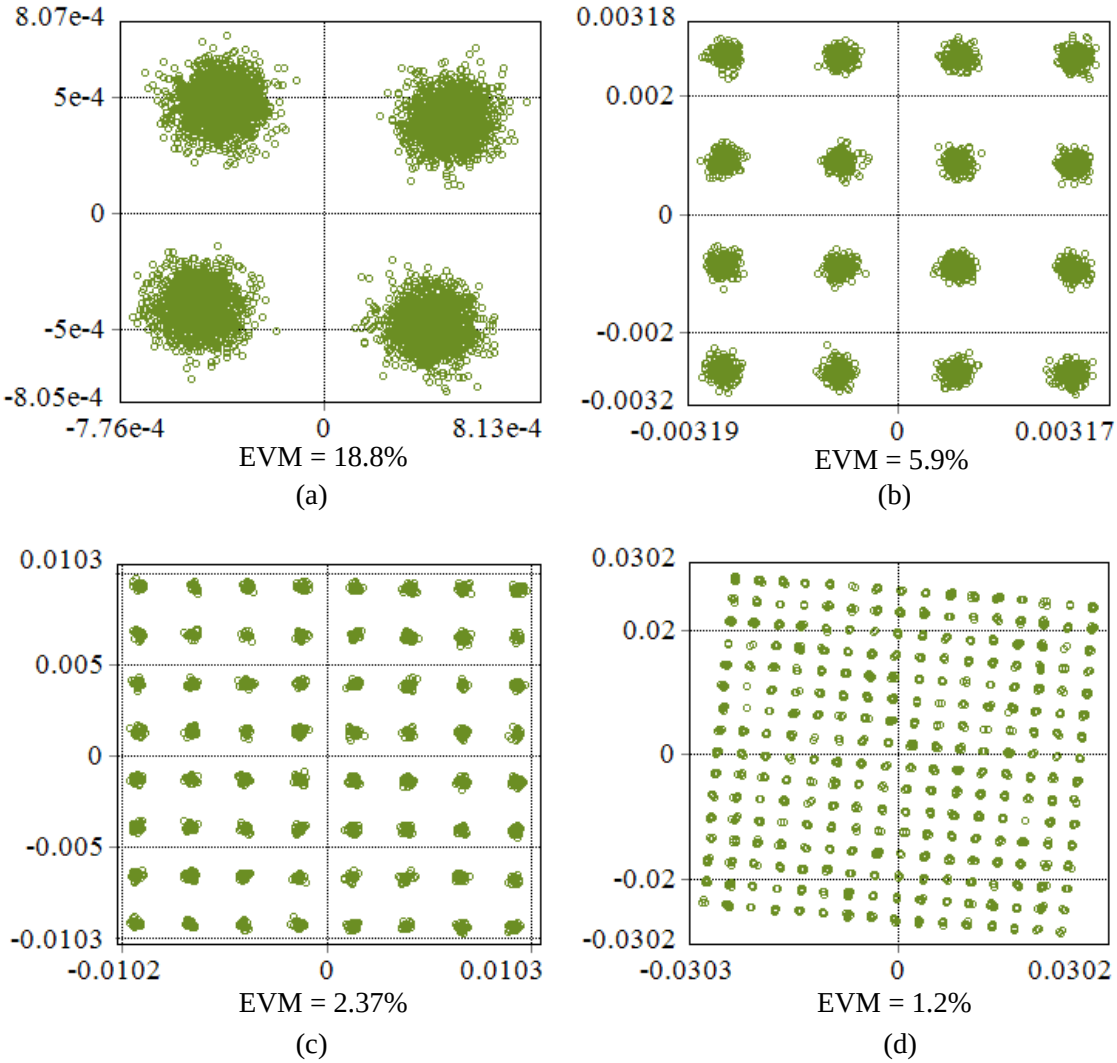

Figure 3- 7: Constellation Diagram of: (a) 4-QAM, (b) 16-QAM, (c) 64-QAM, and (d) 256-QAM Measured at (100 km SMF + 20 km DCF)

Figures 3.7 (a, b, c and d) illustrate the constellation diagrams for each of (4, 16, 64 and 256) QAM signals, respectively. These constellations are measured at 120 km RoF transmission over the (SMF-DCF) combination. They also show a distortion included in their constellation, which is resulted from the nonlinear noise of the optical components and also because of the power attenuation and dispersion in both SMF and DCF segments.

Figure 3.8 shows the BER analysis as a function of the received optical power (ROP) for four OOK baseband signals each with a bit rate of 2.5 Gb/s. It can be seen that an error-free signals are received at the CS side for all channels.

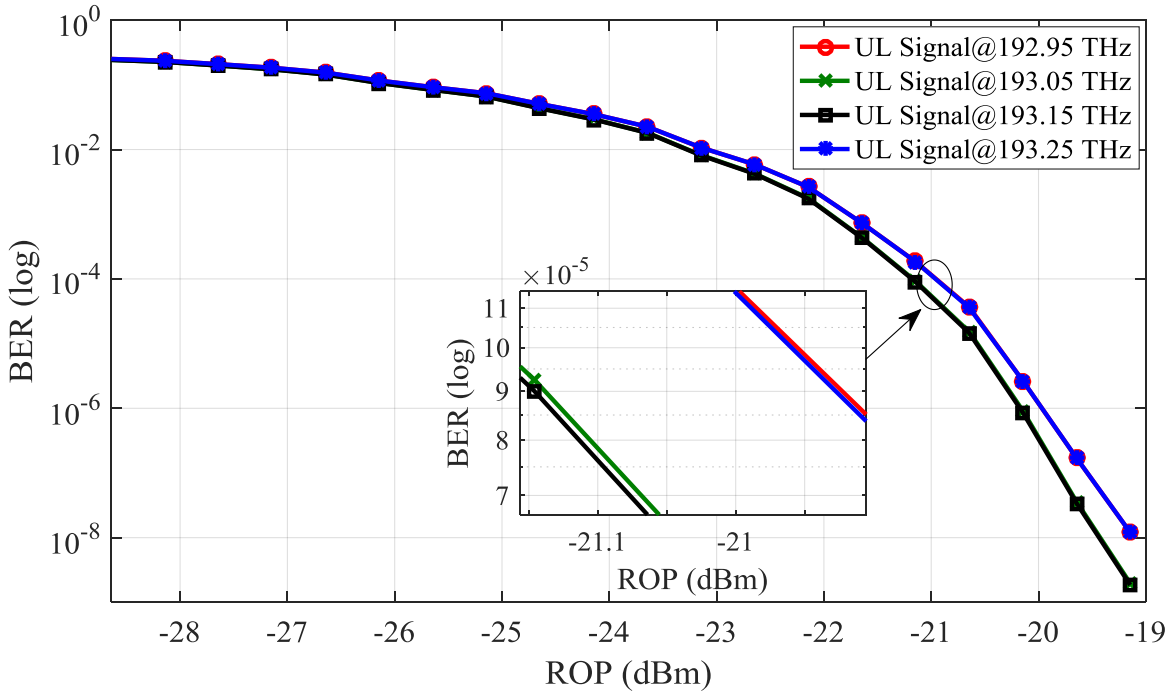

Figure 3- 8: BER Performances versus ROP for Four Upstream Signals Each at 2.5 Gb/s.

The ROP is changed using a galaxy block provided by the simulator produces an ASE noise (emulated as a Gaussian-distributed optical white noise) to the input signal, and a swept attenuator that produces attenuation values between (10 - 20) dB with a step increment of 0.5 dB placed at the CS side before the PIN detector. This galaxy block contains a “Repeat Signal Operation” module to provide multiple copies of the input signal. Thus, a new attenuation is applied to every copy of the input signal, to become an output signal. This module can be placed before a BER estimator, and will feed the estimator with multiple copies of the output of the fibre, each with a different attenuation. A BER versus ROP can be created by inputting the BER estimate to the y-input of a numerical 2D analyzer, and feeding the x-input of the analyzer with a power measurement.

The power measurement is obtained using a power meter module that measures the ROP values in dBm at each simulation running. It can be noted as well that there is an average power penalty of about 0.5 dB between the BER performance of channels 2 and 3 and the BER performance of channels 1 and 4 started after a ROP of about -24 dBm. This is because channels (2 and 3) are exposed to a dispersion value in fibre different than those for channels (1 and 4) depending on the utilised upstream carrier frequency. On one side, it has been mentioned in chapter 2 that the chromatic dispersion is changed as a function to the operating wavelength. On the other side, it has been mentioned earlier in this chapter that the negative dispersion of the DCF is calculated in order to cancel out the positive dispersion caused by the SMF with respect to the reference optical frequency. In another word, the reference optical frequency, which is 193.1 THz, is set to be the zero dispersion frequency in our design. As a result, optical frequencies used for channels 2 and 3 transmissions are centred around the zero dispersion frequency with frequency gap of 100 GHz between them while channels 1 and 4 are placed around this zero dispersion point with 300 GHz frequency gap between them. Consequently, channels 1 and 4 exposed to higher dispersion values than channels 2 and 3 causing that power penalty between them during transmission.

The eye diagram is also observed for the upstream data transmission for 120 km (SMF + DCF) transmission as shown in figure 3.9. It shows a clear eye opening, which means clear signal reception and a satisfied performance.

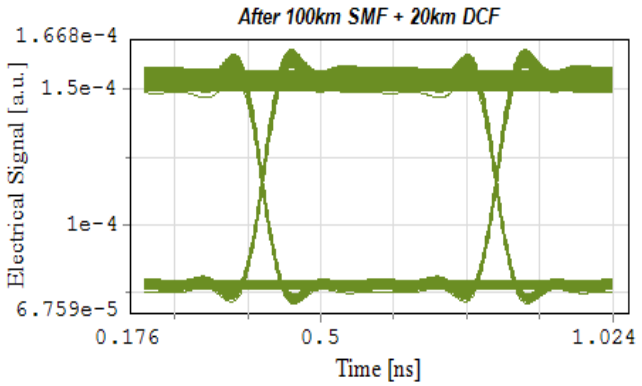

Figure 3- 9: Eye Diagram of Upstream OOK Signal

3.7 Chapter Conclusion

Analogue RoF communication systems provide cost-effective solutions to the highly increasing demands of high bit rate application. Much of the research carried out aims not only reducing the implementation cost but on improving the system's performance and extending the transmission length as well.

In this chapter, a bidirectional ARoF link transmitting four multiplexed downlink RF channels using DWDM technique each with a bit rate of 2.5 Gb/s and modulated using different QAM formats has been designed. The main findings of the ARoF link designed in this chapter can be summarised as follows:

1- The dispersion problem in fibre has been effectively handled by combining the SMF with DCF and utilizing high-order modulation schemes.
2- Transmission of (4, 16, 64 and 256) QAM signals are deployed over RoF combination of 100 km SMF and 20 km DCF using four wavelengths separated by 0.8 nm channel spacing.
3- For the uplink, the need for an additional light source at the BS is avoided by reusing the same optical carrier for the upstream transmission of 4-OOK baseband signals each at 2.5 Gb/s bit rate.
4- EVM values below the 3GPP standard limits for every transmitted QAM signal have been achieved for long-haul transmission distances started from about 100 km up to 120 km.
5- Simulation results have proved the system's ability to achieve SER values of 10^{-4} for the downlink channels for 120 km transmission length at highly satisfactory OSNR values.
6- Because M-QAM is an effective modulation format for the next generation RAN, this scheme can provide a significant improvement on both system reliability and flexibility.

Chapter 4

Efficient Transmission of a DRoF System

4.1 Overview

As mentioned in section (2.11), DRoF represents the technology of transmitting the digitised RF signals over an optical fibre link. With the advent of a high speed ADC and DAC components, DRoF technology has attracted more attention within the last few years. It can, for instance, stabilise the Dynamic Range of the DRoF link independent of the fibre length provided that the power of the received optical signal stays within the optical receiver sensitivity limits. However, in DRoF transmission, the optical link requires a high bandwidth due to the digitisation processes, which in turn, represent the major challenge from the perspectives of DRoF implementation and deployment.

In this chapter, a physical layer design of a DRoF system which uses an optical duobinary modulation scheme to reduce the spectral occupancy of the transmitted signals is proposed. In this system, a transmission of a digitized 16-Quadrature Amplitude Modulation (16-QAM) radio frequency signal with 2.5 Gb/s over a Standard Single Mode Fibre (SSMF) is presented. Optical duobinary transmission is realized with a reduced complexity using a simple differential precoder and a single-arm Mach-Zehender Modulator (MZM). The performance of the proposed system is compared with a DRoF system that utilizes a Non-Return-to-Zero (NRZ) coding scheme. Simulation results reveal that the proposed DRoF system is capable of transmitting a digital signal of 10 Gb/s over

an SSMF that can reach up to 70 km distance without dispersion compensation requirement. To prove this concept, transmission figure of merits, such as the EVM and the BER is evaluated according to the limits established by the 3GPP specification. Moreover, system performance is studied according to the wavelength plan allocated to TWDM-PON by ITU-T-G.989.2 standards for (NG-PON2). As a result of improvement, this system can effectively support high data rate requirement of DRoF transmission over Common Public Radio Interface (CPRI) protocol.

4.2 Introduction

Mobile Network Operators (MNOs) should be prepared to meet the rapid growth in mobile data traffic. A recent study conducted by Cisco showed that mobile data traffic will reach 49 exabytes per month by 2021 [1]. Cloud-Radio Access Network (C-RAN) has been recently proposed to attend the increasing bandwidth demands. It introduces an innovative RAN architecture based on the separation of the baseband processing units (BBUs) in a single place called the Central Office (CO) from the radio element of the Base Station (called Remote Radio Head RRH). Connecting the BBUs to the corresponding RRHs is accomplished through an optical fibre link called the “fronthaul” [100].

Radio over Fiber (RoF) technology can support a long reach transmission network with high data rates by integrating wireless and optical networks. Most importantly, it can be seamlessly integrated with the existing optical access networks such as FTTX and WDM-PON [5]. As mentioned in section (2.9), two types of RoF transmission networks exist, namely, Analog RoF (ARoF) and Digital RoF (DRoF). On ARoF, traffic transported over optical fiber by modulating the light with radio signals in the analogue domain. Radio Frequency (RF) signal transmission over ARoF systems suffers from nonlinear distortion called Intermodulation Distortion (IMD) caused by optical transmitters. Furthermore, it is highly vulnerable to the chromatic dispersion effect caused by fibre, which limits the transmission distance to a few kilometres. This explains why ARoF has not been standardized yet. On the other hand, DRoF transmission is expected to overcome these

impairments due to its robustness to fibre nonlinear effects. The transmission of the digital signal minimizes the nonlinear effects presented on the ARoF transmission allowing the system to maintain its dynamic range independent from the fibre length until the received signal goes below the receiver sensitivity. For these reasons, operators and radio equipment manufacturers are in favour of implementing DRoF technology in fronthaul link. Two industrial standards have emerged for DRoF transmission, namely Common Public Radio Interface (CPRI) and Open Base Station Architecture Initiative (OBSAI). Mapping methods of CPRI are more efficient than OBSAI as CPRI support the concept of digital Distributed Antenna System (DAS). Hence, most global vendors have chosen CPRI for their products. However, DRoF requires high optical bandwidth to support the high data rate produced from the digitalization process to RF signals. This represents one of the major challenges in DRoF implementation, which may limits its performance and increases the cost.

4.3 Related Work

In the following, majority of the conducted work done so far on DRoF is summarised:

1- Authors in [70] have designed an analytical modal that can be used to determine the key parameters of ADC/DAC components utilised in DRoF system. The research findings have resulted in a set of parameters that have been used for the transmission of a digitised 16-QAM RF signal.

2- In [101], performance analysis of a digitised 16-QAM unidirectional DRoF system as a separate transmission scenario and with a coexistence scenario based on ITU-T G.989 standards is presented. Based on that analysis, a trade-off between the ADC bit resolution and ADC sampling rate must be considered to avoid severe restrictions on the transmission performance. However, the results have shown that a DRoF system with only 4 bit ADC resolution is fairly compatible with the ITU-T G.989 specifications by means of the allocated wavelength plan.

3- A digitised transmission of SCM RF signal that composed of a three QPSK modulated signals using an external modulation and a CW laser source is presented in [102]. It has been shown that the DAC can cover the received digital signal at different frequencies without the needs for a mixer and local oscillator.
4- A comparison study between the analogue and digital transmission of multiple RF signals, which are all utilising a single ADC/DAC is demonstrated in [103]. The comparison has revealed that the SNR and dynamic range in the case of DRoF is less severe relative to the ARoF case.
5- A novel methodology to transmit the DRoF signals efficiently is presented in [104]. In which, a digital processing technology based on using Field Programmable Gate Array (FPGA) platform to digitise the RF signals. This system is typical for an in-building digital DAS communication system. It has been shown that the delay produced on the FPGA board to transmit and receive a digitised 64-QAM RF signal is less than 2 μs.

4.4 State of the Art

Up-to-date, three different techniques have been suggested to mitigate the limitations associated with DRoF links deployment. They are Bandpass Sampling, Delta-Sigma Digitisation and All-Photonic ADC (AF-ADC) techniques. In the following sections, a brief description to the operation principles of each of these technologies is presented, but previously, the A/D conversion process is explained to understand its main drawbacks and how they have been tackled using the nominated techniques.

4.5 Conventional Analogue-to-Digital (A/D) Conversion

Conventional A/D converter transforms the continuous time input signal x(t) into a discrete time digital output signal. In fact, it samples the input signal at a fixed sampling

rate (fs=1/Ts), where Ts represents the sampling interval. Each sample is approximated by a finite precision which can be then transformed into a digital code [105]. Figure 4-1 shows the block diagram of a basic A/D conversion process. It shows three different stages need to be passed the analogue input signal to be converted to a digital format. Firstly, an anti-aliasing filter is utilised to prevent the spectral aliasing of the signal in the frequency domain during the sampling process. Secondly, sample-and-hold circuits to maintain the sampled signal at a constant level so that to be digitised by the ADC during the sample interval. Finally, it is the process of converting the continuous time sampled signal into a discrete time digital signal using quantisation process, where each sample is expressed by a unique digital number with (N) bits.

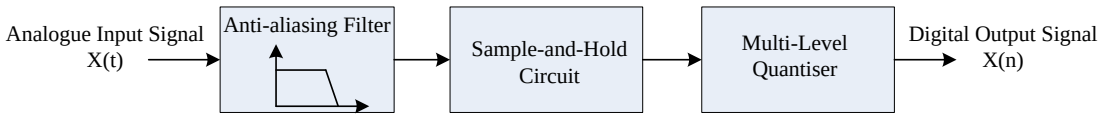

Figure 4 - 1: Conventional (A/D) Conversion Process

Quantisation process introduces an error signal known as the quantisation noise. It is the difference between the generated code number and the original signal. This error signal is constrained by the sampling frequency and the bit resolution of the utilised ADC. In an N-bit ADC, there are 2^N quantisation levels which also represent the resolution of the converter. The interval between consecutive levels (q_s), which is referred to as the quantisation step size, is given by:

$$q = \frac{1}{2^{N-1}} \tag{4.1}$$

The samples value is then approximated to the nearest quantisation level as shown in figure 4-2.

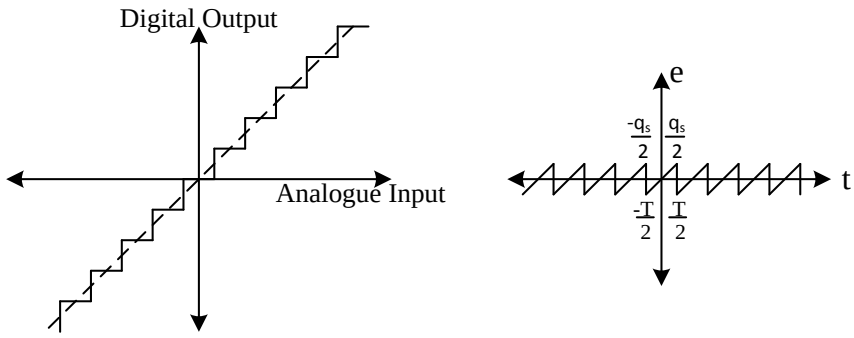

Figure 4 - 2: Quantisation Error Transfer Function

The quantisation error is small in the case of a small magnitude input signal. It is in the order of one Least Significant Bit (LSB) in amplitude [105]. However, its impact is more sever in the case of large input signals. As a result, the ADC digital output *x(n)* can be considered as the sum of the sampled signal $x^*(t)$ and the quantisation error signal *e(n)*:

$$x(n) = x^*(t) + e(n) \tag{4.2}$$

It can be seen from figure 4-2 that the noise probability can occur equally anywhere inside the interval ($-q_s/2, q_s/2$), and hence, the noise power (σ_e) can be determined as:

$$\sigma_e{}^2 = E[e^2] = \frac{1}{q_s}\int_{(-q_s)/2}^{q_s/2} e^2\, de = \frac{q_s{}^2}{12} = \frac{2^{-2N}}{3} \tag{4.3}$$

where, σ_e represent the steady state quantisation noise, and *E* denotes the statistical expectation. Therefore, quantisation noise is uniformly distributed over the whole frequency range of the signal as shown in figure 4-3. The noise spectral density is then obtained by:

$$N(f) = \frac{q_s{}^2}{12 f_s} = \frac{2^{-2N}}{3 f_s} \tag{4.4}$$

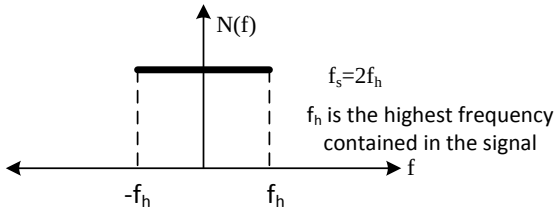

Figure 4 - 3: Noise Spectrum of Nyquist ADC

4.5.1 Bandpass Sampling Theory

This theory has found its application for DRoF since the year 2000 [106]. It implies that the sampling rate depends on the bandwidth of the signal, not only on the highest frequency involved in the spectrum of that signal according to Nyquist's sampling theorem. As a result, it significantly alleviates the excessive sampling rate requirement in the design of ADC/DAC. To explain the principles of the bandpass sampling theory, let us consider the spectrum of RF signal with a bandwidth of B, while the highest and lowest frequencies are f_H and f_L respectively, as shown in figure (4.4a). Figure (4.4b) shows the sampled version of the RF signal, in which, we can observe that the original spectrum of the signal is repeated periodically at intervals equal to the sampling frequency value. The sampling frequency (f_{sam}) must appropriately be chosen so that to ensure a perfect reconstruction of the analogue RF signal and to prevent the spectral aliasing as well. As a consequent, the original signal can simply be recovered by employing a BPF [106].

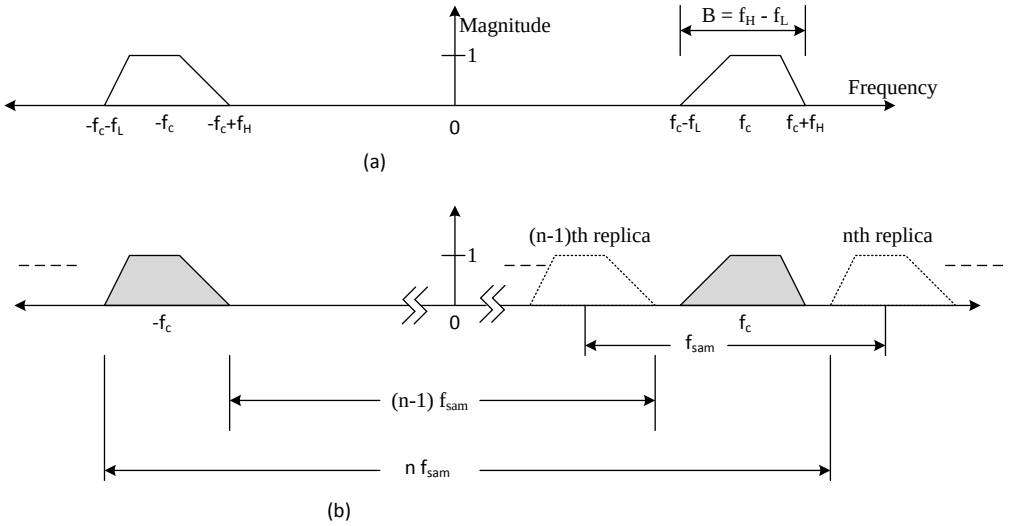

Figure 4 - 4: Frequency Spectrum of (a) the Analogue Signal, (b) the Sampled Version

$$\frac{2f_H}{n} \leq f_{sam} \leq \frac{2f_L}{n-1} \tag{4.5}$$

$$1 \leq n \leq I_g\left[\frac{f_H}{f_H - f_L}\right] \tag{4.6}$$

where, *n* is an integer that represents the spectral replica's position relative to the original spectrum, and I_g is a function that gives the highest integer that is less than or equal to the quantity assigned to it. Equation (4.5) can be plotted for different values of *n* with respect to the normalised highest frequency in the signal as shown in figure 4-5. It clearly shows that the allowed values of the sampling frequency lay in the white regions, whereas the forbidden values in the shaded areas. Therefore, for a particular value of *n*, the sampling frequency can be chosen in accordance to the corresponding white region to avoid aliasing of the spectral replicas. It can be observed also that the higher the value of *n*, the lower the required sampling frequency value.

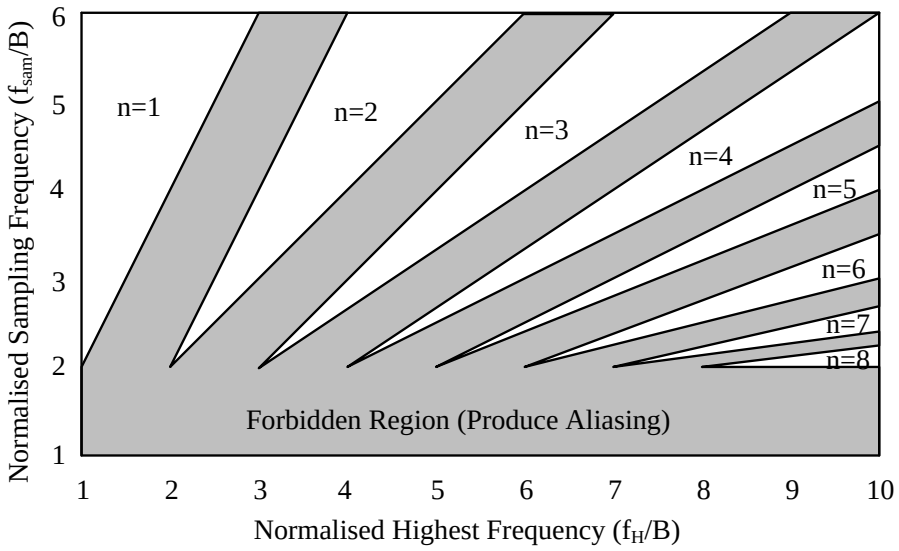

Figure 4 - 5: Allowed (White) and Forbidden (Shaded) Sampling Frequency

Theoretically, some investigations have been carried out since the year 2010 to examine the feasibility of bandpass sampling in DRoF for existing cellular networks [68], [69], [71]. However, it has been found that in the case of broadband RF signals, the design of the ADC/DAC with high speed may be restrictive. Consequently, it is preferable to digitise the modulated Intermediate Frequency (*IF*) signal after being down-converted using an oscillator at the CS side instead of the RF signal, as it will be discussed later in this chapter.

4.5.2 (A/D) Conversion Based Sigma-Delta (Σ-Δ) Modulation

Conventional A/D conversion is primarily steered and affected by quantisation noise. Despite it is a simple and an open-loop technique, undesired effects, such as distortion and timing jitter will be added the digitised signal causing deterioration to the overall performance. A/D and D/A conversion can be divided into two categories depending on the converter sampling frequency as a Nyquist rate or oversampling converters. For the Nyquist rate ADC/DAC, as the name implies, sampling frequency (f_s) must be as low as the requirement set by Nyquist's criteria, i.e. more than twice the input signal bandwidth (*B*), to prevent the spectral aliasing and to alleviate the sharp requirement of the anti-

aliasing filter [107]. In many applications, high resolution and linearity ADC/DAC are required. Besides, the quantisation noise is uniformly distributed over the Nyquist zone in the Nyquist ADCs [108]. To address these limitations, oversampling converters are proposed, which perform the sampling process at much higher rates than the Nyquist rate. There are two main types of oversampling converters, which are both based on a feedback configuration, called Delta modulator and Sigma-Delta (Σ-Δ) modulator [109].

In delta modulation, the quantisation is performed to the changes in the input signal from sample to sample instead of quantising the absolute value of the signal at each sample. Figure (4.6a) shows the block diagram of delta modulator. As a result, the modulator's output signal is a stream of pulses that represent the encoding of the difference between the analogue input signal and the quantised signal as shown in figure (4.6b).

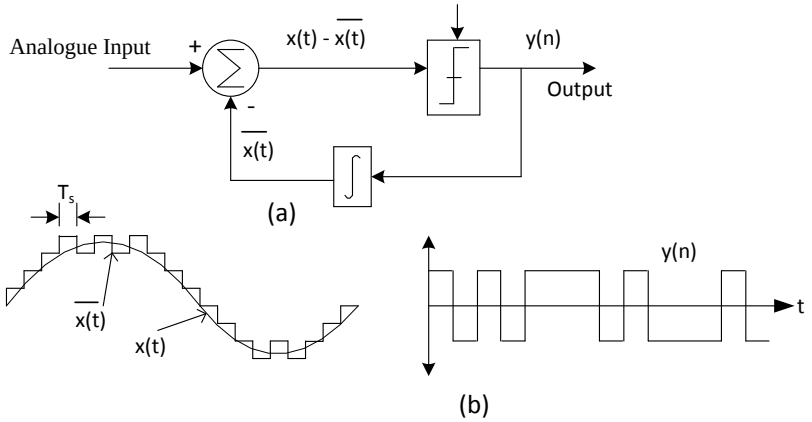

Figure 4 - 6: Delta Modulator: (a) Basic Block Diagram, (b) Quantiser Input and Output Signals

Here, we are going to concentrate on (Σ-Δ) modulator as it is a cost-effective alternative to the Nyquist ADC and can ultimately be integrated on DRoF systems [110]. (Σ-Δ) converter makes use of the oversampling and noise shaping techniques to reduce the quantisation error and to increase the resolution. Figure 4-7 shows the basic elements of (Σ-Δ) modulator. The accuracy of the conversion in (Σ-Δ) modulation is improved by passing the digital output through a 1-bit DAC and adding (sigma) the resulting analogue signal to the input signal (the signal before delta modulation), and hence reducing the error introduced by the delta-modulation. The arrangement shown in figure 4-7 is so-called the first-order (Σ-Δ) modulator.

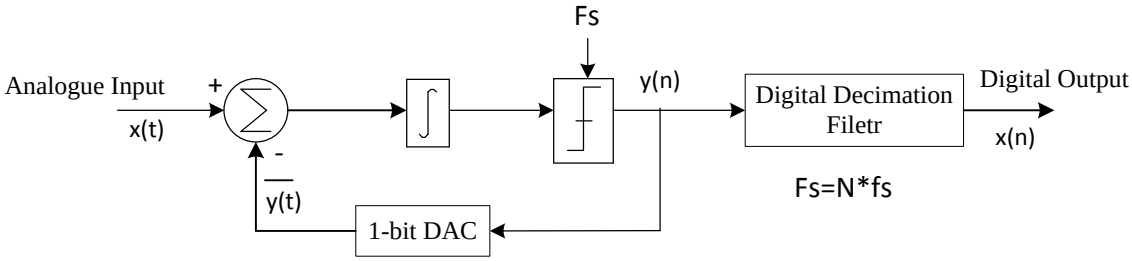

Figure 4 - 7: Block Diagram of a First-Order Sigma-Delta (Σ-Δ) Modulator

The main feature of such (A/D) converter is the enclosing of a 1-bit DAC in a feedback loop in order to shape the spectrum of the both the input signal and the quantisation noise. It low-pass filters the signal and high-pass filters the noise. Meaning, the (Σ-Δ) modulator pushes the quantisation noise into a higher frequency bands, and so, it can be filtered out by a filter. This is what is referred to as the noise shaping process. The modulator can be analysed in the z-domain as follows:

$$Y(z) = X(z)STF(z) + Q(z)NTF(z) \tag{4.7}$$

where, *Y(z)* is the modulator transfer function; *X(z)* and *Q(z)* is the z-transform of the input signal and quantisation noise, respectively; *STF(z)* and *NTF(z)* are the corresponding transfer functions of both the input signal and the quantisation error, which are given by:

$$STF(z) = \frac{H(z)}{H(z)+1} \tag{4.8}$$

$$NTF(z) = \frac{1}{H(z)+1} \tag{4.9}$$

where, *H(z)* represents the loop transfer function, and:

$$H(z) = \frac{z^{-1}}{1 - z^{-1}} \tag{4.10}$$

As a result, equation (2.26) can be rewritten as:

$$Y(z) = z^{-1}X(z)) + (1 - z^{-1})Q(z) \quad (4.11)$$

Typically, the Dynamic Range (D_R) of the k^{th} order modulator is:

$$D_R = 6.02L + 1.76 + 10\log_{10}\left(\frac{2k+1}{\pi^{2k}}\right) + (2k+1)\,10\log_{10}(OSR) \quad (4.12)$$

where *OSR* is the oversampling ratio and *L* is the number of quantized bits.

However, (Σ-Δ) modulation faces some stability issues due to nonlinearities in the feedback DAC resulting in nonlinearities for the whole conversion process [109]. As the DAC output needs to follow the input signal very accurately, any nonlinearity in the DAC results in a distorted signal at the output of the comparator, and therefore, corrupts the overall modulator performance. One possible solution to avoid this issue is the implementation of higher order cascaded (Σ-Δ) modulator. Authors in [111] have proposed a second-order (Σ-Δ) modulator with a multi-level quantiser to address the stability issue for the sake of a digitised transmission of a 32 LTE aggregated carrier components over a 25 km SMF.

4.5.3 Photonic Analogue-to-Digital Converter

Photonic ADCs (PADCs) have attracted a great interest within the last few years [112]. It is a device, in which, the input is an optical signal and the output is a digital optical signal. One preferred standpoint of PADCs is that they are equipped for eliminating the effect of electronic jitter presented in the Electronic ADCs (EADCs) and to improve the sampling frequency. PADCs can be subdivided into 4 classes:

1- Photonic Assisted ADCs: They are EADCs as they perform both sampling and quantisation in the electronic domain, but they use photonics to improve some limiting properties associated with EADCs.

2- Photonic Sampled ADCs: This kind performs the sampling in the optical domain and quantisation in the electrical domain.

3- Photonic Quantised ADCs: In this technique, the domains of operation of both sampling and quantisation are reversed.
4- Photonic Sampled and Quantised ADCs: Obviously, both quantisation and sampling are performed in the optical domain.

However, most researchers [113][114] have focused on photonic sampled ADCs to take the advantage of short duration optical pulse and low pulse-to-pulse jitter. Figure 4-8 shows the basic components of an optically sampled ADC. In which, optical pulse trains with a timing jitter of about one femtosecond are typically generated by an ultra-stable Mode-Locked Laser (MLL). This pulse train is then modulated using fast optical modulator, typically MZM, with an RF signal that needs to be digitised. Therefore, the amplitude of each pulse at the modulator's output is proportional to the RF signal value at the relative pulse time. The modulated optical pulses are then detected using a high-speed photodetector to produce electrical pulses of current. The detector output current is then amplified and converted into electrical digital samples after being electronically quantised using the EADC.

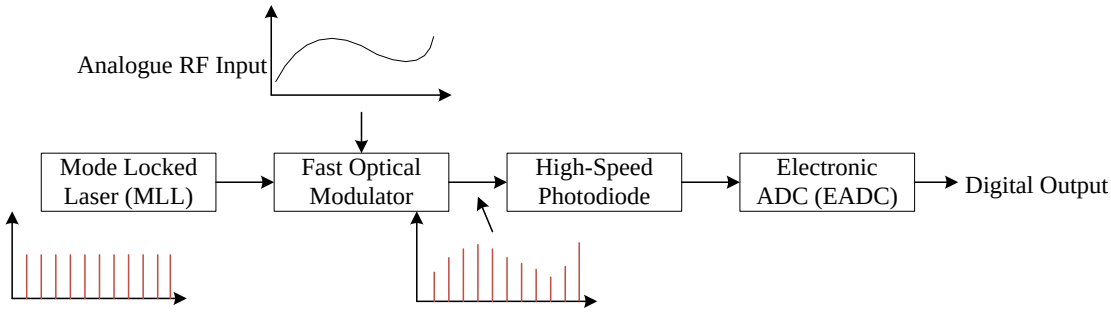

Figure 4 - 8: Optically Sampled ADC

To improve the performance of the photonic sampled ADC, a scheme with wavelength or time de-multiplexing is utilised as shown in figure 4-9. As this system contain an analogue optical link, its performance is characterised by means of the link SNR, Spur Free Dynamic Range (SFDR), the bandwidth of the optical modulator, modulation depth, photodiode bandwidth and saturation current [115][116].

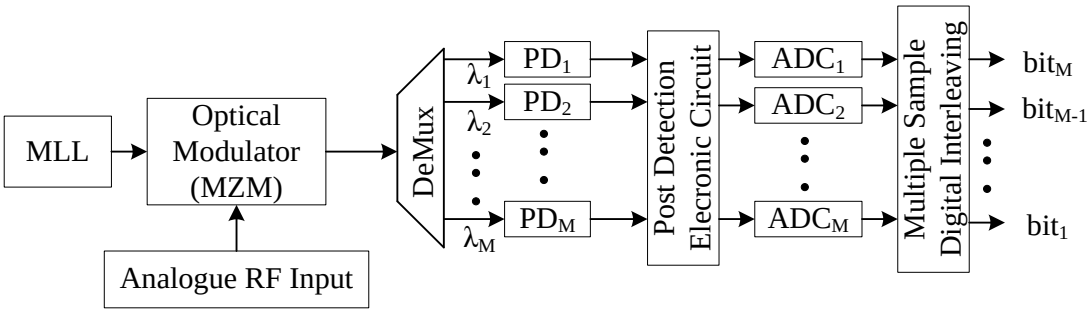

Figure 4 - 9: Optically Sampled ADC with a Wavelength De-Multiplexing

4.5.3.1 Limitations of the Photonic ADCs

Although photonic sampled ADC improves the sampling rate and jitter, it has several limiting issues:

1- This system, like any other optical link, requires linear modulator response, which can be obtained only when using low modulation index. This is, in turn, requires an optical power beyond the practical requirements [18].

2- Photodiode high linearity requirement. It must be linear over the whole range of operating power. Besides, it must turn on very rapidly and it should have low noise [117].

3- The EADC must be clocked at the same sampling rate of the MLL, which means that the sampling time and jitter are both optically controlled [109].

4.6 Baseband vs IF Sampling

Nyquist sampling theorem states that in order to recover an analogue signal from its sampled version, the sampling frequency (f_{sam}) must be chosen at least equal to two times or greater than the highest frequency (f_h) contained in the analogue signal.

$$2f_h \leq f_{sam} \leq \infty \qquad (4.13)$$

Baseband sampling involves direct sampling to the entire baseband signal as shown in figure (4.10), where the incoming signal sent straight to the ADC for conversion after being treated by an anti-aliasing filter to avoid aliasing effect at the frequency domain of the sampled signal. Analogue signal digitization passes through three stages, namely sampling, quantisation and coding.

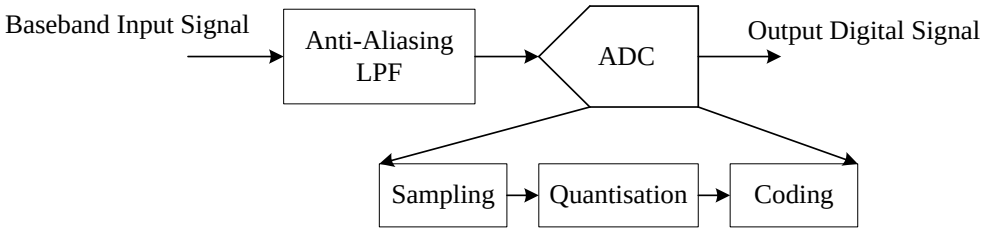

Figure 4 - 10: Baseband Sampling

Due to the Nyquist sampling constraint, baseband sampling has not been possible until recently, as ADC sampling rates have increased to accommodate the highest frequencies included in the input RF signal. However, this calls for fast DSP and/or FPGAs to keep up with the digitized rates. Not to mention how expensive these high speed digital circuitry would be.

A more practical, cost-effective and easy to implement a solution to relax the ADC sampling rate requirement is the RF-to-IF down-conversion process as shown in figure 4-11.

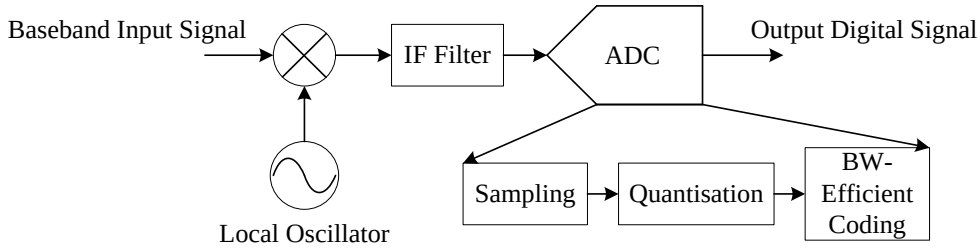

Figure 4 - 11: Intermediate Frequency Sampling

It takes the incoming signal and down-converts it using a mixer with a local oscillator to a lower Intermediate Frequency (*IF*). The signal modulation and bandwidth are retained, but the ADC sampling rate requirements are much lower. With this architecture, fewer circuits and filters are needed, lowering the cost and complexity. On the other hand, heterodyne receivers are required at the BS side for IF-to-RF up-conversion process.

Substantially, this process has been thoroughly optimized in performance, focuses ADC performance on the essential signal and allows for ADC with the best resolution accuracy and dynamic range.

As a result, *IF* sampling technique will be adopted through the digitising process handled in this thesis in order to ease the ADC sampling rate requirements. Moreover, all previous DRoF links presented in section (4.3) have utilized NRZ as a coding scheme to the sampled signal. To achieve a high performance and cost-effective DRoF link, the bandwidth-efficient coding scheme will be considered instead.

4.7 Duobinary Signal Generation

As mentioned in section (2.4), duobinary is a form of coding known as partial response signalling, in which binary digits are mapped into a three-level signal (-1,0,1). A signal with *b* levels can be generated by a series of delay and add circuits. A duobinary signal is generated using a single delay of duration *T*. The spectral density *S(f)* of a multilevel signal is given as:

$$S(f) = \frac{(b-1)^2 A^2 T}{4} \mathrm{sinc}^2[(b-1)^2 fT] \qquad (4.14)$$

According to (4.14), spectral width decreases with increasing signal levels as shown in Figure 4-12. Putting in our consideration the Nyquist criteria which imply that the transmission bandwidth must be greater than or equal to 1/2T for zero inter symbol interference (ISI), DB signalling is the most sensible and useful subset [118].

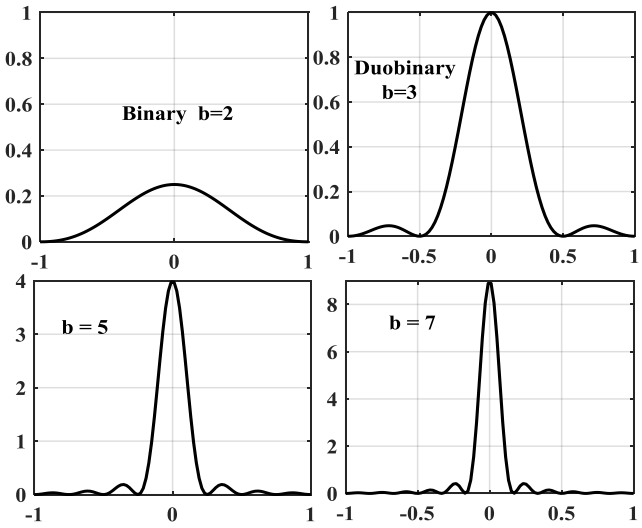

Figure 4 - 12: Power spectral density for poly-binary signals

4.7.1 Proposed Duobinary Precoder Design

Precoding the input bit stream is essential in duobinary transmitter to avoid error propagation and additional hardware complexity at the receiver. It was mentioned in section (2.14) that the conventional duobinary pre-coder uses an inverter, an XOR gate and a feedback tap with 1-bit delay as shown in figure 4-13a. This feedback tap is hard to implement at high data rates such as 10 Gb/s.

In our proposal, the pre-coder does not involve delay as shown in figure 4-13b. It is realized by connecting an inverter and an AND gate followed by a toggle flip-flop (T-ff) which is used here as a divide-by-2 counter. The designed precoder is implemented using

an inverter and (AND) gate followed by a Toggle flip-flop (T-ff), which is used as a divider by two counter to perform the same precoder function. Here, the T-ff clock is AND gated with the inverse version of the input data. Hence, the counter changes state only when the input data are high, and remains the same when these are low, which is equivalent to a module 2 function.

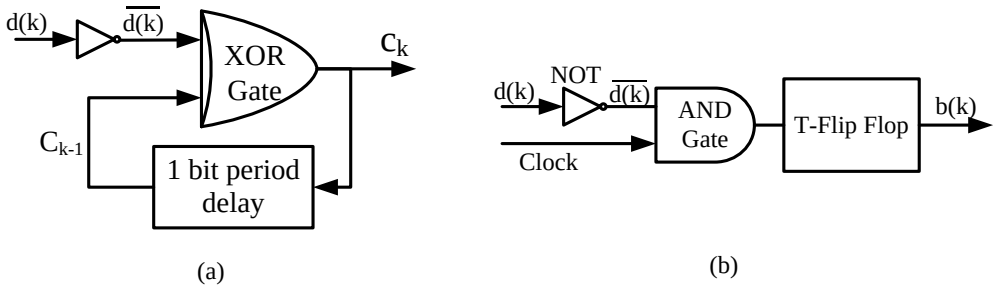

Figure 4 - 13: Duobinary Pre-coder: (a) Conventional Pre-coder, (b) Proposed Pre-coder

In the proposed duobinary coding scheme, which is shown in figure 4-14, the duobinary encoder is realised using a 5^{th} order Low Pass Filter (LPF) with Bessel transfer function and 2.5 GHz cut-off frequency. The purpose of the LPF is to generate the three level electrical signal for the 10 Gb/s Duobinary system. A single driver amplifier is utilised after the encoder to provide the required bias voltage to the optical transmitter.

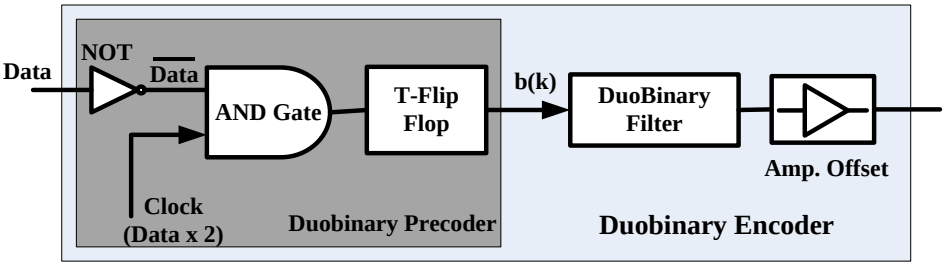

Figure 4 - 14: Proposed Duobinary Coding Scheme

4.7.2 Proposed Duobinary Transmitter

The Duobinary signal can be applied to an optical modulator biased at ($V_{\pi}/2$) to generate a three-level intensity modulated optical Duobinary signal as shown in figure 4-15a. Biasing the optical modulator at this point is essential to maintain the three optical intensity levels through the transmission. To keep up this criterion, the optical modulator extinction ratio in the case of Duobinary signal transmission must be degraded compared to the value used in the binary signal transmission case. As a consequence, the transmitted Duobinary signal might be susceptible to noise.

To overcome this limitation, a three-level optical electric-field signal can be created using MZM biased at its full biasing voltage as shown in figure 4-15b. In this form, the three electric field levels are translated to only two optical intensity levels, where a 0 is represented by a zero level and a 1 is transmitted by either an optical pulse (+E) or a $\boldsymbol{\pi}$ phase shifted pulse (-E), depending on the precoder formula. Therefore, this type of data signaling is sometimes called as an Amplitude Modulation Phase Shift Keying (AM-PSK) Duobinary modulated signal.

The generated (AM-PSK) duobinary signal has two levels in terms of the optical power, while it has three levels in terms of the optical electric-field domain. Thus, the signal optical electric-field spectrum, which the chromatic dispersion effects on, is still be halved relative to the conventional binary signal transmission. Subsequently, this format does not only increase the optical extinction as only two levels are being detected, but also reduces effectively the chromatic dispersion effects comparing to the conventional transmission formats.

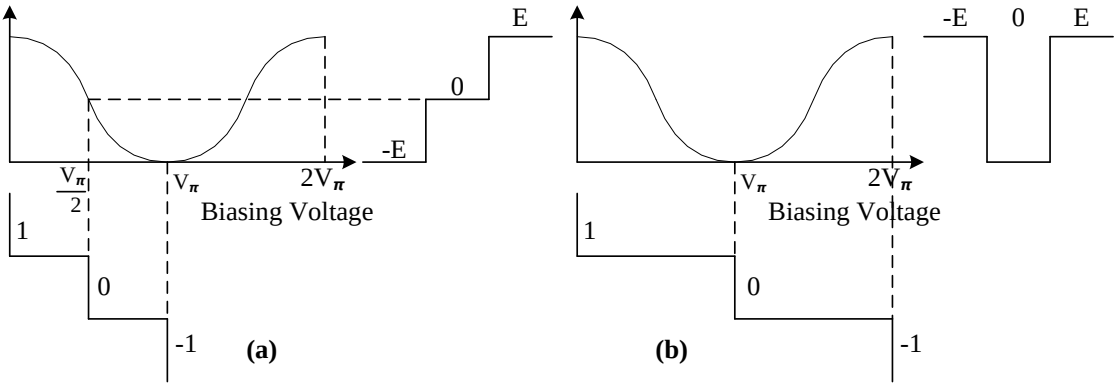

Figure 4 - 15: : MZM Biasing Conditions for Generating: (a) A Regular Duobinary Intensity Modulated Signal, (b) an AM-PSK Duobinary Modulated Signal

In our simulation, Duobinary transmitter uses a single driver amplifier with 2Vπ swing voltage to bias a standard single arm MZM at its null. Using such a single-arm MZM to generate the Duobinary modulated signal reduces the setup complexity and improves the transmission performance.

4.8 Efficient Transmission of a Digitised 16-QAM RF Signal

Against the related work and state of the art presented in sections (4.3) and (4.4) respectively, a cost-effective physical layer DRoF link is designed. In particular, the digitized transmission of a 16-QAM RF signal over SMF between the CS and BS is conceived.

Our ultimate goal is to improve the DRoF link performance more than the previous DRoF solutions discussed in section (4.3) by reducing the produced optical bandwidth. To achieve that, an optical duobinary coding/modulation scheme is proposed for the transmission of DRoF system without significantly increasing complexity. It is really important to mention that this work does not encompass the wireless transmission, but rather focuses on the fibre link design only. It will be shown that the proposed system reduces the spectral occupancy of the transmitted signals as well as counters the Inter-

Symbol Interference (ISI) effect induced by the chromatic dispersion. It will be tested as a separate transmission scenario for a digitized 16-QAM radio frequency signal. To highlight its proficiency, a comparison study will be conducted with a legacy DRoF system that uses non-return-to-zero (NRZ) coding scheme. Finally, DRoF transmission will be studied in coexistence with TWDM-PON standards with respect to the wavelength plan to ensure its compatibility with this technology.

4.9 Simulation Design of the Proposed DRoF Link

Figure (4.34) shows the structure of the proposed DRoF system which is implemented using VPItransmissionMaker^{TM} 9.5 simulator. In transmitter side, a data rate of 2.5 Gb/s is generated using Pseudo Random Binary Sequence (PRBS). This data is modulated with a carrier frequency of 5 GHz using the 16-QAM transmitter component provided by the simulator. The generated analogue 16-QAM RF signal is then down-converted to an intermediate frequency (IF) of 400 MHz using a combination of Local Oscillator (LO) at 4.6 GHz and mixer followed by a Low Pass Filter (LPF) with Bessel transfer function and order of 3. Table I shows simulation parameters used for the proposed DRoF system.

Table 4- 1 SIMULATION PARAMETERS

Parameter	**Value**
Modulation	16-QAM
Fiber Attenuation	0.2 dB/km
Fiber Dispersion	21 ps/nm.km
Laser Emission Frequency	187.266×10^{12} Hz
Laser Linewidth	1.0×10^{6} Hz
APD Responsivity	0.8 A/W
APD Thermal Noise	1.0×10^{-12} A/Hz$^{1/2}$

The direct baseband method of data communication is useful only for short distances provided the path is independent of any source of interference. If not, then there will be severe distortion in amplitude and the reception will be noisy. The only alternative for transmitting this baseband signal error-free is by way of some modulation which can reduce the noise factor induced by amplitude distortion. So, the baseband signal is always modulated for communication over long distances whether by wired or wireless communication[106].

Frequency down-conversion is essential before digitizing the RF signal in order to ensure that the produced IF signal will satisfy the Nyquist Criteria in sampling theorem, this is to avoid signal aliasing. Prior to digitalization process, IF signal has been normalized in our simulation according to the ADC dynamic range. The first step in digitizing the analogue IF signal is quantization, in which, the signal is divided into a number of levels according to the selected bit-resolution of the ADC. After that, the quantized signal is converted into a serial bit stream with a rate that is equal to the product of ADC sampling frequency by the ADC bit resolution. This was all achieved by using the ADC and the (integer-to-bit) components provided by the simulation program. Converting the bit stream into a baseband digital signal is achieved by the encoder. In our proposal, the digital data are encoded using the duobinary encoder presented in figure 4-13b. Here, digital data are differentially encoded using a simple binary digital circuit that consists of NOT Gate, AND Gate followed by a Toggle flip-flop (T-ff) so that to allow for easier recovery of binary data at the receiver. The output of the duobinary pre-coder is then encoded using LPF with a cut-off frequency of 7.5 GHz to obtain a 3-level electrical DB signal.

Finally, the produced signal is externally modulated using a single-arm Mach-Zehnder Modulator (MZM) biased at its null point resulting in a significant reduction of the transmitter complexity. The output optical signal will exhibit two levels in terms of power while preserving three-level nature in optical phase. The optical spectrum of the produced DRoF signal using NRZ coding and duobinary coding is shown in the inset of the figure 4-16.

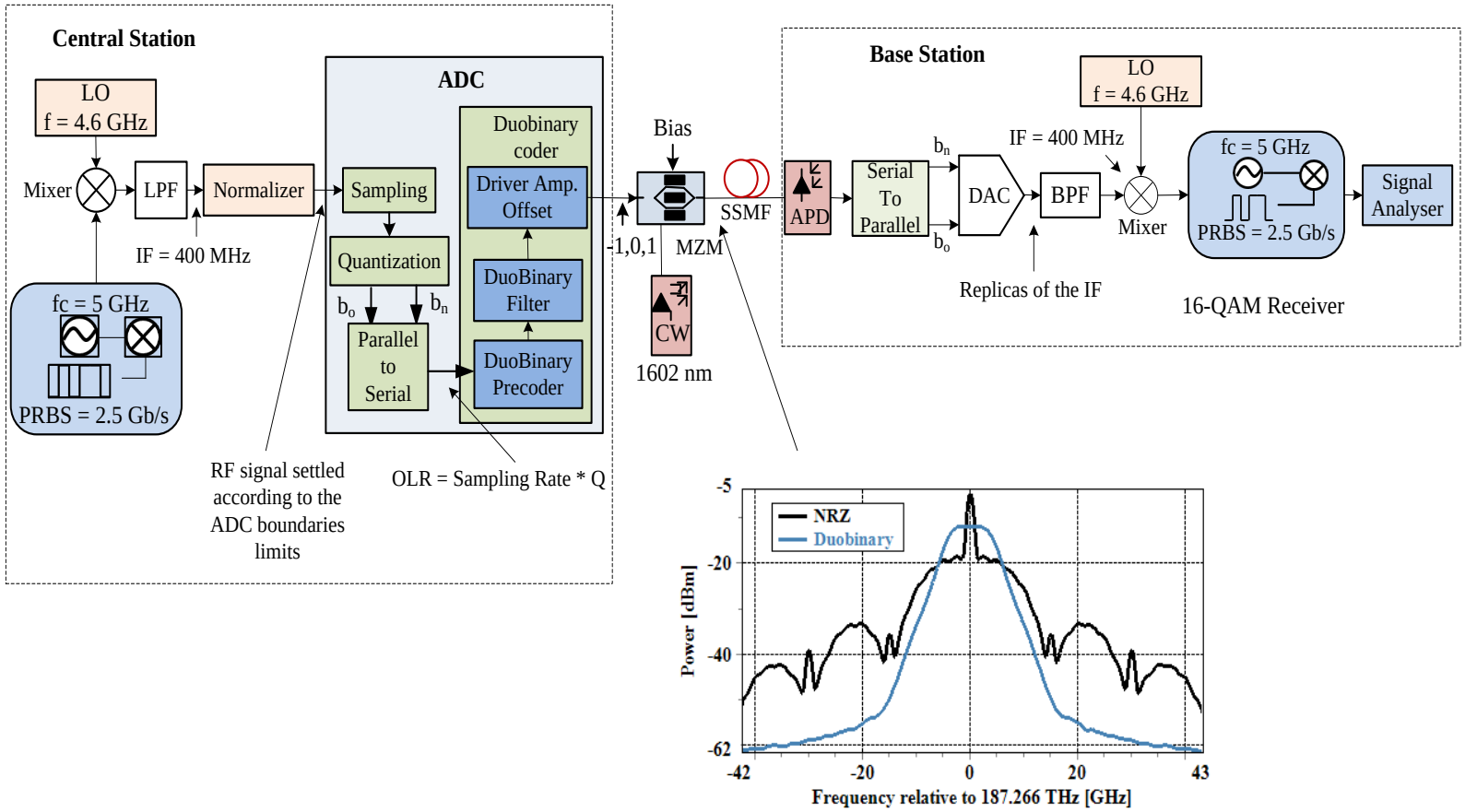

Figure 4 - 16: Proposed DRoF System

Most recent studies have shown that Next Generation-Passive Optical Network (NG-PON2) is the first PON standard to go beyond 10 Gb/s total bandwidth [20]. Hence, it was suggested that the NG-PON2 is the most promising candidate to provide the front-haul services using DRoF over CPRI interface. Time-Wavelength Division Multiplexing PON (TWDM-PON) was suggested to be the primary solution for NG-PON2 deployment. Moreover, according to the latest amendments to ITU-T-G989.2 (NG-PON2 specifications) [10], TWDM-PON is allocated between 1524-1544 nm in the C band for the upstream transmission, and between 1596-1603 nm for the downstream transmission. Therefore, in our proposed system, the modulated signal is transmitted over an (SSMF) using an optical source at 1602 nm emitted by CW laser source, which is equivalent to 187.266 THz, to examine the compatibility of our system upon NG-PON2 standards. A dispersion value of 21 (ps/nm.km) is considered in the simulation so that to be compatible with the used wavelength. Digitization process suffers from different types of interference such as jitter and quantization noise. Quantization noise directly influences the system performance as it limits its dynamic range. This error noise is distributed uniformly between ±LSB (Least Significant Bit) of the ADC. Signal to Quantization Noise Ratio (SQNR) for (M-QAM) signal is given by (4.15) [80]:

$$SQNR = 20\log_{10}\left[\left(\frac{\sqrt{M}+1}{3\sqrt{M}-3}\right)^{\frac{1}{2}}\sqrt{3}\,2^{Q}\right] = 6.02Q + 10\,log_{10}\left(\frac{\sqrt{M}+1}{\sqrt{M}-1}\right) \qquad (4.15)$$

where Q is the ADC resolution and M is the number of bits per symbol. According to (4.15), increasing the resolution yields to a significant improvement in the SQNR by about 6 dB. On the other hand, increasing Q will produce high optical line rate (OLR) (OLR = Sampling Frequency (*fs*) * Q), which will increase the system impairments. For this reason, ADC bit resolution has a great impact on DRoF implementation and performance.

At the receiver side, the optical signal is detected using APD photo-detector to obtain the baseband electrical signal, which is then converted from serial to parallel digital data. To recover the original analogue signal, parallel bit streams are processed using Digital to

Analog Converter (DAC). It must be noted that the analogue signal produced from the DAC will have spectral replicas of the original IF signal at intervals equal to the DAC sampling frequency. This is explained by (4.16), which states that the equivalent spectrum *R'(f)* of any RF signal *R(f)* sampled by a rectangular sampling function is obtained by convoluting an impulse train by a unit pulse functions [119], where *d* is the sampling rectangular pulse width, δ is the Dirac delta function, *Ts* denotes the sampling interval which is mutual to the DAC sampling frequency *fs*.

$$\acute{R}(f) = R(f)\, x \left(d \sum_{n=-\infty}^{+\infty} \left(\frac{\sin(n\pi d)}{n\pi d} \right) \delta \left(f - \frac{n}{T_s} \right) \right) \qquad (4.16)$$

A Gaussian transfer function Band Pass Filter (BPF) centred at the IF frequency with a bandwidth of 0.8 GHz is used to extract the IF signal from its replicas. The original RF signal is obtained through the frequency up-conversion process using LO and mixer. The received signal is then supplied to a 16-QAM receiver component provided by the software to evaluate the system performance in terms of the EVM and the BER merits.

4.10 Performance Results and Discussion of the Designed 16-QAM DRoF Link

The obtained results are discussed in this section to evaluate the proposed DRoF system performance. As noted earlier, the overall bit rate in the optical link could be extremely high which needs a higher requirement of the optoelectronic devices. It has been mentioned in section (4.3) that a trade-off between the ADC sampling rate and the ADC bit resolution might be needed to mitigate heavy bandwidth demands on the optical link. We aimed here to reduce the produced optical bandwidth using a bandwidth-efficient modulation scheme, which is based on DB coding. To evaluate our proposed system, we

compared it with a DRoF system uses the legacy NRZ coding. In figure 4-17, the EVM is plotted versus the fibre length for a certain value of resolution (Q=4). With this value of ADC resolution, the produced optical line rate is 10 Gb/s.

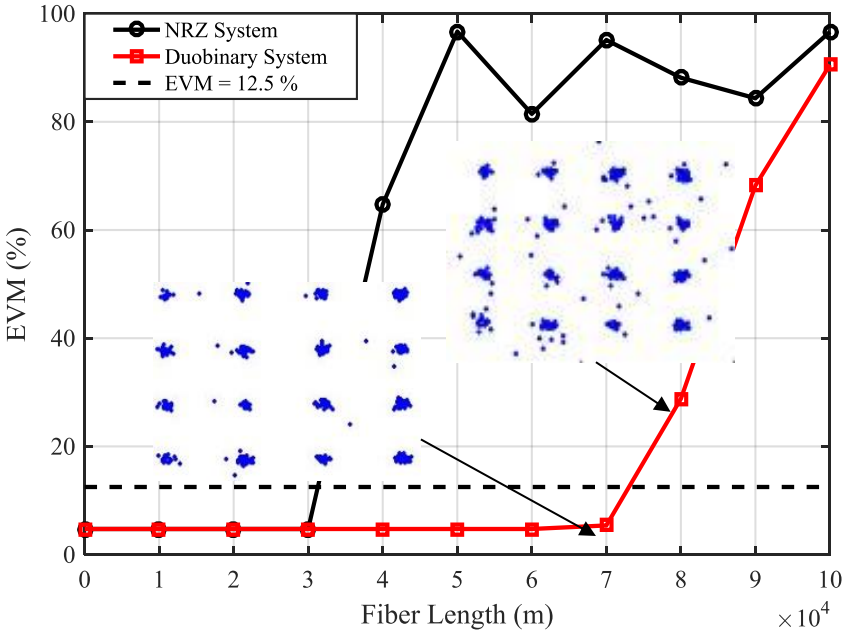

Figure 4 - 17: EVM versus Fibre Length measured at ADC Resolution = 4 bits

It can be seen that the EVM in the NRZ system remains constant until 30 km only and below the limit of 12.5% which is the required limit according to the 3GPP specifications. As the distance is increased, EVM values are increased accordingly due to the chromatic dispersion effect in the fibre. On the other hand, the proposed system is capable of maintaining EVM values up to 70 km of transmission distance for the same 10 Gb/s digital signal. Employing the DB modulation in DRoF transmission has two advantages. First, DB coding reduces the spectral bandwidth of the baseband signal, and consequently the overall optical bandwidth. Second, the ISI effect induced by the chromatic dispersion in fibre is reversed positively by using the DB precoding scheme. A small penalty between 60 and 70 km is experienced, but the transmission is not that much affected, and the EVM value still below the requirement as illustrated by the constellation diagrams shown in the inset of figure 4-17.

4.10.1 Effect of ADC/DAC Bit Resolution on the Link Performance

BER performance versus the received optical power is presented in figure 4-18 for various ADC/DAC resolution values. All measurements were taken at 20 km transmission distance so that to emphasize the impact of increasing the bit resolution on the BER as a function of the receiver sensitivity. To achieve a fair and acceptable performance comparison, BER of $1.0e^{-6}$ is considered as a sensitivity measurement level for both systems. In the NRZ system, figure 4-18(a), to achieve an acceptable BER performance, ADC bit resolution must not exceed 5 bits, leaving the system more affected by the quantization noise and bandwidth limited as well. A power penalty of 4.5 dB is measured as the bit resolution increases from 3 to 5 due to the dispersion effect signifying the impact of increasing the ADC bit resolution on the transmission performance. Figure 4-18(b) depicts the BER performance in the duobinary system for various bit resolution values. It can be seen that the BER performance in the proposed system is less affected by increasing the ADC bit resolution even if this causes an increase in the bandwidth requirement. Unlike NRZ system, duobinary system has nearly the same receiver sensitivity value of -17.1 dBm measured at resolution values of 5-to-8 bits to satisfy the BER limit. A small penalty of 0.6 dB is observed between the performances of 3-to- 5 bits. This confirms that a DRoF system based on duobinary modulation scheme can transmit a digital signal of 20 Gb/s (8 bits * 2.5 GHz) with receiver sensitivity better than the compared system, which can only transmit a maximum bit rate of 12.5 Gb/s (5 bits * 2.5 GHz).

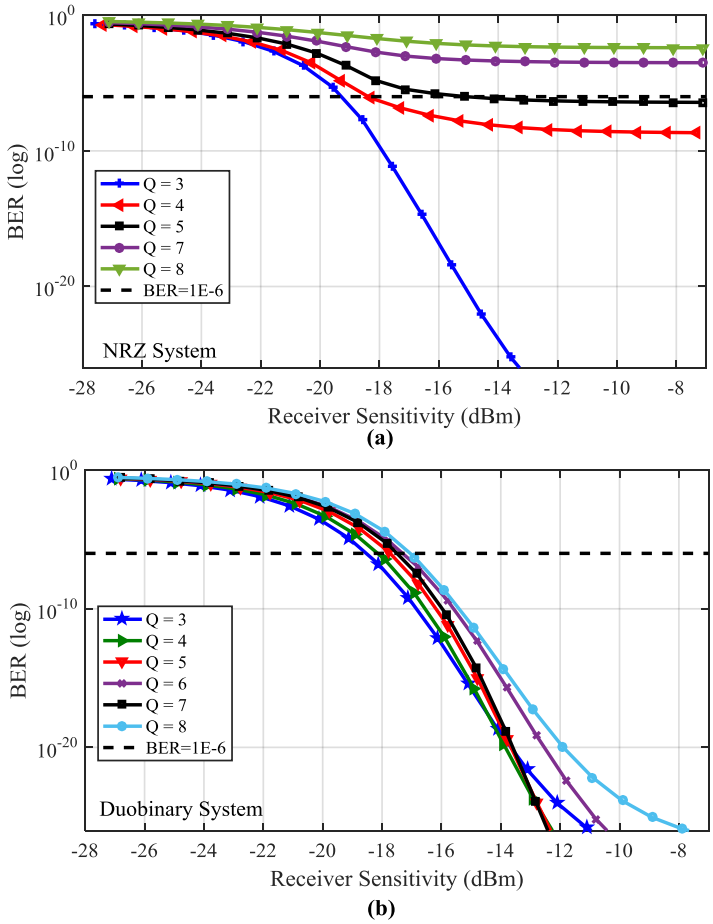

Figure 4 - 18: BER versus Receiver Sensitivity Measured at 20 km Fibre Distance: (a) DRoF System Uses NRZ Coding, (b) DRoF System Uses Duobinary Coding

Similarly, BER performance was calculated versus the OSNR for various bit resolution (from 3 to 8) bits. The OSNR is changed by creating a sweep control parameter that varies the OSNR values between (0 – 35) dB using this module and running the simulation repeatedly in accordance to the variation happening in the OSNR while measuring the received BER at each iteration. Figure 4-19(a) shows that BER threshold is reached at a resolution value of 5 bit in the NRZ system and the measured OSNR value is equal to 31 dB. Figure 4-19(b) illustrates BER performances of the duobinary system at different ADC

resolution bits as a function to the received OSNR. These results show that the duobinary system with ADC bit resolution of 8 can improve the power budget by 4 dB measured at BER of 10^{-6} relative to the NRZ system with a resolution of 5 bits only.

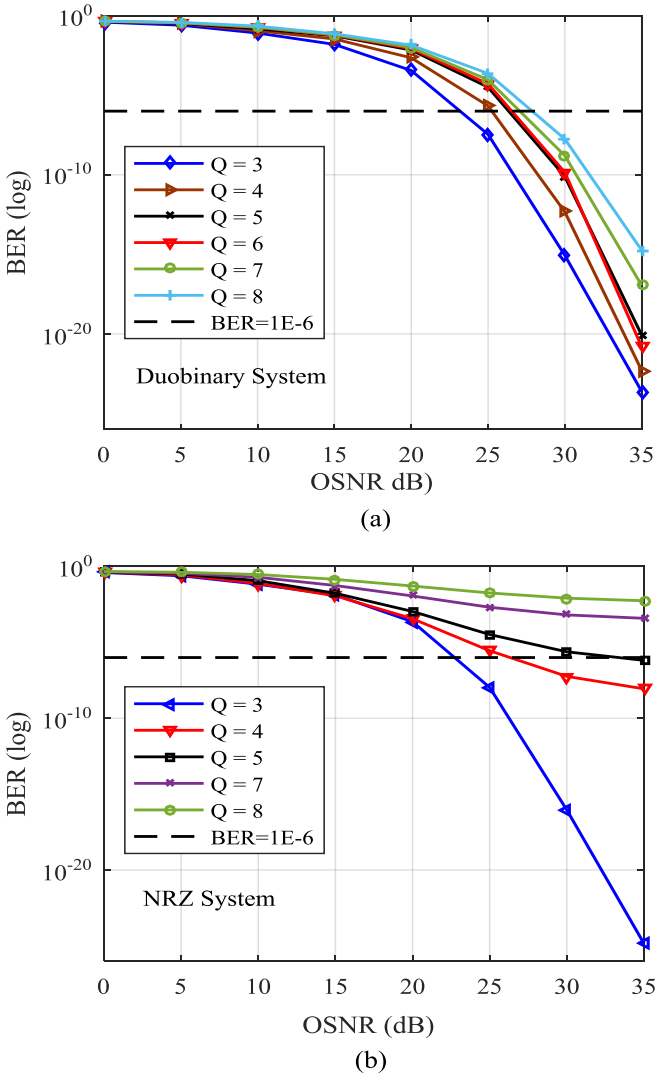

Figure 4 - 19: BER versus OSNR Measured at 20 km Fibre Distance: (a) DRoF System Uses Duobinary Coding, (b) DRoF System Uses NRZ Coding

To highlight how the duobinary system contributes to overall OLR, we calculated the SQNR at 20 km fibre distance for different ADC resolution values and compared with the theoretical SQNR obtained from equation (4.15) as shown in figure 4-20. While SQNR values increasing linearly by 6 dB in accordance with the resolution bits, duobinary system proves that it is possible to achieve high data rate transmission that reaches up to 10 Gb/s and BER $1e^{-9}$ at satisfactory SQNR values around 30 dB.

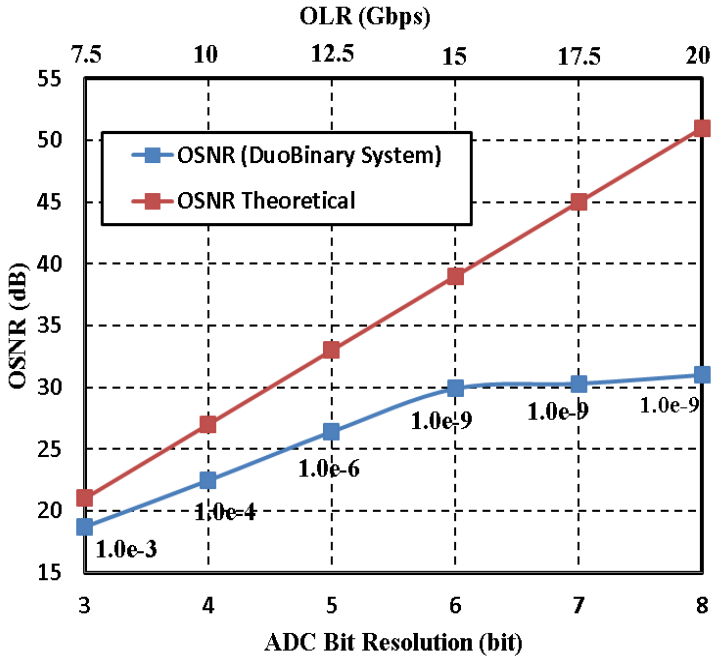

Figure 4 - 20: Comparing the Duobinary System's SQNR with the Theoretical Values

4.11 Chapter Conclusion

In this chapter, a detailed study of the digitized transmission of the RF signals over fibre (DRoF) has been presented. The techniques used for digitizing the analogue signals have been reported. In order to achieve a cost-effective physical layer design to the DRoF link, baseband sampling technique has been considered with the aid of RF-to-IF conversion. The implementation challenge that DRoF systems faces, which is mainly, high optical

bandwidth requirement has been investigated. The main conclusion of this chapter can be summarized as follows:

- An optical bandwidth-efficient modulation scheme based on Duobinary coding has been proposed to reduce the spectral occupancy of the transmitted DRoF signal over fibre.
- The intersymbol interference (ISI) effect induced by the chromatic dispersion in fibre has been addressed as well using the proposed transmission scenario.
- To highlight the designed system proficiency, performance comparison with a DRoF system uses the legacy non-return-to-zero (NRZ) coding scheme has been conducted.
- Simulation results have shown that a DRoF system employs Duobinary modulation is highly resilient to dispersion effect as well as to the ADC resolution bits.
- It has been shown that the proposed link allows the DRoF signals to be transmitted over longer fibre distances relative to the previous DRoF solutions.
- It has been shown that the proposed system is compatible with the NG-PON2 standard by means of the wavelength plan. Moreover, all measurements taken have been tested and verified according to the 3GPP specifications.

Chapter 5

Advanced Design of DRoF Transmission Link

5.1 Overview

The high optical bandwidth requirement in Digital Radio over Fibre (DRoF) technology represents one of the major design constraints. In this chapter, a DRoF system that integrates the duobinary coding scheme with the optical single sideband (OSSB) transmission is proposed. This system reduces the spectral occupancy of the transmitted signals as well as the chromatic dispersion effects induced by fibre in both the electrical and optical domains. The OSSB signal is created by driving two cascaded optical modulators with a combination of a baseband digital signal and the Hilbert Transform of that signal. The transmission performance of a digitised 16-Quadrature Amplitude Modulation 16-QAM radio frequency signal with a bit rate of 1.25 Gb/s over a Standard Single Mode Fibre (SSMF) is investigated. By means of simulation, the results show that the transmission length can be extended by 75% and 16.6% relative to the case of transmitting a DRoF signal using Double Sideband (DSB) and Single Sideband (SSB) transmission formats, respectively. The power budget is improved by 10 dB compared to the SSB case with respect to the measured OSNR at 70 km fibre distance while maintaining the EVM below the value specified by the 3GPP release 13.

5.2 Introduction

Radio over Fibre (RoF) technology has been considered as the most promising solution to cope with the exponential growth in mobile data traffic. Such RoF technology can provide the essential platform required to build a Centralised Radio Access Network (C-RAN). Under C-RAN, a new architecture is proposed based on connecting the Remote Radio Heads (RRHs) to a central baseband processing unit (BBU) via an optical distribution network called the "fronthaul". However, transmitting RF signals over fibre in the analogue domain needs to have an infrastructure that is capable of supporting high carrier frequencies by adopting analogue optical devices with high linearity. Analog RoF (ARoF) systems are highly vulnerable to nonlinear distortion, such as Intermodulation Distortion (IMD) and the link dynamic range degrades linearly with increasing transmission distance. Furthermore, the Chromatic Dispersion (CD) effect in such a communication system represents one of the major challenges that limit both the transmission bandwidth and distance, consecutively. Telecommunication operators have considered the fronthaul link as a purely digital entity that is based on either the Common Public Radio Interface (CPRI) or the Open Base Station Architecture Initiative (OBSAI) protocols. In accordance with the above, Digital RoF (DRoF) has recently been suggested as a feasible alternative to ARoF, as it can remove linearity concerns in the optical devices. The key components in DRoF systems are the Analog-to-Digital Converter (ADC) and Digital-to-Analog Converter (DAC), which are employed to digitise RF signals, hence enabling the optical modulation to be performed in the digital domain.

However, the digitisation process produces an extremely high digital transmission rate that requires high optical bandwidth since it is equal to the product of the ADC sampling rate by the ADC bit resolution. DRoF performance can be improved by increasing the sampling rate and/or the bit resolution, but this may place high Capital Expenditure (Capex) and Operational Expenditure (Opex) challenges in terms of hardware

implementation [73]. Many approaches have been proposed to circumvent the high optical bandwidth bottleneck related to this technology [120].

On the other hand, the use of multilevel modulation and partial response signalling has attracted substantial research interest, as they can reduce the spectral width of the baseband signal [121], [122]. Much of the research on increasing the bandwidth efficiency of Mobile Front-Haul (MFH) based DRoF technology has relied on multilevel modulation formats [111], [123], with relatively complex demodulation schemes at the receiver side. In the same context, transmitting the digital signal in an Optical Single Sideband (OSSB) form allows for the effects of chromatic dispersion to be reduced relative to transmission in double sideband (DSB) form [124].

In this chapter, a transmission scenario based on the integration of a duobinary coding scheme with a digital (OSSB) modulation format is proposed for DRoF transmission. As a result, in this system, the overall transmission bandwidth is reduced over two stages; First, in the electrical domain using duobinary encoding and the second, in the optical domain using OSSB transmission. By doing so, the performance of DRoF link is greatly improved as the nonlinear impairments are directly related to the transmission bandwidth. The utilised OSSB structure is modified in terms of the biasing voltages and the driving signals in order to be compatible with the three-level duobinary signal. Also, the use of duobinary signalling has two advantages over the conventional coding schemes, such as Non-Return-to-Zero (NRZ). First, it is more tolerant to chromatic dispersion compared to NRZ and hence, offers a reach extension. Second, it introduces the Inter-Symbol Interference (ISI) induced by the chromatic dispersion in a controlled manner that reverses its effect positively at the receiver side.

A comparative study is demonstrated between the proposed system and each of a DRoF link based on the OSSB and Optical Double Sideband (ODSB) transmission formats, which both use the NRZ encoding scheme. A comprehensive analysis and performance evaluation of the proposed system is undertaken using VPITransmission Maker as a simulation tool, which is only focused on the optical network design.

5.3 Related Work

The most recent work in the area of bandwidth optimization of DRoF links are summarized as follows:

1- Two transmission approaches to reduce the optical bandwidth of high data rates transmission requirement in the Mobile Fronthaul (MFH), namely an analogue based-IFoF and an Ethernet-Based digital MFH have been investigated in [120]. Both solutions have achieved an EVM less the 3GPP LTE threshold for transmitting 10 Gb/s data rate over 20-40 km fibre distances. However, for higher data rates, the investigated approached are limited to few kilometres of distance due to the chromatic dispersion effect.

2- Experimental demonstration of a digitized MFH based on one-bit and two-bit Δ-Σ modulation to replace the high optical bandwidth on DRoF based-CPRI have been presented in [111]. A 32 LTE carrier aggregated signals were digitized and transmitted using 4-levels Pulse Amplitude Modulation (PAM-4) over 25 km optical distance. Results have shown that high order QAM up to 256QAM and 1024QAM with EVM than 5% and 2.1%, respectively can be achieved. Moreover, it has been proved that the fronthaul capacity can be increased by four times relative to the conventional CPRI-based MFH without significant EVM penalty.

3- The performance of a DRoF system transmitting high order QAM signals has been evaluated in [72]. The simulation results have shown that the DRoF systems can reach longer distances than ARoF while maintaining the standard EVM limit of the QAM signals.

4- Analysis and experimental demonstration of a DRoF system uses an Envelope Delta-Sigma Modulation (EDSM) are presented in [110]. It has been verified that this system can support the requirements of a (760 MHz – 2.6 GHz) 3GPP LTE bands and IEEE 802.11g WLAN standards.

5- Experimentally, an improved MFH link employing high order Δ-Σ modulation and PAM-4 format have been proposed in [125]. It has been verified that a digitized transmission of a 32 4G-LTE carrier aggregation signals with a data rate of 39.32 Gb/s based-CPRI protocol is achievable. The overall quantization noise was obtained with 68% improvement for the average EVM performance compared to the MFH based on single-bit Δ-Σ modulation.

5.4 Optical Single Sideband Transmission

The frequency spectrum of a signal modulated using one of the amplitude modulation schemes, such as OOK-NRZ, m-QAM and PAM is double sided with redundant information conveyed in both the lower and upper sidebands of the carrier signal. Single Sideband (SSB) transmission has been proposed to reduce the bandwidth occupancy by a factor of two and to improve the SNR at the receiver in systems with analogue RF signals modulated onto an optical carrier [126]. A similar approach has been utilised with the digitised transmission of the information signals over fibre [127][124].

The main focus of this chapter is employing OSSB transmission format in the DRoF link design. The first benefit is to increase both the spectral efficiency and the link performance as the fibre nonlinearities are mostly dependant on the transmission bandwidth. A second and even more significant advantage behind transmitting the DRoF signal in the OSSB form is that it allows for chromatic dispersion to be reduced in relative to the customary transmission in the DSB form. This is attributed to the fact that the spectral bandwidth of the transmitted signals has been reduced by a factor of two. It was mentioned in chapter 2 that the GVD is proportional to the square value of the frequency. Therefore, if the optical bandwidth is reduced by a factor of two, dispersion penalty due to first order GVD would be reduced by a factor of four.

5.5 Generating of Digital OSSB Signal

Several approached have been proposed to directly generate a broadband, digital OSSB signal. However, the main goal is to create an OSSB transmitter that is chirp-free to excess dispersion penalty on transmission, and relatively easy to implement. An SSB signal can be created using Hartly modulator, which can be represented as [128]:

$$S(t)_{SSB/_{U,L}} = m(t)\cos(2\pi f_c t) \mp \hat{m}(t)\sin(2\pi f_c t) \quad (5.1)$$

where, plus and minus signs produce the lower and upper sidebands, respectively. *m(t)*, is the modulating signal. *m^(t)*, is the Hilbert Transform (HT) of the modulating signal, where a 90^o phase shift is performed to all frequencies contained in that modulating signal. Figure 5-1 shows the block diagram for generating an SSB signal using Hartly modulator.

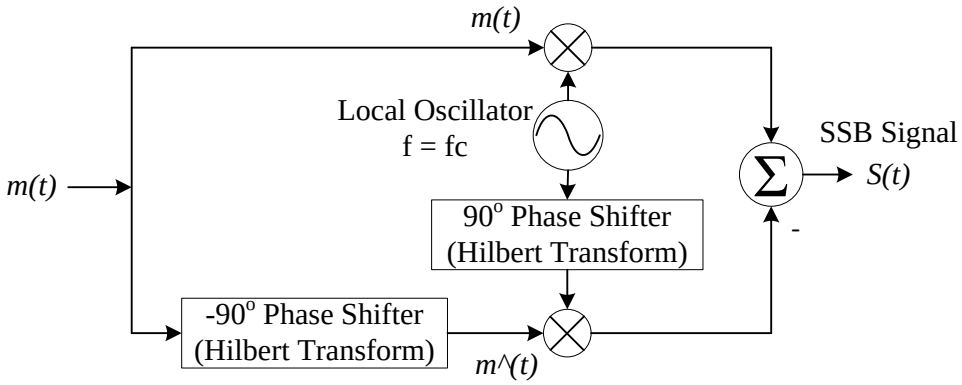

Figure 5- 1: Hartly Modulator for Generating SSB Signal

Mathematically, Hartly modulator can be implemented for both digital and analogue RF signals. A baseband SSB signal can be obtained using the complex representation of that baseband modulating signal, which is given by:

$$g(t) = m(t) \mp j\hat{m}(t) \quad (5.2)$$

Equation (5.2) gives rise to the SSB signal of (5.1), which can be shown that it has both an amplitude and phase modulation components as follows:

1- Amplitude modulation component is represented by the real part of the complex form of (5.2):

$$|g_r(t)| = \sqrt{m^2(t) + \hat{m}^2(t)} \quad (5.3)$$

2- Phase modulation component is given by:

$$\emptyset = g_i(t) = \tan^{-1}\left[\frac{\mp\hat{m}(t)}{m(t)}\right] \quad (5.4)$$

As a result, a digital OSSB signal can be generated by cascading a chirp-free amplitude optical modulator driven by the real part of the baseband modulating the signal, with a phase modulator driven by the HT of that baseband signal [77].

5.6 Design of the Proposed Digital OSSB Transmitter

Figure 5-2 below shows a schematic diagram of the OSSB modulator used in the proposed DRoF system.

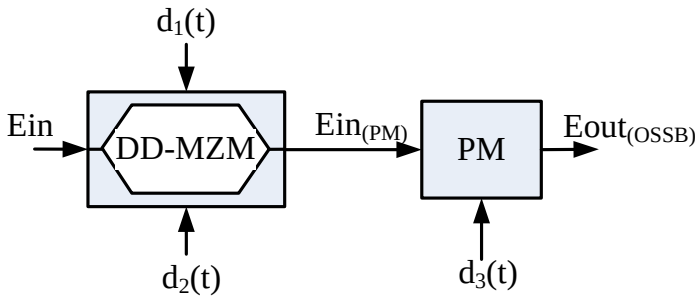

Figure 5- 2: Optical Single Sideband Transmitter Configurations

It consists of a Dual Drive Mach Zehnder Modulator (DD-MZM) followed by a Phase Modulator (PM). An OSSB baseband digital signal is achieved using this configuration without the requirement for an optical filter. The electrical field output of the chirp-free DD-MZM and PM is represented in (5.5) and (5.6), respectively:

$$E_{out(DD-MZM)} = E_{in(PM)} = \frac{E_{in}}{2} exp\left(j\pi \frac{d_1}{V_\pi}\right) + \frac{E_{in}}{2} exp\left(j\pi \frac{d_2}{V_\pi}\right) \quad (5.5)$$

$$E_{out(PM)} = E_{out(OSSB)} = E_{in(PM)} exp\left(j\pi \frac{d_3}{V_\pi}\right) \quad (5.6)$$

where, V_π is the modulator biasing voltage, whilst d_1, d_2 and d_3 are the electrical drive signals, which were set up in our simulation as follows:

$$d_1(t) = xV_\pi m(t) - \frac{V_\pi}{2} \quad (5.7)$$

$$d_2(t) = -xV_\pi m(t) + \frac{V_\pi}{2} \quad (5.8)$$

$$d_3(t) = xV_\pi \hat{m}(t) \quad (5.9)$$

where x is the modulation index, $m(t)$ is the original version of the encoded baseband digital signal and $m\hat{}(t)$ is the Hilbert Transform of $m(t)$. Mathematically, the SSB signal can be obtained by using the Tylor series expansion to solve the resultant equation from substituting each of (5.7), (5.8) and (5.9) into (5.5) and (5.6), and by taking only the first order terms (i.e. the linear terms).

$$E_{out(OSSB)} = exp(j\omega_\circ t) exp\left(jz\hat{m}(t)\right) \cos\left(zm(t) - \frac{\pi}{4}\right) \quad (5.10)$$

where, $z = \pi x$. It can be seen from (5.10) that the output SSB signal represents the cascade of amplitude modulation (cosine term) and phase modulation (exponential term).
By means of simulation, all above analysis have been set up by considering *m(t)* is the ADC output baseband digital signal, *m^(t)* is the Hilbert Transformed version of *m(t)*, V_π equal to 5 V, and x equal to 0.2.

5.7 Hilbert Transformer Design

The discrete time impulse response of the Hilbert Transformer or 90^o phase shifter is given as [128]:

$$h(n) = \begin{cases} \frac{2}{\pi}\frac{\sin^2(n\pi/2)}{n} & for\ n \neq 0 \\ 0 & for\ n = 0 \end{cases} \qquad (5.11)$$

Figure 5-3 shows the impulse response of an ideal Hilbert transformer.

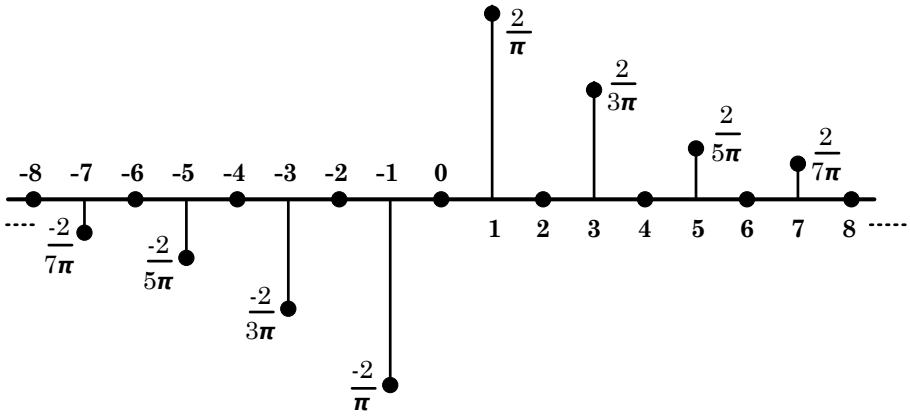

Figure 5- 3: Impulse Response of an Ideal Hilbert Transformer

Thus, a discrete time Hilbert transform can be formulated using a casual low-pass Finite Impulse Response (FIR) digital filter with constant group delay since they have the same impulse responses. The ideal FIR transfer function is expressed as [129]:

$$H(z) = \sum_{n=0}^{N-1} h[n] z^{-n} \tag{5.12}$$

where n is the filter order, N is the filter length and z^{-n} represents the unit delay (τ) between filter's taps, which can be calculated as:

$$Unit\ Delay = \tau = \frac{N-1}{2 * f_s} \tag{5.13}$$

where f_s is the sampling frequency.

In our proposal, the Hilbert transformer needed for the drive signal of PM is designed by considering an anti-symmetric FIR digital filter with an odd length of 7 (order 6), as shown in figure 5-4 below, since it is more stable. The FIR filter order is truncated to this order as the improvement in the performance using more than 6 taps is minimal.

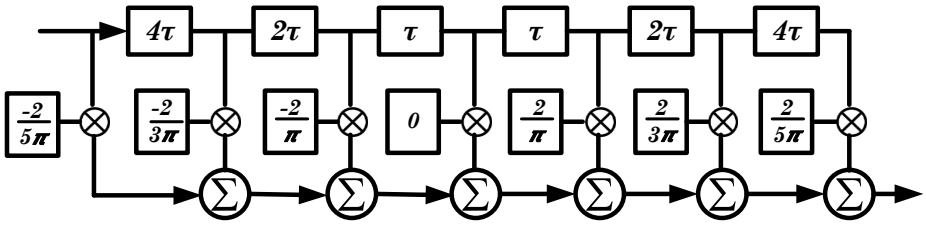

Figure 5- 4: FIR Filter Designed as Hilbert Transformer

5.8 Integration of OSSB Transmission with Duobinary Signalling

It was mentioned in chapter 2 that one technique of limiting the chromatic dispersion impact is to reduce the optical bandwidth that is required to transmit a given bit rate. It was also mentioned in chapter 4 that transmitting the digital signal in duobinary format reduces the chromatic dispersion as the effective transmission bandwidth for duobinary transmission is one-half relative to the conventional binary transmission. Moreover, it has been found that encoding the digital data at the transmitter using duobinary signalling scheme introduces the ISI in a controlled manner at the receiver which counteracts its effect.

Implementing the duobinary signalling in the OSSB transmission would then result in an even more bandwidth reduction. With this implementation, the transmission bandwidth is furtherly reduced from both the duobinary coding format and the OSSB status to the optical electric-field signal. However, it must be mentioned that integrating the duobinary signalling with the OSSB transmitter would only be possible if the biasing points of the MZM are chosen so that to maintain the three levels manner of the Duobinary signal through the transmission. In this case, $m(t)$ in equation (5.10) would represent the three-level signal. Therefore, the amplification parameter (x) of $m(t)$ must be relatively small, so that to maintain the three-level signal and hence to deter signal distortion upon detection, and also to gain a good sideband cancellation in the resultant optical signal.

5.9 Proposed System Simulation

The proposed system is simulated using VPItransmission Maker V9.5 and the system structure is shown in figure 5-6. In this system, a carrier frequency of 5 GHz is modulated with a bit rate of 1.25 Gb/s using a 16-QAM modulation scheme. The modulated RF signal is then down-converted into an Intermediate Frequency (IF) of 400 MHz to alleviate the sampling frequency requirements of the existing ADC, according to the Nyquist criteria in the sampling theorem. Frequency down-conversion is established using a combination of a

Local Oscillator (LO) of 4.6 GHz and mixer, followed by a Band Pass Filter (BPF) with BW of 400 MHz. This bandwidth value was chosen since it covers the minimum bandwidth requirements for the 16-QAM RF signal with a data rate of 1.25Gb/s [80]:

$$B = \left(\frac{f_b}{\log_2 M}\right) \tag{5.14}$$

where B is the minimum Nyquist bandwidth, f_b is the channel capacity (bps) and M is the number of discrete signal or voltage levels. The dynamic range limits of the utilised ADC lie between 0 and -1 and thus, a normaliser is used to match the amplitude of the input signal in accordance with the ADC limits. The digitisation process is performed by the ADC component provided by the simulator.

In our design, the intention was to use a different coding scheme and consequently, the existing ADC processes are redesigned so as to be compatible with our requirements. Initially, the signal is quantised into a number of levels given by 2^n, where n is the ADC bit resolution and thus, the signal is transferred into a discrete time signal with multi-level integer values. The digital bit stream is obtained by an integer-to-bit converter. The obtained bit stream is converted into a serial sequence and then coded using the duobinary coding scheme presented in chapter 4. The output of the duobinary precoder is pulse-shaped using a Butterworth LPF with 3-dB cut-off frequency at 2.5 GHz, which is 25% of the resultant bit rate, so as to achieve a 3-level baseband signal. The eye diagram of the corresponding electrical duobinary signal is shown in the inset (a) of Fig. 8, which has two eyes since duobinary has two decision thresholds. Whilst the duobinary signal is a 3-level signal in terms of the electrical domain, it exhibits two levels in terms of the optical power while preserving a 3-level nature in the optical phase. This is, in turn, reduces the ISI effect as an opposite phase between any adjacent one-bits will be introduced. At the optical stage, the digitised RF signal is externally modulated using the following categories: Optical Double Sideband (ODSB) that applies the Non-Return-to-Zero (NRZ) coding scheme, Optical Single Sideband (OSSB) transmission using the NRZ coding scheme as well and finally, OSSB that employs duobinary coding format. Regarding the

ODSB transmission, the DD-MZM is set up as a balanced Mach-Zehnder Modulator by disabling the upper DC and the lower RF drive inputs as shown in figure 5-5.

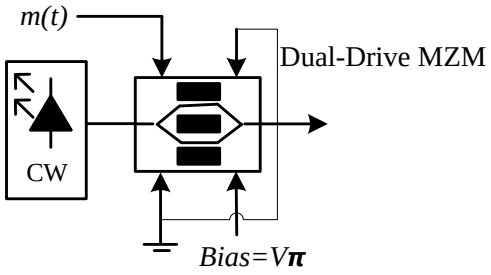

Figure 5- 5: Digital Optical DSB Transmitter

It is important to note that the three transmission scenarios use the same pulse-shape LPF characteristics, which is placed after the coding stage. In the proposed system, the OSSB transmission is performed using the configuration shown in figure 5-6, in which the duobinary coded modulating signal is fed to two paths. One goes to the Low Pass FIR digital filter presented in figure 5-4 to achieve the Hilbert Transformation (HT) required for the drive signal of the PM. The second path is applied equally to each arm of the dual-drive MZM (DD_MZM), which has the same DC bias voltage of ($V\boldsymbol{\pi}/2$) for each arm in order to drive the modulator between the maximum and minimum extinction ratio. The amplitude of the RF drive signals applied to each arm is equal to $V\boldsymbol{\pi}$ multiplied by the modulation depth (x). The output of the DD-MZM and the FIR digital filter are both modulated using the PM to obtain the required OSSB signal, which is then transmitted over a Standard Single Mode Fibre (SSMF) using a continuous wave (CW) laser source with a wavelength of 1552nm.

A PIN photo-detector is used at the receiver side to detect the transmitted baseband signal, which is regrouped from serial to parallel in order to be processed by the DAC component so as to recover the analogue IF signal. The DAC output signal has spectral replicas repeated at frequency points equal to the sampling frequency (f_s) [119], as shown in the inset of figure 5-6. Therefore, a Gaussian function BPF centred at the IF value is used after the DAC to extract the IF signal from its replicas. Finally, an LO and mixer are used to

regenerate the RF signal, which is analysed in terms of the received BER, EVM, Q-factor, Eye-Opening Penalty and OSNR, using the 16-QAM receiver component provided by the simulation software

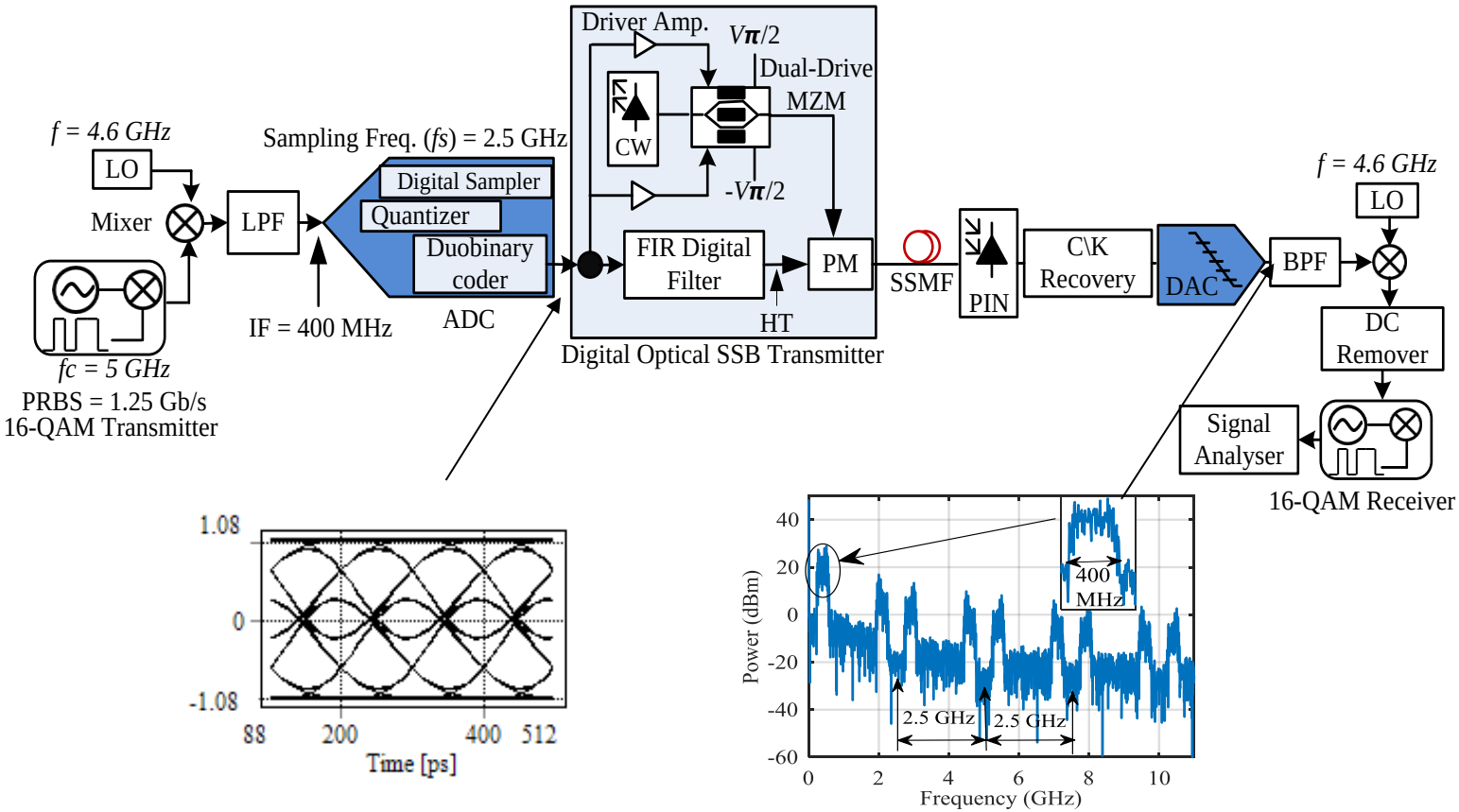

Figure 5- 6: Proposed System Structure

5.10 Simulation Results and Discussion

The overall bit rate in the DRoF transmission system is equal to the product of the ADC sampling rate by the ADC bit resolution. It is evident that DRoF system with ADC bit resolution of 4 bits and ADC sampling rate of 2.5 GHz can achieve acceptable performance [104], thus all measurements were taken at these values. In other words, the transmission of a 5 GHz 16-QAM RF signal with a bit rate of 1.25 Gb/s is mapped into a digital signal with an overall bit rate of 10 Gb/s for the optical link. To show the distinction of the proposed system, the performance of the designed transmission technique has been compared to those of two other transmission formats, namely ODSB and OSSB, using the same simulation parameters that are listed in table 5-1 below.

Table 5- 1 SIMULATION PARAMETERS

Parameter	**Value**
Modulation	16-QAM
Fiber Attenuation	0.2 dB/km
Fiber Dispersion	16 ps/nm.km = 16×10^{-6} s/m^2
Laser Emission Frequency	193.1×10^{12} Hz
Laser Linewidth	1.0×10^{6} Hz
APD Responsivity	0.9 A/W
ADC Resolution	4 bits

The MZ modulator in the case of ODSB is driven to full extinction, while the DD_MZM and PM in the OSSB case are driven to levels so that they optimise the received EVM. This was achieved by using a modulation depth x of 0.2 and biasing voltage V$\boldsymbol{\pi}$ of 5 V in the OSSB case. The comparison of the produced DRoF optical spectrum for the three transmission scenarios is shown in figure 5-7. It clearly demonstrates that the OSSB spectrum has not completely cancelled the unwanted sideband, which is the upper

sideband and the suppression ratio is about 4.38 dB. This imperfect suppression is a result of the signal driving the PM as it is not the perfect Hilbert Transform of the modulating signal.

It also can be seen that the OSSB transmission that employs duobinary coding scheme requires much less bandwidth while reserving the same data rate. In addition, more than 2 dB suppression ratio was achieved in the unwanted sideband. This contributes to the high bandwidth reduction due to the use of the duobinary coding scheme that shows more effect on the optical spectrum than that of the OSSB.

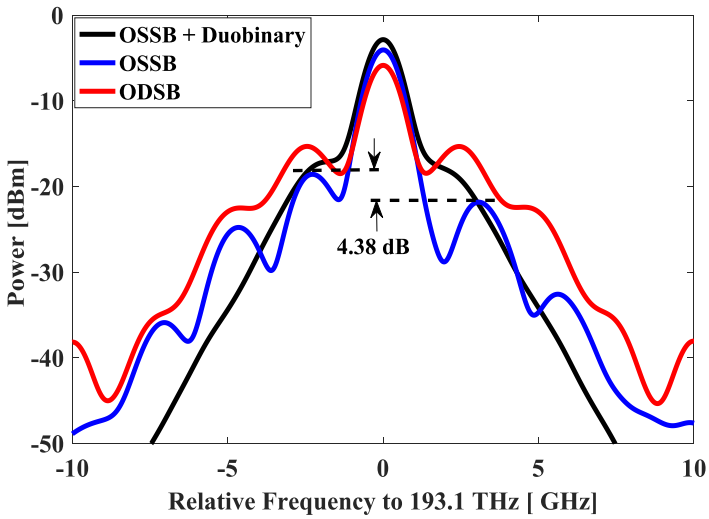

Figure 5- 7: Optical Spectrum of the Three Transmission Scenarios

It should be noted that the value of the sampling frequency default parameter in the simulation session was chosen to be 80 GHz. According to (13), the delay time τ between the FIR filter taps is calculated to be 31.25 ps for the incoming 10 Gb/s bit rate. Figure 5-8 plots the receiver sensitivity of the three compared systems versus fibre distance. To achieve a fair comparison, the receiver sensitivity was calculated based on a received BER of 10^{-4}, which is acceptable for a 16-QAM transmission system without the requirement of error correction.

It must be noted that receiver sensitivity is defined as the minimum average received optical power required to achieve a fixed BER. It is measured in our simulation by using a receiver sensitivity evaluator that evaluates the receiver sensitivity defined as a received optical power required for achieving the specified BER level. The required BER value of 10^{-4} is provided by the external BER estimators. The input BER value is converted to the effective Q-factor. The latter is evaluated for different optical powers in multiple module runs. The change in the optical power is achieved using the same galaxy block that provides ASE noise and a swept attenuation values (0 – 20) dB. Finally, the receiver sensitivity is calculated for the selected BER value for different fibre distances.

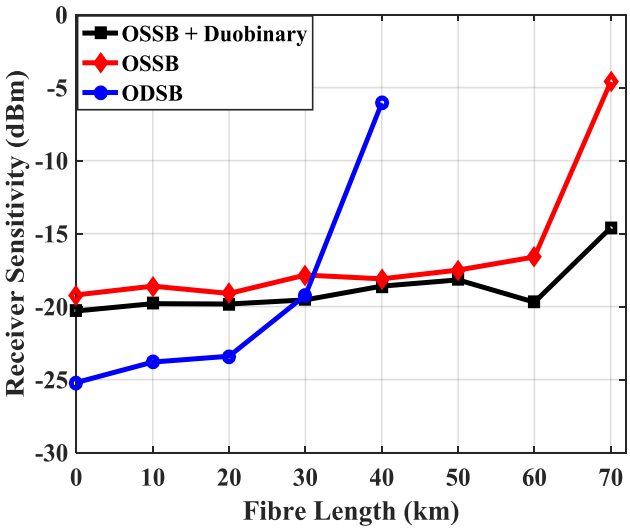

Figure 5- 8: Receiver Sensitivity versus Fibre Distance

It can be seen from figure 5-8, that the transmission of the DRoF signal in OSSB format can achieve better receiver sensitivity than ODSB at distances over than 30 km. It is also evident that there is a power penalty of about 5 to 6 dB at 0 km in the case of both OSSB and the proposed formats with respect to ODSB. This is because the MZ modulator is not being driven to the full extinction in the case of OSSB, unlike in the case of ODSB. The receiver sensitivity improves further when the DRoF system employs the proposed transmitting scenario due to the use of the duobinary coding scheme, which reduces the chromatic dispersion effect, resulting in a -66.44% sensitivity enhancement at 70 km fibre

distance relative to the OSSB case. However, link performance is degraded after this fibre length, because of the additional effects, such as the fibre non-linear effects and the accumulated fibre attenuation.

The Quality factor (Q factor) is related to the received BER by:

$$BER = \frac{1}{2} erfc \frac{Q}{\sqrt{2}} \tag{5.15}$$

This relationship implies that the minimum value of Q that will satisfy a BER of 10^{-9} is 6 as it can be shown in figure 5-9 below. Hence, this Q factor value is considered as the threshold level to compare between the three transmission schemes.

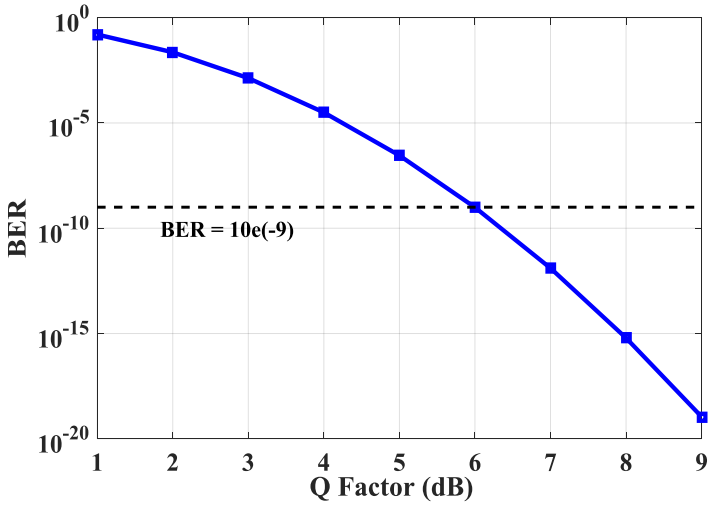

Figure 5- 9: Q Factor versus BER

Figure 5-10 shows the measured Q factor versus the Optical Signal-to-Noise Ratio (OSNR). The simulation results of figure 5-10 were taken at a fibre length of 20 km. It indicates that the threshold level cannot be reached in the case of the ODSB transmission scenario. This confirms the feasibility of the suggested bandwidth-efficient transmission

schemes for DRoF systems. It should be noted that the OSSB scheme can achieve the threshold value of Q at OSNR values higher than 29 dB. It should also be stressed that the OSNR of the proposed scheme is enhanced by 5.8 dB relative to the OSSB system in meeting the same requirement. This enhancement is contributed to the major reduction in the chromatic dispersion effect by utilising the duobinary coding in the proposed scheme.

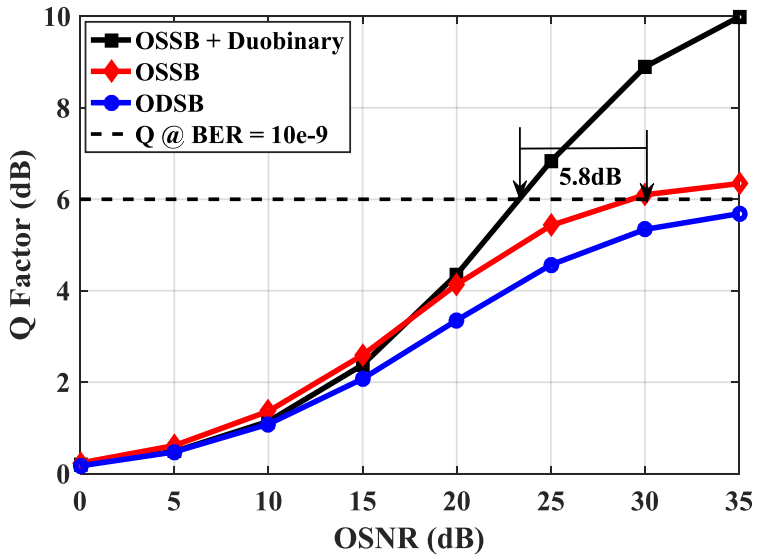

Figure 5- 10: Q Factor versus OSNR

Eye diagrams of the transmitted signals were used to evaluate the transmission performance of the compared systems. The Eye-Opening Penalty (EOP) is used to measure the degradation in the eye diagrams, which is defined as the ratio of the non-distorted reference eye, namely the Eye Opening Amplitude (EOA), which can be obtained from the back-to-back measurement and the eye opening of the distorted eye, i.e. the Eye Opening Height (EOH). In fact, EOP is the ratio of the inside and outside the opening of the eye diagram as shown in the inset of figure 5-11. EOP is usually given in dB as [130]:

$$EOP(dB) = 10\log\left(\frac{EOA}{EOH}\right) \tag{5.16}$$

Figure 5-11 shows the measured EOP against the fibre distance. It can be seen that the EOP increases exponentially with increasing distance. In the figure, EOH in the ODSB case closes after 30 km distance owing to the EOP approaching infinity, according to (5.16), since the eye diagram is completely closed at 40 km distance. In the OSSB case, the EOH does not close until 50 km distance, where 8.1 dB of the EOP is obtained since the optical bandwidth is half that of the ODSB case.

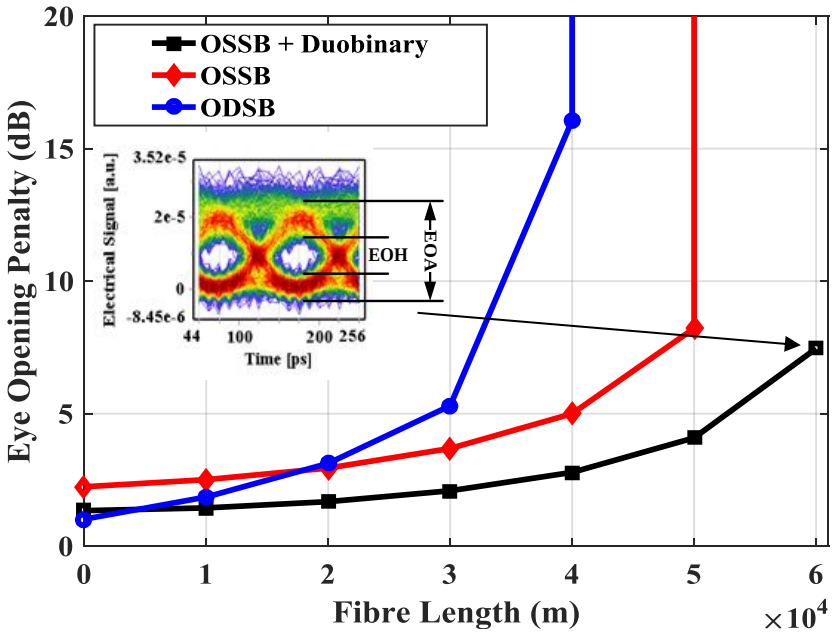

Figure 5- 11: Eye Opening Penalty versus Fibre Length

In the proposed system, the digital signal is pre-compensated for the CD effect via duobinary coding. This has resulted in a further extension to the fibre distance in terms of the measured EOP. In addition, a significant improvement can be observed in the EOP along the whole transmission distance relative to the OSSB case, because of the optical bandwidth is more reduced. As a result, the EOH can be partially reopened for a distance beyond the OSSB case, but it can never be reopened after 60 km due to the second order effect of the CD.

Another important finding is depicted in figure 5-12 regarding the measured Error Vector Magnitude (EVM) of the 16-QAM digitised RF signal at different fibre distances. Initially, it should be mentioned that the minimum requirement for the EVM value, according to the

3rd Generation Partnership Project (3GPP) specifications for a 16-QAM signal, is 12.5%. Regarding the ODSB transmission scenario, the measured EVM values remain constant from 0 to 40 km of fibre distance, despite the signal is subjected to an 8 dB penalty resulted from the fibre attenuation despite the signal has imposed to 8 dB penalty of fibre attenuation. This confirms the fact that DRoF systems are capable of maintaining the signal dynamic range independent from the fibre length until it goes below the receiver sensitivity. Similarly, measured EVM values remain stable and below the 3GPP requirement in the case of OSSB transmission, but this time for a long distance that reaches up to 50 km. This increment is directly related to the optical bandwidth reduction. However, the attenuation and dispersion effects become more severe after this distance, thus causing a distortion in the received constellation diagram, as shown in the inset of figure 5-12. In the proposed scenario, it should be noted that there is an observable EVM enhancement of 7% along the whole transmission distance when compared with the other ones. It is evident that the received I/Q symbols forming the constellation diagram are mainly penalised by the ISI effect produced by the CD. Employing the duobinary coding reduces the ISI effect and consequently, the received symbols are more concentrated, which improves the EVM values, as shown in the inset of figure 5-12. Moreover, the transmission distance is increased up to 70 km, while still satisfying the EVM requirement. This resulted from the further reduction in the optical bandwidth presented in this transmission scheme.

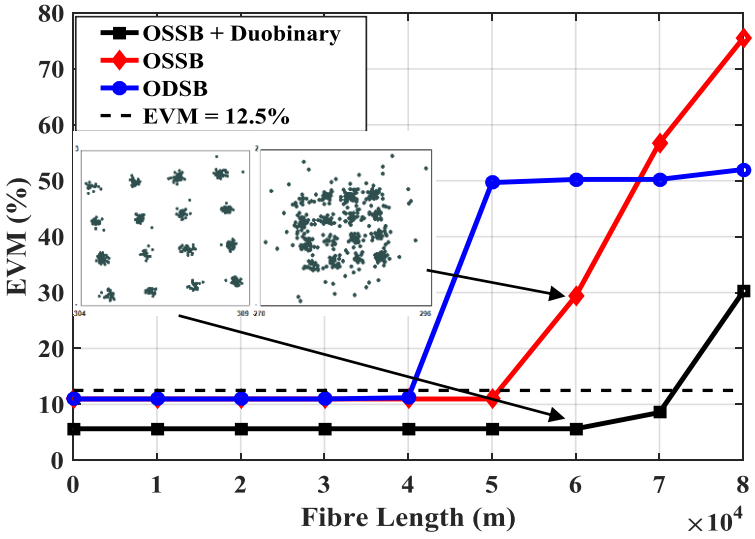

Figure 5- 12: Error Vector Magnitude versus Fibre Length

5.11 Chapters Conclusion

In this chapter, the performance of the digitized transmission of the RF signals over fibre (DRoF) has been greatly improved. A further reduction to the optical bandwidth requirement of the DRoF link has been achieved. The techniques used for the single sideband transmission of the optically modulated digital signals have been studied. The main conclusion of this chapter can be summarized as follows:

1- A transmission scenario to the DRoF signals based on the integration of digital optical single sideband transmission with duobinary coding scheme has been proposed.
2- The proposed scheme reduced the dispersion effects introduced in the fibre by first, diminishing the spectral occupancy of the transmitted optical signal and second, by countering the ISI effects induced by the chromatic dispersion.
3- For comparison, two other transmission scenarios, based on optical double sideband and optical single sideband modulation schemes, respectively, have been considered.
4- Simulation results have proven that by employing the proposed scenario in DRoF technology, transmission distance can be extended up to 70 km without dispersion compensation requirement.
5- Moreover, it has been shown that this transmission scenario can achieve the EVM and BER limits required by the 3GPP specifications, thus confirming that radio interfaces, such as CPRI, might be compatible with the proposed system.

Chapter 6

Conclusions and Future work

In this chapter, the thesis work is concluded and the accomplishments of the research objectives are summarised. This thesis studies the two main categories of RoF technologies that may form a genuine part of the future high bandwidth RAN aiming to find solutions for the deployment challenges while coping with the ever increasing high data rate demands.

This thesis presented three contributions addressing, by means of simulation, the main challenges associated with the physical layer design of the fronthaul link for the next generation RAN based on applying ARoF and DRoF transmission techniques. The findings of this research have proven from thorough simulation environments the capability of the designed links to achieve high-quality signal spectrums, increased transmission distances and low power budgets with reduced implementation cost.

6.1 Chapter Summaries

The overall summary of each chapter in this thesis can be reported as follows:

6.1.1 Chapter 2 - Optical Communication Systems (Literature Review)

In chapter 2, the operating principles of the main components used in optical communication systems are reviewed. Firstly, the optical transmitters are discussed in section 2.2 including the generation of the optical signal using a CW laser source. The optical signal is modulated either directly or externally with the RF signal using an optical modulator. However, for high-frequency signals (RF ≥ 10 GHz), external modulators are

required. Section 2.2.2 described the operation principles of the most commercial external modulators used in optical transmission systems, in particular, MZM and DD-MZM.

The optical receiver, which performs the OE conversion process, is detailed in section 2.3. Operation principles of the most commonly used photo-detector, known as PIN photo-detector is presented.

The optical fibre types are discussed in section 2.4.1. The major types of impairments imposed by the optical fibre link on the transmitted signals are discussed in sections 2.5, 2.6 and 2.7. The first kind of impairments is the attenuation, which occurs due to light absorption by the silica fibre and Rayleigh scattering phenomenon. Secondly, fibre nonlinearities are discussed in section 2.7. It causes a severe impact on the transmission when increasing the light intensity. Finally, the major impairment type in optical communication systems is discussed in section 2.6, which is the dispersion. As discussed in that section, it causes pulse broadening at the output of the optical fibre link causing the ISI effect at the received signal. Fibre-induced dispersion types are illustrated in section 2.6, among them, chromatic dispersion has the major effect on optical transmission. Since addressing the chromatic dispersion effect is the main focus in this thesis, this gives rise to review the most commonly approaches dedicated to limit or reverse the chromatic dispersion effect, particularly DCF and CFBG technologies.

RoF technology is introduced in section 2.9. The two main multiplexing methods of RoF communication systems, namely SCM and WDM are discussed. The ARoF transmission system is briefly introduced in section 2.10, where the RF carrier in modulated with the baseband data and then transmitted over fibre using an optical carrier. In section 2.10.1, the practical impairments associated with ARoF transmission philosophy are presented. The conventional DRoF system is discussed in section 2.11, in which the RF signal is digitised at the transmitter before being transmitted over fibre. As discussed in section 2.11, RF signal digitisation process is accomplished using an electronic ADC and then converted to a series binary digital signal to be externally modulated by an optical signal. Due to the digitalisation process, the optical link required a high bandwidth, which represents a major challenge in DRoF deployment.

Based on this literature, a typical multilevel transmission technique based on Duobinary encoding is proposed. It can modify the transmission format of the information signal so that the required optical bandwidth is reduced. As a consequence, optical transmission can partially be increased by reducing the effective transmission bandwidth. In the same context, bandwidth-efficient modulation formats which can be used in digital optical systems to limit the chromatic dispersion effect are discussed in section 2.13.

6.1.2 Chapter 3 - Analogue RoF Transmission System

Chapter 3 investigates the simulation design of the ARoF transmission system and presents the achieved contributions in that area. The optical physical layer design of an ARoF system that is used for facilitating the A-FH transmission of four RF channels each with 5 GHz RF carrier and 2.5 Gb/s data rate via DWDM-RoF system is designed. The proposed design investigates the deployment of these channels upon using different QAM combination for each RF signal. Accordingly, a 4-QAM, 16-QAM, 64-QAM and 256-QAM signals are multiplexed forming the DL signals and transmitted over SSMF. Each RF channel carried by a separate wavelength while a frequency gap of 0.8 nm was set between adjacent wavelengths to enable an optimised bandwidth utilisation cooperated with an extended RoF capacity.

In order to control the chromatic dispersion induced in the SSMF at zero dispersion point, a DCF has been utilised; thus, the transmission distance has been significantly increased up to 120 km. This transmission increase was not possible without employing an EDFA with 20 dB gain to compensate for the high value of accumulated attenuation resulted from both SMF and DCF. Another contribution was added to the designed link concluded by proposing a simplified wavelength reuse scheme based on using PS followed by an optical BPF located at the BS side. For UL transmission, four OOK baseband signals each with 2.5 Gb/s were multiplexed and transmitted back to the transmitter using the same DL wavelengths.

The performance of the designed link is assessed on the basis of the received SER and EVM values for every single channel. These results have shown that the EVM values are still within the 3GPP standardised limits specified for each nominated QAM combination along 120 km transmission distance. Most importantly, simulation results have shown that employing higher modulation formats can contribute to a further transmission increase as they would require less optical bandwidths. Furthermore, the performance results have displayed clear constellation diagrams for the received channels even after 120 km transmission length. Finally, it was shown that the designed ARoF link has a BER $< 10^{-6}$ for UL channels at a ROP of -20 dBm proving that the link is of high integrity; thus, the aim of achieving a highly qualified A-FH link based on ARoF technology has been achieved.

6.1.3 Chapter 4 - Efficient Transmission of a DRoF Link

In chapter 4, a DRoF communication system is detailed. The digitisation of the analogue RF signal is performed using the legacy baseband sampling theorem to achieve a simplified link design compared to the other digitisation processes. In section 4.9, a cost-effective physical layer design of DRoF link that addresses the high optical bandwidth requirement is designed. The proposed link transmits the digitised version of a 16-QAM signal with 5 GHz carrier frequency and 1.25 Gb/s data rate over an SSMF. In order to effectively reduce the resultant optical bandwidth, Duobinary encoding scheme has been utilised in the designed link instead of the conventional encoding formats, such as NRZ. ADC resolution's bit is the major source of performance limitation in DRoF link design as it is the main reason for the produced high data rates. In contrast, simulation results of the proposed link have shown a high-quality signal performance even with ADC resolution of 8 bits in terms of the received EVM and BER.

To quantify the quality of the proposed link, performance results have been compared with another DRoF link utilises NRZ encoding scheme. It was observed that the designed link is capable to maintain EVM values below 12.5%, which is the 3GPP standard value for

16-QAM signal, for transmission distances reach up to 70 km without dispersion compensation requirements. Moreover, the BER results have recorded a value of 10^{-6} upon the received optical sensitivity of about -17 dBm showing the high resiliency of the designed link to both the dispersion effect and ADC resolution bits against high bit rate transmission of 10 Gb/s.

6.1.4 Chapter 5 - Advanced Design of a DRoF Transmission Link

In chapter 5, a more advanced performance of a DRoF communication link is simulated. The main aim of this chapter is how to develop a transmission technique such that to fourthly reduce the resultant optical bandwidth of the DRoF link. A new transmission approach based on transmitting the Duobinary encoded digital signal using an optical SSB modulation system is demonstrated. The proposed optical SSB system was optimised so that to be compatible with the proposed encoding scheme in terms of modifying the biasing voltages of the modulators and modelling an FIR digital filter to achieve the required Hilbert Transformation to the modulating digital signal.

Based on the simulation results, it was determined that the proposed DRoF link could offer a significant improvement and a transmission extension over a conventional optical DSB and optical SSB that uses NRZ encoding. Furthermore, it was shown that the designed link has a BER of 10^{-9} measured at a quite satisfactory OSNR value of 23 dB after 20 km transmission distance of a 10 Gb/s data rate. At this point of improvement, optical spectrum results have displayed that the major limiting factor of high optical bandwidth requirements associated with DRoF deployment has been addressed confirming the achievement of the research aim.

6.2 Thesis Future Work

The following points can be performed as a future work of this research:

1- The simulations demonstrated in this thesis have shown promising solutions regarding the deployment of the fronthaul link based on both RoF technologies while increasing the transmission length and data rates. Therefore, the next step to support and confirm these achievements could be an experimental work with measurements on ARoF and DRoF systems performances.

2- Designing a full duplex multi-RF signal transmission over the reduced bandwidth occupancy DRoF links proposed in this research and to evaluate the performance in comparing it with the ARoF transmission.

3- Investigating the implementation of different multi-levels modulation schemes, such as PAM-4 in terms of the chromatic dispersion management and to compare it with the proposed DRoF links upon different transmission scenarios.

4- Design and implementation of a different wavelength reuse scheme to achieve a cost-efficient bidirectional RoF link. This scheme based on transmitting a pilot optical carrier generated at the CO by frequency shifting the original optical signal. The original optical carrier will be modulated by the RF signal and then multiplexed with the pilot signal to be transmitted over the same fibre. A de-multiplexer would be used at the BS side to extract both the modulated optical signal for detection and the pilot optical signal to be used for the upstream transmission.

References

[1] Cisco Systems 2017, “Cisco Visual Networking Index: Global Mobile Data Traffic Forecast Update, 2016–2021 White Paper,” 2017.

[2] R. Ramaswami and K. Sivarajn, *Optical Networks: A Practical Perspective*, 2ndEdition ed. Academic Press, 2002.

[3] M. Tornatore, G.-K. Chang, and G. Ellinas, *Fiber-Wireless Convergence in Next-Generation Communication Networks*. Springer, 2017.

[4] Y. Yang, C. Lim, and A. Nirmalathas, “Investigation on transport schemes for efficient high-frequency broadband OFDM transmission in fibre-wireless links,” *J. Light. Technol.*, vol. 32, no. 2, pp. 267–274, 2014.

[5] H. Al-Raweshidy and S. Komaki, *Radio over fiber technologies for mobile communications networks*, 1st Editio. Artech House, 2002.

[6] J. Wu, Z. Zhang, Y. Hong, and Y. Wen, “Cloud radio access network (C-RAN): A primer,” *IEEE Netw.*, vol. 29, no. 1, pp. 35–41, 2015.

[7] A. Checko *et al.*, “Cloud RAN for Mobile Networks - A Technology Overview,” *IEEE Commun. Surv. Tutorials*, vol. 17, no. 1, pp. 405–426, 2015.

[8] A. De La Oliva, J. A. Hernandez, D. Larrabeiti, and A. Azcorra, “An overview of the CPRI specification and its application to C-RAN-based LTE scenarios,” *IEEE Commun. Mag.*, vol. 54, no. 2, pp. 152–159, 2016.

[9] C. Lanzani and S. P. Manager, “Open Base Station Architecture :,” 2008. [Online]. Available: www.obsai.com.

[10] “NG-PON2 Specification,” *ITU-T-G.989.2 Amendment 1*, 2014. [Online]. Available: http://www.itu.int/rec/T-REC-G.989.2/en.

[11] E. FORESTIERI, *Optical Communication Theory and Techniques*. Pisa, Italy: Springer, 2005.

[12] A. E. Siegman, *Lasers*. University Sience Books, 1986.

[13] G. P. Agrawal, *Fiber-Optic Communication Systems*, Third Edit. New York: John Wiley & Sons, 2002.

[14] X. Qian, P. Hartmann, J. D. Ingham, R. V Penty, and I. H. White, "Directly-Modulated Photonic Devices for Microwave Applications (INVITED)," *IEEE MTTS Int. Microw. Symp. Dig. 2005*, vol. 44, no. 0, pp. 909–912, 2005.

[15] Y. Fu, X. Zhang, B. Hraimel, T. Liu, and D. Shen, "Mach-Zehnder: A review of bias control techniques for mach-zehnder modulators in photonic analog links," *IEEE Microw. Mag.*, vol. 14, no. 7, pp. 102–107, 2013.

[16] Y. N. Wijayanto *et al.*, "Metamaterial antenna integrated to LiNbO3 optical modulator for millimeter-wave-photonic links," *2015 Int. Symp. Antennas Propagation, ISAP 2015*, pp. 2–5, 2016.

[17] "VPI Photonics. VPITransmissionMaker Optical Systems 9.5." Tech. Rep., 2015.

[18] P. L. Kelley, I. P. Kaminow, and G. G. P. Agrawal, *Nonlinear fiber optics*. 2001.

[19] I. P. KAMINOW and T. LI, *OPTICAL FIBER TELECOMMUNICATIONS IV B SYSTEMS AND IMPAIRMENTS*. USA: Academic Press, 2002.

[20] M. Cvijetic, *Optical Transmission Systems Engineering*. Boston • London: Artech House, 2004.

[21] R. Gaudino *et al.*, "Perspective in next-generation home networks: Toward optical solutions?," *IEEE Commun. Mag.*, vol. 48, no. 2, pp. 39–47, 2010.

[22] C. D. Encyclopedia, "Numerical Aperture Computer Definition," 2011. [Online]. Available: http://encyclopedia2.thefreedictionary.com/fiber+optics+glossary.

[23] A. Das, A. Nkansah, N. J. Gomes, I. J. Garcia, J. C. Batchelor, and D. Wake, "Design of low-cost multimode fiber-fed indoor wireless networks," *IEEE Trans. Microw. Theory Tech.*, vol. 54, no. 8, pp. 3426–3432, 2006.

[24] A. M. J. Koonen and M. G. Larrode, "Radio-Over-MMF Techniques-Part-II: Microwave to Millimeter-Wave Systems," *J. Light. Technol.*, vol. 26, no. 13–16, pp. 2396–2408, 2008.

[25] D. R. Anderson, L. Johnson, and F. G. Bell, *Troubleshooting Optical-Fiber Networks*. California, US: Elsevier Academic Press, 2004.

[26] S. V. Kartalopoulos, *Next Generation Intelligent Optical Networks*. Oklahoma, USA: Springer, 2008.

[27] I. P. Kaminow, T. Li, and A. E. Willner, *Optical Fiber Telecommunications.*

Burlington. Burlington, US: AP Academic Press, 2008.

[28] J. T.Moring, *Communications Engineering Desk Reference*. Oxford, UK: AP, 2009.

[29] L. N. Binh and N. Q. Ngo, *Ultra-Fast Fiber Lasers*. New York, US: CRC Press, 2011.

[30] K. Okamoto, *Fundamentals of Optical Waveguides*. Tokyo, Japan: Academic Press of Elsevier, 2006.

[31] J. R. Vacca, *Optical Networking Best Practices Handbook*. New Jersey, USA: Wiley & Sons, 2007.

[32] J. P. Vasseur, M. Pickavet, and P. Demeester, *Network Recovery Protection and Restoration of Optical, SONET-SDH, IP, and MPLS*. San Francisco ,USA: Elsevier Academic Press, 2004.

[33] A. Kobyakov, M. Sauer, and D. Chowdhury, "Stimulated Brillouin scattering in optical fibers," *Adv. Opt. Phot.*, vol. 2, pp. 1–59, 2010.

[34] A. V Harish and J. Nilsson, "Optimization of Phase Modulation Formats for Suppression of Stimulated Brillouin Scattering in Optical Fibers," *IEEE J. Sel. Top. Quantum Electron.*, vol. 24, no. 3, pp. 1–10, 2018.

[35] M. Baskaran and R. Prabakaran, "Photonic generation of microwave pulses using Stimulated Brillouin Scattering (SBS)-based carrier processing and data transmission for Radio over Fiber (RoF) systems," *Proc. 2016 IEEE Int. Conf. Wirel. Commun. Signal Process. Networking, WiSPNET 2016*, pp. 372–375, 2016.

[36] C. A. Codemard *et al.*, "Resonant SRS Filtering Fiber for High Power Fiber Laser Applications," *IEEE J. Sel. Top. Quantum Electron.*, vol. 24, no. 3, pp. 1–9, 2018.

[37] B. E. A. Saleh and M. C. Teich, *Fundamental of Photonics*, Second Edi. Wiley - Interscience, 2007.

[38] R. H. Stolen and C. Lin, "Self-phase-modulation in silica optical fibers," *Phys. Rev. A*, vol. 17, no. 4, pp. 1448–1453, 1978.

[39] F. Zernike and J. E. Midwinter, *Applied Nonlinear Optics*. Wiley- Inrerscience, 1974.

[40] N. Sultana and M. S. Islam, "The effects of cross-phase modulation and third order dispersion on pulses and pulse broadening factor in the WDM transmission system,"

Proc. 2013 2nd Int. Conf. Adv. Electr. Eng. ICAEE 2013, no. Icaee, pp. 282–285, 2013.

[41] F. Ramos, J. Marti, and V. Polo, "Compensation of Chromatic Dispersion Effects in Microwave / Millimeter-Wave Optical Systems Using Four-Wave-Mixing Induced in Dispersion-Shifted Fibers," *IEEE Photonics Technol. Lett.*, vol. 11, no. 9, pp. 1171–1173, 1999.

[42] B. Chomycz, *Planning Fiber Optic Networks*. New York, USA: McGraw-Hill, 2009.

[43] R. J. Nuyts, Y. K. Park, and P. Gallion, "Dispersion equalization of a 10 Gb/s repeatered transmission system using dispersion compensating fibers," *J. Light. Technol.*, vol. 15, no. 1, pp. 31–41, 1997.

[44] S. M. Nejad and N. Ehteshami, "A novel design to compensate dispersion for square-lattice photonic crystal fiber over E to L wavelength bands," *Commun. Syst. Networks Digit. Signal Process. (CSNDSP), 2010 7th Int. Symp.*, pp. 0–4, 2010.

[45] R. Kashyap, *Fiber Bragg Gratings*. San Diego, USA: Academic Press, 1999.

[46] K. O. Hill and G. Meltz, "Fiber Bragg grating technology fundamentals and overview," *J. Light. Technol.*, vol. 15, no. 8, pp. 1263–1276, 1997.

[47] B. Mukherjee, *Traffic Grooming for Optical Networks Optical Networks Series Editor :* .

[48] H. Al-Raweshidy and S. Komaki, *Radio over Fibre for Mobile Communications Networks*, 1st Editio. Artech House.

[49] D. Wake *et al.*, "A comparison of radio over fiber link types for the support of wideband radio channels," *J. Light. Technol.*, vol. 28, no. 16, pp. 2416–2422, 2010.

[50] C. Cox, E. Ackerman, R. Helkey, and G. E. Betts, "Techniques and Performance of Intensity- Modulation Direct-Detection Analog Optical Links," vol. 45, no. 8, p. 1375— 1383.

[51] S. Pato, F. Ferreira, P. Monteiro, and H. Silva, "On supporting multiple radio channels over a SCM-based distributed antenna system: A feasibility assessment BT - 2010 12th International Conference on Transparent Optical Networks, ICTON 2010, June 27, 2010 - July 1, 2010," pp. 3–6, 2010.

[52] V. A. Thomas, M. El-Hajjar, and L. Hanzo, “Performance Improvement and Cost Reduction Techniques for Radio Over Fiber Communications,” *IEEE Commun. Surv. Tutorials*, vol. 17, no. 2, pp. 627–670, 2015.

[53] H.-G. Weber and M. Nakazawa, *Ultrahigh-Speed Optical Transmission Technology*. 2007.

[54] A. Moscoso-Mártir *et al.*, “Silicon Photonics WDM Transceiver with SOA and Semiconductor Mode-Locked Laser,” vol. 25, no. 1, pp. 1395–1401, 2016.

[55] J. S. S.Uma, “Human Interaction Pattern Mining Using Enhanced Artificial Bee Colony Algorithm S.,” *Int. J. Innov. Res. Comput. Commun. Eng.*, vol. 3, no. 10, pp. 10131–10138, 2015.

[56] B. With, W. D. M. Ring, C. Lim, A. Nirmalathas, S. Member, and M. Attygalle, “On the Merging of Millimeter-Wave Fiber-Radio,” *October*, vol. 21, no. 10, pp. 2203–2210, 2003.

[57] J. Yu, Z. Jia, L. Yi, Y. Su, G. K. Chang, and T. Wang, “Optical millimeter-wave generation or up-conversion using external modulators,” *IEEE Photonics Technol. Lett.*, vol. 18, no. 1, pp. 265–267, 2006.

[58] J. Yu, Z. Jia, L. Xu, L. Chen, T. Wang, and G. K. Chang, “DWDM optical millimeter-wave generation for radio-over-fiber using an optical phase modulator and an optical interleaver,” *IEEE Photonics Technol. Lett.*, vol. 18, no. 13, pp. 1418–1420, 2006.

[59] A. Kaszubowska, P. Anandarajah, and L. P. Barry, “Multifunctional Operation of a Fiber Bragg Grating in a WDM/SCM Radio Over Fiber Distribution System,” *IEEE Photonics Technol. Lett.*, vol. 16, no. 2, pp. 605–607, 2004.

[60] G. H. Smith, D. Novak, and C. Lim, “A millimeter-wave full-duplex fiber-radio star-tree architecture incorporating WDM and SCM,” *IEEE Photonics Technol. Lett.*, vol. 10, no. 11, pp. 1650–1652, 1998.

[61] Z. Xu *et al.*, “Carrier-reuse WDM-PON using a shared delay interferometer for separating carriers and subcarriers,” *IEEE Photonics Technol. Lett.*, vol. 19, no. 11, pp. 837–839, 2007.

[62] Q. Guo and A. V. Tran, “Demonstration of a 40 Gb/s Wavelength-Reused WDM-

PON Using Coding and Equalization [Invited],” *J. Opt. Commun. Netw.*, vol. 5, no. 10, p. A119, 2013.

[63] P. Lecoy, *Fibre-Optic Communications*, Third Edit., vol. 6. John Wiley & Sons, 2010.

[64] T. S. Cho and K. Kim, “Optimization of radio-on-fiber systems employing ODSB signals by utilizing a dual electrode Mach-Zehnder modulator against IM3,” *IEEE Photonics Technol. Lett.*, vol. 18, no. 9, pp. 1076–1078, 2006.

[65] M. R. Phillips, T. E. Darcie, D. Marcuse, G. E. Bodeep, and N. J. Frigo, “Nonlinear Distortion Generated by Dispersive Transmission of Chirped Intensity-Modulated Signals,” *IEEE Photonics Technol. Lett.*, vol. 3, no. 5, pp. 481–483, 1991.

[66] S. Betti, E. Bravi, and M. Giaconi, “Nonlinear distortions due to the ‘dispersive’ transmission of SCM optical signals in the presence of chirping effect: An accurate analysis,” *IEEE Photonics Technol. Lett.*, vol. 9, no. 12, pp. 1640–1642, 1997.

[67] E. Chen and A. Murphy, *Broadband Optical Modulators: Science, Technology, and Applications*. 2011.

[68] J. M. B. Oliveira, L. M. Pessoa, D. Coelho, J. S. Tavares, and H. M. Salgado, “Digitised radio techniques for Fibre-wireless applications,” *Int. Conf. Transparent Opt. Networks*, pp. 4–7, 2014.

[69] W. Ampalavanapillai, Nirmalathas; Prasanna , A. Gamage; Christina, Lim; Dalma, Novak; Rodney, “Digitized Radio Over Fiber Technologies for Converged Optical Wireless Access Network,” *J. Light. Technol.*, vol. 28, no. 16, pp. 2366–2375, 2010.

[70] P. A. Gamage, A. Nirmalathas, C. Lim, D. Novak, and R. Waterhouse, “Design and analysis of digitized RF-over-fiber links,” *J. Light. Technol.*, vol. 27, no. 12, pp. 2052–2061, 2009.

[71] A. Nirmalathas, P. A. Gamage, C. Lim, D. Novak, R. Waterhouse, and Y. Yang, “Digitilized RF transmission over fiber,” *IEEE Microw. Mag.*, vol. 10, no. 4, pp. 75–81, 2009.

[72] R. S. Oliveira, N. S. Moritsuka, R. C. Santos, and R. P. Almeida, “Low Cost Digital Radio over Fiber System Low Cost Digital Radio over Fiber System,” 2015. [Online]. Available: http://www.researchgate.net/publication/264942874.

[73] A. Saadani *et al.*, “Digital Radio over Fiber for LTE-Advanced: Opportunities and Challenges,” *Opt. Netw. Des. Model. (ONDM), 2013 17th Int. Conf.*, pp. 194–199, 2013.

[74] K. V. Prasad, *Principles of Digital Communication Systems and Computer Networks Preface*. Charles River Media, 2005.

[75] L. N. Binh, *Digital Optical Communications*. New York: CRC Press, 2008.

[76] L. W. Couch, “BASEBAND PULSE AND DIGITAL SIGNALING,” in *DIGITAL AND ANALOG COMMUNICATION SYSTEMS*, Eighth Edi., New Jersey, USA: Pearson Education, 2013, pp. 164–184.

[77] J. Conradi, “Bandwidth-Efficient Modulation Formats for Digital Fiber Transmission Systems,” in *OPTICAL FIBER TELECOMMUNICATIONS IV B SYSTEMS AND IMPAIRMENTS*, California, US: Elsevier Science, 2002, pp. 862–902.

[78] M. K. Simon, “Bandwidth-Efficient Digital Modulation with Application to Deep - Space Communications,” *Deep Sp. Commun. Navig. Ser.*, vol. 3, p. 237, 2001.

[79] F. Xiong, *Digital Modulation Techniques*, Second Edi. Boston, UK: Artech House, 2006.

[80] P. S. R. Diniz, E. A. B. Silva, and S. L. Netto, *Digital Signal Processing: System Analysis and Design*, Second Edi. Cambridge University Press, 2010.

[81] W. Leon and I. Couch, *Baseband Pulse and Digital Signaling’ in ‘Digital and Analog Communication Systems*, Eighth Edi. New Jersey, USA: Pearson Education, 2013.

[82] J. Wei, K. Grobe, C. Wagner, E. Giacoumidis, and H. Griesser, “40 Gb/s Lane Rate NG-PON using Electrical/Optical Duobinary, PAM-4 and Low Complex Equalizations,” *Opt. Fiber Commun. Conf.*, no. c, p. Tu3C.5, 2016.

[83] J. Builting, *Introduction to Duobinary Encoding and Decoding*. Elektor Electronics, 1990.

[84] W. Ji and J. Chang, “Design of WDM-RoF-PON for wireless and wire-line access with source-free ONUs,” *IEEE/OSA J. Opt. Commun. Netw.*, vol. 5, no. 2, pp. 127–133, 2013.

[85] A. N. Geboren, *Radio-over-Fibre Technology for Broadband Wireless Communication Systems door*. Netherlands, 2005.

[86] J. E. Mitchell, "Integrated Wireless Backhaul Over Optical Access Networks," *J. Light. Technol.*, vol. 32, no. 20, pp. 3373–3382, 2014.

[87] W. Ji and J. Chang, "The radio-on-fiber-wavelength-divisionmultiplexed- passive-optical network (WDM-RoF-PON) for wireless and wire layout with linearly-polarized dual-wavelength fiber laser and carrier reusing," *Opt. Laser Technol.*, vol. 49, pp. 301–306, 2013.

[88] V. Sarup and A. Gupta, "Performance analysis of an ultra high capacity 1 Tbps DWDM-RoF system for very narrow channel spacing," *IFIP Int. Conf. Wirel. Opt. Commun. Networks, WOCN*, 2014.

[89] J. Yu, M. F. Huang, D. Qian, L. Chen, and G. K. Chang, "Centralized lightwave WDM-PON employing 16-QAM intensity modulated OFDM downstream and OOK modulated upstream signals," *IEEE Photonics Technol. Lett.*, vol. 20, no. 18, pp. 1545–1547, 2008.

[90] W. Hung, C. K. Chan, L. K. Chen, and F. Tong, "An optical network unit for WDM access networks with downstream DPSK and upstream remodulated OOK data using injection-locked FP laser," *IEEE Photonics Technol. Lett.*, vol. 15, no. 10, pp. 1476–1478, 2003.

[91] P. Downlink and I. Uplink, "Cost-Effective Radio-over-Fiber Systems Employing," pp. 8–10, 2009.

[92] P. Healey *et al.*, "Spectral slicing WDM-PON using wavelength-seeded reflective SOAs," *Electron. Lett.*, vol. 37, no. 19, p. 1181, 2001.

[93] E. Wong, C. J. Chang-hasnain, W. Hofmann, and M. C. Amann, "Uncooled, Optical Injection-Locked 1.55 gm VCSELs for Upstream Transmitters in WDM-PONs," *Ofc*, pp. 1–3, 2006.

[94] H. Kim, "Radio over RSOA-based WDM-PON," *2011 IEEE Int. Top. Meet. Microw. Photonics - Jointly Held with 2011 Asia-Pacific Microw. Photonics Conf. MWP/APMP 2011*, pp. 238–241, 2011.

[95] C. Yeh, H. Chien, and S. Chi, "Cost-Effective Colorless RSOA-Based WDM-PON

with 2.5 Gbit/s Uplink Signal," in *IEEE Optical Fiber Communication Conference*, 2008, pp. 2–4.

[96] S. Bindhaiq, N. Zulkifli, A. Sahmah, M. Supa, and R. Q. Shaddad, "Capacity Improvement of TWDM-PONs Exploiting the 16-QAM Technique for Downstream Side With a Nonlinearity Effect Study for Upstream DML," *J. OPT. COMMUN. NETW*, vol. 7, no. 10, pp. 1018–1024, 2015.

[97] A. Qasim, T. Mehmood, U. Ali, Q. U. Khan, and S. Ghafoor, "Dual-Ring Radio Over Fiber System with Centralized Light Sources and Local Oscillator for millimeter-wave Transmission," in *20th International Multitopic Conference (INMIC 17)*, 2017, no. 17, pp. 2–6.

[98] "LTE, 3GPP TS 24.229 V13.5.1." [Online]. Available: http://www.3gpp.org/release-13.

[99] V. S. R. Krishna and R. Singhal, "Dual carrier multiplexed M-QAM signals modulated optical SSB transmission over fiber," *IFIP Int. Conf. Wirel. Opt. Commun. Networks, WOCN*, vol. 16, no. 2, 2016.

[100] I. A. Alimi, A. L. Teixeira, and P. P. Monteiro, "Toward an Efficient C-RAN Optical Fronthaul for the Future Networks: A Tutorial on Technologies, Requirements, Challenges, and Solutions," *IEEE Commun. Surv. Tutorials*, vol. 20, no. 1, pp. 708–769, 2018.

[101] R. S. Oliveira, C. R. L. Frances, J. C. W. A. Costa, D. F. R. Viana, M. Lima, and A. Teixeira, "Analysis of the cost-effective digital radio over fiber system in the NG-PON2 context," *2014 16th Int. Telecommun. Netw. Strateg. Plan. Symp. Networks 2014*, pp. 1–6, 2014.

[102] Y. Yang, C. Lim, P. Gamage, A. Nirmalathas, A. P. Scm, and D. Scheme, "Demonstration of SCM Signal Transmission based on Digitized Radio-over-Fiber Technique," *Converter*, pp. 14–17, 2009.

[103] P. M. Wala, "A new microcell architecture using digital optical transport," *IEEE 43rd Veh. Technol. Conf.*, pp. 585–588, 1993.

[104] Y. Yang, A. Nirmalathas, and C. Lim, "Digitized RF-over-fiber as a cost-effective and energy-efficient backhaul option for wireless communications," *Ann. des*

Telecommun. Telecommun., vol. 68, no. 1–2, pp. 23–39, 2013.

[105] A. V. Oppenheim, R. W. Schafer, and J. R. Buck, *Discrete Time Signal Processing (2nd edition)*, Second Edi. New Jersey, USA: Prentice-Hall, 1999.

[106] R. E. Ziemer and W. H. Tranter, *Principles of Communication Systems, Modulation, and Noise*, Seventh Ed. USA: John Wiley & Sons, 2014.

[107] R. G. Vaughan, N. L. Scott, and D. R. White, "The theory of bandpass sampling," *Softw. Radio Technol. Sel. Readings*, vol. 39, no. 9, pp. 126–137, 2001.

[108] R. H. Walden, "Analog-to-digital converter survey and analysis," *IEEE J. Sel. Areas Commun.*, vol. 17, no. 4, pp. 539–550, 1999.

[109] R. Gaggl, *Delta-Sigma A/D-Converters Practical Design for Communication Systems*, vol. 39. Villach, Austria: Springer, 2013.

[110] S. Hori *et al.*, "A digital radio-over-fiber downlink system based on envelope delta-sigma modulation for multi-band/mode operation," *IEEE MTT-S Int. Microw. Symp. Dig.*, vol. 2016–Augus, no. 1, pp. 16–19, 2016.

[111] J. Wang *et al.*, "Digital Mobile Fronthaul Based on Delta–Sigma Modulation for 32 LTE Carrier Aggregation and FBMC Signals," *J. Opt. Commun. Netw.*, vol. 9, no. 2, p. A233, 2017.

[112] S. R. Abdollahi, H. S. Al-Raweshidy, A. Ahmadinia, and R. Nilavalan, "An all-photonic digital radio over fiber architecture," *2011 IEEE Swedish Commun. Technol. Work. Swe-CTW 2011*, pp. 62–67, 2011.

[113] L. Gates, L. Brzozowski, and E. H. T. Sargent, "All-Optical Analog-to-Digital Converters ," vol. 19, no. 1, pp. 114–119, 2001.

[114] H. Zmuda, E. N. Toughlian, G. Li, and P. LiKamWa, "A photonic wideband analog-to-digital converter," *IEEE Aerosp. Conf. Proc.*, vol. 3, pp. 31461–31472, 2001.

[115] Q. Wu, H. Zhang, M. Yao, and W. Zhou, "All-Optical Analog-to-Digital Conversion Using Inherent Multiwavelength Phase Shift in LiNbO 3," vol. 20, no. 12, pp. 1036–1038, 2008.

[116] Y. Peng, H. Zhang, Q. Wu, X. Fu, Y. Zhang, and M. Yao, "A Novel Proposal of All-Optical Analog-to-Digital Conversion with Unbalanced MZM and Filter

Array," in *15th Asia-Pacific Conference on Communications*, 2009, pp. 485–486.

[117] P. W. Juodawlkis, J. J. Hargreaves, and J. C. Twichell, "Impact of photodetector nonlinearities on photonic analog-to-digital converters," *Summ. Pap. Present. Lasers Electro-Optics. CLEO '02. Tech. Diges*, vol. 2, no. 1, pp. 11–12, 2002.

[118] L. N. Binh, "Partial Responses and Single-sideband Modulation Formats," in *Digital Optical Communication*, CRC Press, 2008, pp. 331–365.

[119] W. Tranter, K. Shanmugan, T. Rappaport, and K. Kosbar, "Sampling and Quantizing," in *Principles of Communication Systems Simulation with Wireless Applications*, Englewood Cliffs, NJ: Prentice Hall, 2003, pp. 55–90.

[120] M. Hinrichs, L. F. del Rosal, C. Kottke, and V. Jungnickel, "Analog vs. next-generation digital fronthaul: How to minimize optical bandwidth utilization," *2017 Int. Conf. Opt. Netw. Des. Model.*, vol. 1, pp. 1–6, 2017.

[121] J. J. V. Olmos, L. F. Suhr, and B. Li, "Five-level polybinary signaling for 10 Gbps data transmission systems," *Opt. Express*, vol. 21, no. 17, pp. 417–422, 2013.

[122] L. F. Suhr, P. Madsen, I. T. Monroy, and J. J. V. Olmos, "Analog-based duobinary-4-PAM for electrical bandwidth limited optical fiber links," *Opt. Appl.*, vol. 46, no. 1, pp. 71–78, 2016.

[123] J. J. Vegas Olmos *et al.*, "Challenges in polybinary modulation for bandwidth limited optical links," *J. Lasers, Opt. Photonics*, vol. 2, p. 150, 2016.

[124] M. Niknamfar and M. Shadaram, "OSSB and ODSB configurations for RoF transmission over DWDM link," *Int. Conf. Transparent Opt. Networks*, pp. 3–6, 2013.

[125] H. L. I. Aibo *et al.*, "Improving performance of mobile fronthaul architecture employing high order delta-sigma modulator with PAM-4 format," vol. 25, no. 1, pp. 1–9, 2017.

[126] K. Yonenaga and N. Takachio, "A Fiber Chromatic Dispersion Compensation Technique With An Optical SSB Transmission In Optical Homodyne Detection Systems," *IEEE Photonics Technol. Lett.*, vol. 5, no. 8, pp. 949–951, 1993.

[127] M. Sieben, J. Conradi, and D. E. Dodds, "Optical single sideband transmission at 10 Gb/s using only electrical dispersion compensation," *Light. Technol. J.*, vol. 17, no.

10, pp. 1742–1749, 1999.

[128] A. A. Oppenheim, R. W. Schafer, and J. R. Buck, “Discrete Hilbert Transforms’,” in *Discrete-Time Signal Processing*, Second Edi., Prentice-Hall, 1999, pp. 775–799.

[129] A. A. Oppenheim, R. W. Schafer, and J. R. Buck, “Filter Design Techniques’,” in *‘Discrete-Time Signal Processing*, Second Edi., Prentice-Hall, 1999, pp. 465–478.

[130] M. Seimetz, “System Simulation Aspect,” in *High-Order Modulation for Optical Fiber Transmission*, Springer, 2009, pp. 127–131.